

Hiroshima University Doctoral Thesis

**Sulfur Atom Effect on Photo-
uncaging Reaction of (Coumarin-
4-yl)methyl Derivatives**

((クマリン-4-イル)メチル誘導体の光脱ケ
ーシング反応に対する硫黄原子の影響)

2024

Department of Chemistry,
Graduate School of Science,
Hiroshima University

NGUYEN HAI DANG

Table of Contents

1. Main thesis

Sulfur Atom Effect on Photo-uncaging Reaction of (Coumarin-4-yl)methyl
Derivatives

((クマリン-4-イル)メチル誘導体の光脱ケージング反応に対する硫黄原子の影響)

2. Articles

(1) "Crucial Roles of Leaving Group and Open-Shell Cation in Photoreaction of (Coumarin-4-yl)methyl Derivatives"

Hai Dang Nguyen and Manabu Abe*
J. Am. Chem. Soc. **2024**, 146, 10993-11001.

(2) "Sulfur Atom Effect on the Photochemical Release of Benzylamine from Caged Amines"

Hai Dang Nguyen and Manabu Abe*
Chem. Lett. **2024**, 53, 1-4.

3. Thesis supplements

(1) "Crucial Roles of Leaving Group and Open-Shell Cation in Photoreaction of (Coumarin-4-yl)methyl Derivatives"

Hai Dang Nguyen and Manabu Abe*
J. Am. Chem. Soc. **2024**, 146, 10993-11001.

(2) “Sulfur Atom Effect on the Photochemical Release of Benzylamine from Caged Amines”

Hai Dang Nguyen and Manabu Abe*

Chem. Lett. **2024**, 53, 1-4.

(3) “Development of a Two-Photon-Responsive Chromophore, 2-(*p*-Aminophenyl)-5,6-dimethoxy-1-(hydroxyinden-3-yl)methyl Derivatives, as a Photoremovable Protecting Group”

Tuan Phong Nguyen, Hai Dang Nguyen and Manabu Abe*

J. Org. Chem. **2024**, 89, 4691-4701.

Main Thesis

Contents

Chapter 1. General Introduction

- 1-1. Photolabile protecting group and caged compound
- 1-2. Types of photolabile protecting groups
- 1-3. 7-diethylamino(coumarin-4-yl)methyl (DEACM)
- 1-4. Purpose of this study

References

Chapter 2. Sulfur Atom Effect on the Uncaging Reaction of DEACM-based Caged Carboxylic Acid

- 2-1. Introduction
- 2-2. Synthetic routes
- 2-3. Photophysical properties
- 2-4. Photochemical properties
- 2-5. Mechanism
- 2-6. ^{18}O -labeling experiments
- 2-7. Transient Absorption Spectroscopy
- 2-8. Chalcogen atom effect on relative energetic stability of radical pair versus ion pair
- 2-9. References
- 2-10. Experimental Section
- 2-11. Spectra

Chapter 3. Sulfur Atom Effect on the Uncaging Reaction of DEACM-based Caged Amines

- 3-1. Introduction
- 3-2. Syntheses of **2a** and **2b**

- 3-3. Photophysical properties of **2a** and **2b** in DMSO
- 3-4. Photochemical properties of **2a** and **2b**
- 3-5. DFT calculation
- 3-6. References
- 3-7. Experimental Section
- 3-8. Spectra

1-1. Photolabile protecting group and caged compound

Photolabile protecting groups (PPGs)¹⁻¹² have been extensively utilized as effective tools for caging various compounds, including bioactive molecules,^{13,14} organic synthesis precursors,¹⁵ fluorophores,¹⁶⁻²⁰ and gasotransmitters such as H₂S, CO, and NO.²¹⁻²⁶ The concept behind this approach is that functions such as bioactivity and fluorescence in molecules can be temporarily quenched by attaching PPGs. These PPGs can then be selectively removed by exposure to light irradiation (uncaging), releasing the leaving groups, thereby restoring the original functions of the molecules. (Figure 1) In the field of biological chemistry, compounds subjected to this temporary masking are commonly referred as caged compounds.

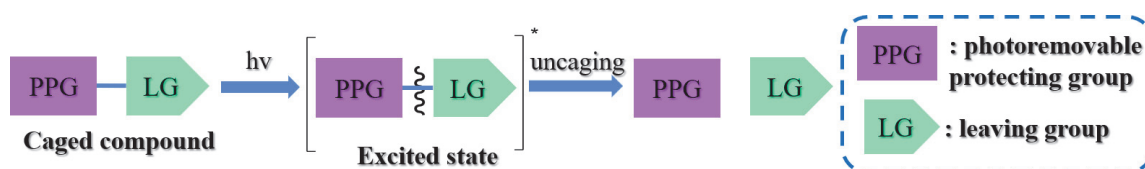


Figure 1. The concept of caged compounds

The distinctive feature of caged compounds is their reliance solely on light as a reagent, making this method mild and minimally invasive. This characteristic is particularly beneficial for selectively removing protecting groups using two colors,²⁷ especially in compounds containing multiple protecting groups.^{14,15} In addition to their practical uses, several new PPGs²⁸ have been designed recent years specifically for biological research. Since the use of the *o*-nitrobenzyl group²⁹ to cage adenosine cyclic 3',5'-phosphate (cAMP),³⁰ vast types of caged bioactive molecules have been developed for neurotransmitters,³¹⁻³⁴ calcium,³⁵⁻³⁹ and peptides,^{40,41} all of which have demonstrated utility in biological applications.⁴²

1-2. Types of photolabile protecting groups

There are two main types of PPGs, classified based on the mechanisms of release of leaving groups. The first group is the *o*-Nitrobenzyl type. The mechanism of photo-uncaging reactions of *o*-Nitrobenzyl-type PPGs is shown

in Figure 2. Under light irradiation, caged compounds on the ground state are excited to the excited state, from which a hydrogen abstraction of *o*-nitro group occurs to generate an aci-nitro intermediate. The aci-nitro intermediate undergoes a cyclization transformation to form a cyclic intermediate, followed by a ring-opening process to generate a hemiacetal intermediate, from which the leaving group is released. Popular representatives for this group are *o*-nitrobenzyl (*o*-NB),⁵ 6-nitropiperonylmethyl (NP),⁴³ 6-nitroveratryl (NV),⁴⁴ 4-amino-4'-1,1'-biphenyl (BP),⁴⁵ 2-(4-nitrophenyl)benzofuran (NPBF),⁴⁶ nitrodibenzofuran (NDBF)⁴⁶ and 6-(4-nitrophenyl)-7,8-dihydronaphthalen-2-amine (NPNA).⁴⁷

The other common group of PPGs is the Photo-S_N1 type. By irradiation, an ion pair is generated via the heterolytic bond dissociation of C-LG bond (Figure 2). The cation is trapped by a nucleophile to generate the product. The last two decades have witnessed a wide range of Photo-S_N1-type PPGs which have been developed such as coumarin-4-yl,⁴⁸ xanthene,⁴⁹ BODIPY,^{7,50-52} quinoline,⁵³ pyrene,⁵⁴ and 2-(*p*-aminophenyl)-1-hydroxyliden-3-ylmethyl (pAPHi).⁵⁵

o-nitrobenzyl type

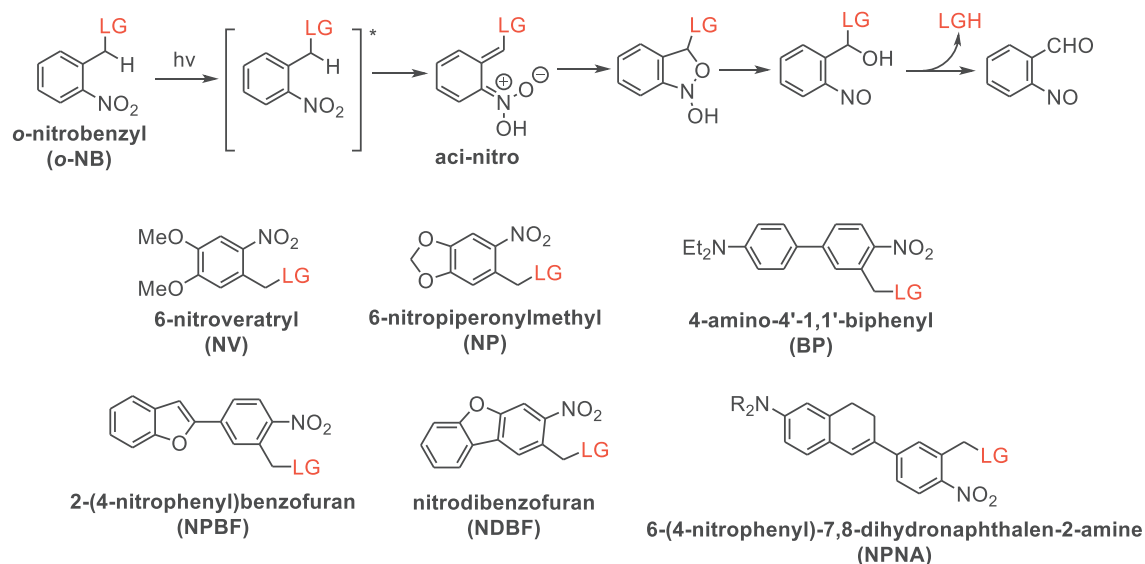


Photo-S_N1 type

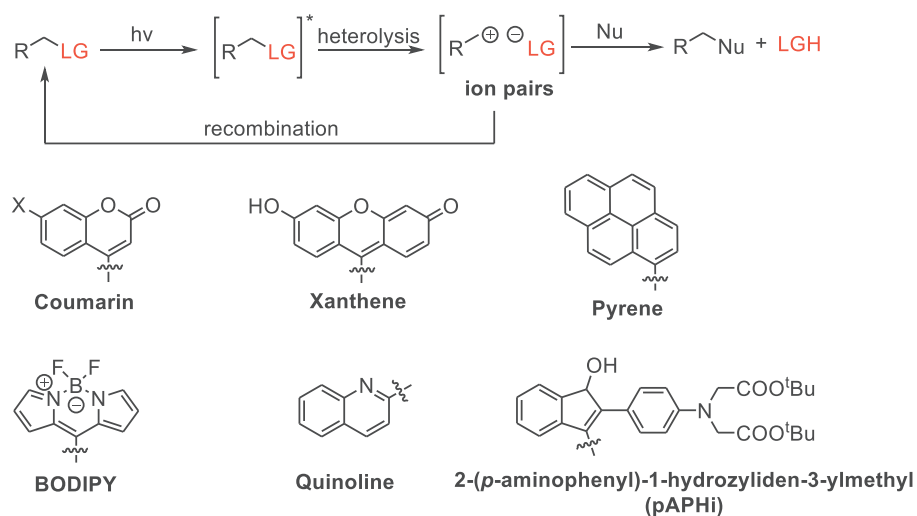


Figure 2. Types of photolabile protecting groups

1-3. 7-diethylamino(coumarin-4-yl)methyl (DEACM)

The 7-diethylamino(coumarin-4-yl)methyl (DEACM) is among the most studied PPGs because of its attractive features such as fast release rates

of leaving groups under light with wavelengths above 400 nm, large extinction coefficients and stabilities under dark condition. In 2018, Rivera-Fuentes and coworkers examined the photochemistry of a series of DEACM-based caged compounds, including different leaving groups.⁵⁶ It could be observed that the lower the pK_a of the leaving groups, the higher the photochemical quantum yield of caged compounds (Figure 3). In other words, the leaving ability of the leaving group has a profound influence on the photochemistry of DEACM-based caged compounds.

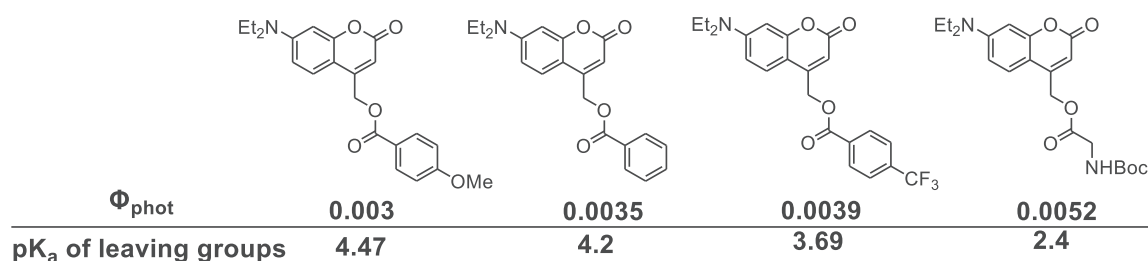
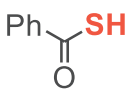
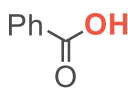
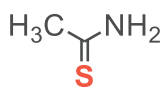
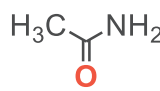


Figure 3. Relationship between pK_a and photochemical quantum yield (Φ_{phot})

1-4. Purpose of this study

It was reported that the pK_a (in DMSO) of thiobenzoic acid is approximately two times lower than that of benzoic acid (Table 1).⁵⁷ Similarly, the pK_a of thioacetamide is significantly lower than that of acetamide. Based on these data, we anticipated that leaving groups containing the sulfur atom would be better in leaving ability as compared to those containing oxygen atom. Therefore, the sulfur atom could have a large influence on the photo-uncaging reactions of DEACM-based caged compounds.

Table 1. pK_a value in DMSO

	 thiobenzoic acid	 benzoic acid	 thioacetamide	 acetamide
pK_a in DMSO	5.2	11.0	18.5	25.5

To clarify our hypothesis, in this study, we synthesized a series of DEACM-based caged carboxylic acids and caged amines and examined their photophysical and photochemical properties to investigate the sulfur atom effect on the photo-uncaging reactions of DEACM-based caged compounds.

References

- (1) Weinstain, R.; Slanina, T.; Kand, D.; Klán, P. Visible-to-NIR-Light Activated Release: From Small Molecules to Nanomaterials. *Chem Rev* **2020**, *120* (24), 13135–13272. <https://doi.org/10.1021/acs.chemrev.0c00663>.
- (2) Barltrop, J. A.; Schofield, P. Photosensitive Protecting Groups. *Tetrahedron Lett* **1962**, *3* (16), 697–699.
- (3) Barton, D. H. R.; Chow, Y. L.; Cox, A.; Kirby, G. W. Photosensitive Protection of Functional Groups. *Tetrahedron Lett* **1962**, *3* (23), 1055–1057. [https://doi.org/10.1016/S0040-4039\(00\)70957-9](https://doi.org/10.1016/S0040-4039(00)70957-9).
- (4) Sheehan, J. C.; Wilson, R. M. Photolysis of Desyl Compounds. *J. Am. Chem. Soc.* **1964**, *86* (23), 5277–5281.
- (5) Patchornik, A., Amit, B. Woodward, R. B. Photosensitive Protecting Groups. *J Am Chem Soc* **1970**, *92* (21), 6333–6335.
- (6) Barton, I. R.; Cox, A.; Kirby, G. W.; Barton, H. R.; Starratt, A. N.; Barltrop, J. A.; Schofield, P.; R Barton, D. H.; Chow, Y. L.; Havlik, A. J.; Kharasch, N. 654. *Photochemical Transformation. Part XIX? Some Photosensitive Protecting Groups*; 1956; Vol. 78.
- (7) Shrestha, P.; Kand, D.; Weinstain, R.; Winter, A. H. Meso-Methyl BODIPY Photocages: Mechanisms, Photochemical Properties, and Applications. *Journal of the American Chemical Society*. American Chemical Society August 16, 2023, pp 17497–17514. <https://doi.org/10.1021/jacs.3c01682>.
- (8) Kand, D.; Liu, P.; Navarro, M. X.; Fischer, L. J.; Rousso-Noori, L.; Friedmann-Morvinski, D.; Winter, A. H.; Miller, E. W.; Weinstain, R. Water-Soluble BODIPY Photocages with Tunable Cellular Localization. *J Am Chem Soc* **2020**, *142* (11), 4970–4974. <https://doi.org/10.1021/jacs.9b13219>.

- (9) Klán, P.; Šolomek, T.; Bochet, C. G.; Blanc, A.; Givens, R.; Rubina, M.; Popik, V.; Kostikov, A.; Wirz, J. Photoremovable Protecting Groups in Chemistry and Biology: Reaction Mechanisms and Efficacy. *Chemical Reviews*. January 9, 2013, pp 119–191. <https://doi.org/10.1021/cr300177k>.
- (10) Brieke, C.; Rohrbach, F.; Gottschalk, A.; Mayer, G.; Heckel, A. Light-Controlled Tools. *Angewandte Chemie - International Edition*. August 20, 2012, pp 8446–8476. <https://doi.org/10.1002/anie.201202134>.
- (11) Abe, M.; Chitose, Y.; Jakkampudi, S.; Thuy, P. T. T.; Lin, Q.; Van, B. T.; Yamada, A.; Oyama, R.; Sasaki, M.; Katan, C. Design and Synthesis of Two-Photon Responsive Chromophores for Near-Infrared Light-Induced Uncaging Reactions. *Synthesis (Stuttg)* **2017**, 49 (5), 3337–3346.
- (12) Bochet, C. G. Photolabile Protecting Groups and Linkers. *J Chem Soc Perkin 1* **2002**, 2 (2), 125–142. <https://doi.org/10.1039/b009522m>.
- (13) Ellis-Davies, G. C. R. Caged Compounds: Photorelease Technology for Control of Cellular Chemistry and Physiology. *Nat Methods* **2014**, 4 (8), 619–628. <https://doi.org/10.1038/nmeth1072.Caged>.
- (14) Sansalone, L.; Zhao, J.; Nguyen, L. T. B.; Gupta, S.; Benson, D. L.; Abe, M.; Ellis-Davies, G. C. R. Bidirectional Neuronal Actuation by Uncaging with Violet and Green Light. *Angewandte Chemie - International Edition* **2024**, 63 (13). <https://doi.org/10.1002/anie.202315726>.
- (15) Albini, A.; Germani, L.; Albini, A.; Fagnoni, M. *Handbook of Synthetic Photochemistry, Wiley 2010.Pdf*; 2010; Vol. null.
- (16) Abou Nakad, E.; Chaud, J.; Morville, C.; Bolze, F.; Specht, A. Monitoring of Uncaging Processes by Designing Photolytical Reactions. *Photochemical and Photobiological Sciences* **2020**, 19 (9), 1122–1133. <https://doi.org/10.1039/d0pp00169d>.

- (17) Sengupta, P.; Van Engelenburg, S. B.; Lippincott-Schwartz, J. Superresolution Imaging of Biological Systems Using Photoactivated Localization Microscopy. *Chem Rev* **2014**, *114* (6), 3189–3202. <https://doi.org/10.1021/cr400614m>.
- (18) Betzig, E. Single Molecules, Cells, and Super-Resolution Optics (Nobel Lecture). *Angewandte Chemie - International Edition* **2015**, *54* (28), 8034–8053. <https://doi.org/10.1002/anie.201501003>.
- (19) Hell, S. W. Nanoscopy with Focused Light (Nobel Lecture). *Angewandte Chemie - International Edition* **2015**, *54* (28), 8054–8066. <https://doi.org/10.1002/anie.201504181>.
- (20) Moerner, W. E. Single-Molecule Spectroscopy, Imaging, and Photocontrol: Foundations for Super-Resolution Microscopy (Nobel Lecture). *Angewandte Chemie - International Edition* **2015**, *54* (28), 8067–8093. <https://doi.org/10.1002/anie.201501949>.
- (21) Zhao, Y.; Bolton, S. G.; Pluth, M. D. Light-Activated COS/H₂S Donation from Photocaged Thiocarbamates. *Org Lett* **2017**, *19* (9), 2278–2281. <https://doi.org/10.1021/acs.orglett.7b00808>.
- (22) Sharma, A. K.; Nair, M.; Chauhan, P.; Gupta, K.; Saini, D. K.; Chakrapani, H. Visible-Light-Triggered Uncaging of Carbonyl Sulfide for Hydrogen Sulfide (H₂S) Release. *Org Lett* **2017**, *19* (18), 4822–4825. <https://doi.org/10.1021/acs.orglett.7b02259>.
- (23) Palao, E.; Slanina, T.; Muchová, L.; Šolomek, T.; Vitek, L.; Klán, P. Transition-Metal-Free CO-Releasing BODIPY Derivatives Activatable by Visible to NIR Light as Promising Bioactive Molecules. *J Am Chem Soc* **2016**, *138* (1), 126–133. <https://doi.org/10.1021/jacs.5b10800>.
- (24) Eroy-Reveles, A. A.; Leung, Y.; Beavers, C. M.; Olmstead, M. M.; Mascharak, P. K. Near-Infrared Light Activated Release of Nitric Oxide from Designed Photoactive Manganese Nitrosyls: Strategy, Design, and

Potential as NO Donors. *J Am Chem Soc* **2008**, *130* (13), 4447–4458.
<https://doi.org/10.1021/ja802581m>.

- (25) Okuno, H.; Ieda, N.; Hotta, Y.; Kawaguchi, M.; Kimura, K.; Nakagawa, H. A Yellowish-Green-Light-Controllable Nitric Oxide Donor Based on: N -Nitrosoaminophenol Applicable for Photocontrolled Vasodilation. *Org Biomol Chem* **2017**, *15* (13), 2791–2796.
<https://doi.org/10.1039/c7ob00245a>.
- (26) Antony, L. A. P.; Slanina, T.; Šebej, P.; Šolomek, T.; Klán, P. Fluorescein Analogue Xanthene-9-Carboxylic Acid: A Transition-Metal-Free CO Releasing Molecule Activated by Green Light. *Org Lett* **2013**, *15* (17), 4552–4555. <https://doi.org/10.1021/ol4021089>.
- (27) Bochet, C. G. Wavelength-Selective Cleavage of Photolabile Protecting Groups. *Tetrahedron Lett* **2000**, *41* (33), 6341–6346.
[https://doi.org/https://doi.org/10.1016/S0040-4039\(00\)01050-9](https://doi.org/https://doi.org/10.1016/S0040-4039(00)01050-9).
- (28) Nguyen, L. T. B.; Abe, M. Development of Photoremovable Protecting Groups Responsive to Near-Infrared Two-Photon Excitation and Their Application to Drug Delivery Research. *Bulletin of the Chemical Society of Japan*. Chemical Society of Japan September 1, 2023, pp 899–906.
<https://doi.org/10.1246/bcsj.20230140>.
- (29) Kaplan, J. H.; Forbush, B. I. I.; Hoffman, J. F. Rapid Photolytic Release of Adenosine 5'-Triphosphate from a Protected Analog: Utilization by the Sodium:Potassium Pump of Human Red Blood Cell Ghosts. *Biochemistry* **1978**, *17* (10), 1929–1935.
<https://doi.org/10.1021/bi00603a020>.
- (30) Engels, J.; Schlaeger, E. J. Synthesis, Structure, and Reactivity of Adenosine Cyclic 3',5'-Phosphate-Benzyl Triesters. *J Med Chem* **1977**, *20* (7), 907–911. <https://doi.org/10.1021/jm00217a008>.
- (31) Araya, R.; Andino-Pavlovsky, V.; Yuste, R.; Etchenique, R. Two-Photon Optical Interrogation of Individual Dendritic Spines with Caged

Dopamine. *ACS Chem Neurosci* **2013**, 4 (8), 1163–1167.
<https://doi.org/10.1021/cn4000692>.

- (32) Sitkowska, K.; Hoes, M. F.; Lerch, M. M.; Lameijer, L. N.; Van Der Meer, P.; Szymański, W.; Feringa, B. L. Red-Light-Sensitive BODIPY Photoprotecting Groups for Amines and Their Biological Application in Controlling Heart Rhythm. *Chemical Communications* **2020**, 56 (41), 5480–5483. <https://doi.org/10.1039/d0cc02178d>.
- (33) Wieboldt, R.; Gee, K. R.; Niu, L.; Ramesh, D.; Carpenter, B. K.; Hess, G. P. Photolabile Precursors of Glutamate: Synthesis, Photochemical Properties, and Activation of Glutamate Receptors on a Microsecond Time Scale. *Proc Natl Acad Sci U S A* **1994**, 91 (19), 8752–8756.
<https://doi.org/10.1073/pnas.91.19.8752>.
- (34) Boinapally, S.; Huang, B.; Abe, M.; Katan, C.; Noguchi, J.; Watanabe, S.; Kasai, H.; Xue, B.; Kobayashi, T. Caged Glutamates with π -Extended 1,2-Dihydronaphthalene Chromophore: Design, Synthesis, Two-Photon Absorption Property, and Photochemical Reactivity. *Journal of Organic Chemistry* **2014**, 79 (17), 7822–7830. <https://doi.org/10.1021/jo501425p>.
- (35) Ellis-Davies, G. C. R.; Kaplan, J. H. Nitrophenyl-EGTA, a Photolabile Chelator That Selectively Binds Ca^{2+} with High Affinity and Releases It Rapidly upon Photolysis. *Proc Natl Acad Sci U S A* **1994**, 91 (1), 187–191. <https://doi.org/10.1073/pnas.91.1.187>.
- (36) Adams, S. R.; Kao, J. P. Y.; Tsien, R. Y. Biologically Useful Chelators That Take Up Ca^{2+} upon Illumination. *J Am Chem Soc* **1988**, 110 (10), 3212–3220. <https://doi.org/10.1021/ja00202a042>.
- (37) Momotake, A.; Lindegger, N.; Niggli, E.; Barsotti, R. J.; Ellis-Davies, G. C. R. The Nitrodibenzofuran Chromophore: A New Caging Group for Ultra-Efficient Photolysis in Living Cells. *Nat Methods* **2006**, 3 (1), 35–40. <https://doi.org/10.1038/nmeth821>.

- (38) Pham, T. T. T.; Jakkampudi, S.; Furukawa, K.; Cheng, F. Y.; Lin, T. C.; Nakamura, Y.; Morioka, N.; Abe, M. P-Nitroterphenyl Units for near-Infrared Two-Photon Uncaging of Calcium Ions. *J Photochem Photobiol A Chem* **2021**, *409* (January), 113154. <https://doi.org/10.1016/j.jphotochem.2021.113154>.
- (39) Jakkampudi, S.; Abe, M.; Komori, N.; Takagi, R.; Furukawa, K.; Katan, C.; Sawada, W.; Takahashi, N.; Kasai, H. Design and Synthesis of a 4-Nitrobromobenzene Derivative Bearing an Ethylene Glycol Tetraacetic Acid Unit for a New Generation of Caged Calcium Compounds with Two-Photon Absorption Properties in the Near-IR Region and Their Application in Vivo. *ACS Omega* **2016**, *1* (2), 193–201. <https://doi.org/10.1021/acsomega.6b00119>.
- (40) Rothman, D. M.; Petersson, E. J.; Vázquez, M. E.; Brandt, G. S.; Dougherty, D. A.; Imperiali, B. Caged Phosphoproteins. *J Am Chem Soc* **2005**, *127* (3), 846–847. <https://doi.org/10.1021/ja043875c>.
- (41) Walker, J. W.; Gilbert, S. H.; Drummond, R. M.; Yamada, M.; Sreekumar, R.; Carraway, R. E.; Ikebe, M.; Fay, F. S. Signaling Pathways Underlying Eosinophil Cell Motility Revealed by Using Caged Peptides. *Proc Natl Acad Sci U S A* **1998**, *95* (4), 1568–1573. <https://doi.org/10.1073/pnas.95.4.1568>.
- (42) Kaplan, J. H.; Somlyo, A. P. Flash Photolysis of Caged Compounds: New Tools for Cellular Physiology. *Trends Neurosci* **1989**, *12* (2), 54–59. [https://doi.org/https://doi.org/10.1016/0166-2236\(89\)90136-7](https://doi.org/https://doi.org/10.1016/0166-2236(89)90136-7).
- (43) Berroy, P.; Viriot, M. L.; Carre, M. C. *Photolabile Group for 5'-OH Protection of Nucleosides: Synthesis and Photodeprotection Rate*; 2001.
- (44) Görner, H. Effects of 4,5-Dimethoxy Groups on the Time-Resolved Photoconversion of 2-Nitrobenzyl Alcohols and 2-Nitrobenzaldehyde into Nitroso Derivatives. *Photochemical & Photobiological Sciences* **2005**, *4* (10), 822–828. <https://doi.org/10.1039/b506393k>.

- (45) Jakkampudi, S.; Abe, M.; Komori, N.; Takagi, R.; Furukawa, K.; Katan, C.; Sawada, W.; Takahashi, N.; Kasai, H. Design and Synthesis of a 4-Nitrobromobenzene Derivative Bearing an Ethylene Glycol Tetraacetic Acid Unit for a New Generation of Caged Calcium Compounds with Two-Photon Absorption Properties in the Near-IR Region and Their Application in Vivo. *ACS Omega* **2016**, *1* (2), 193–201. <https://doi.org/10.1021/acsomega.6b00119>.
- (46) Komori, N.; Jakkampudi, S.; Motoishi, R.; Abe, M.; Kamada, K.; Furukawa, K.; Katan, C.; Sawada, W.; Takahashi, N.; Kasai, H.; Xue, B.; Kobayashi, T. Design and Synthesis of a New Chromophore, 2-(4-Nitrophenyl)Benzofuran, for Two-Photon Uncaging Using near-IR Light. *Chemical Communications* **2016**, *52* (2), 331–334. <https://doi.org/10.1039/c5cc07664a>.
- (47) Boinapally, S.; Huang, B.; Abe, M.; Katan, C.; Noguchi, J.; Watanabe, S.; Kasai, H.; Xue, B.; Kobayashi, T. Caged Glutamates with π -Extended 1,2-Dihydronaphthalene Chromophore: Design, Synthesis, Two-Photon Absorption Property, and Photochemical Reactivity. *Journal of Organic Chemistry* **2014**, *79* (17), 7822–7830. <https://doi.org/10.1021/jo501425p>.
- (48) Givens, R. S.; Matuszewski, B. Photochemistry of Phosphate Esters: An Efficient Method for the Generation of Electrophiles¹. *J Am Chem Soc* **1984**, *106* (22), 6860–6861. <https://doi.org/10.1021/ja00334a075>.
- (49) Šebej, P.; Wintner, J.; Müller, P.; Slanina, T.; Al Anshori, J.; Antony, L. A. P.; Klán, P.; Wirz, J. Fluorescein Analogues as Photoremovable Protecting Groups Absorbing at ~520 Nm. *Journal of Organic Chemistry* **2013**, *78* (5), 1833–1843. <https://doi.org/10.1021/jo301455n>.
- (50) Goswami, P. P.; Syed, A.; Beck, C. L.; Albright, T. R.; Mahoney, K. M.; Unash, R.; Smith, E. A.; Winter, A. H. BODIPY-Derived Photoremovable Protecting Groups Unmasked with Green Light. *J Am Chem Soc* **2015**, *137* (11), 3783–3786. <https://doi.org/10.1021/jacs.5b01297>.

- (51) Peterson, J. A.; Wijesooriya, C.; Gehrmann, E. J.; Mahoney, K. M.; Goswami, P. P.; Albright, T. R.; Syed, A.; Dutton, A. S.; Smith, E. A.; Winter, A. H. Family of BODIPY Photocages Cleaved by Single Photons of Visible/Near-Infrared Light. *J Am Chem Soc* **2018**, *140* (23), 7343–7346. <https://doi.org/10.1021/jacs.8b04040>.
- (52) Slanina, T.; Shrestha, P.; Palao, E.; Kand, D.; Peterson, J. A.; Dutton, A. S.; Rubinstein, N.; Weinstain, R.; Winter, A. H.; Klán, P. In Search of the Perfect Photocage: Structure-Reactivity Relationships in Meso-Methyl BODIPY Photoremovable Protecting Groups. *J Am Chem Soc* **2017**, *139* (42), 15168–15175. <https://doi.org/10.1021/jacs.7b08532>.
- (53) Fedoryak, O. D.; Dore, T. M. Brominated Hydroxyquinoline as a Photolabile Protecting Group with Sensitivity to Multiphoton Excitation. *Org Lett* **2002**, *4* (20), 3419–3422. <https://doi.org/10.1021/ol026524g>.
- (54) Fernandes, M. J. G.; Costa, S. P. G.; Gonçalves, M. S. T. Synthesis and Light Triggered Release of Catecholamines from Pyrenylmethyl Carbamate Cages. *New Journal of Chemistry* **2013**, *37* (8), 2369–2376. <https://doi.org/10.1039/c3nj00247k>.
- (55) Sasaki, M.; Tran Bao Nguyen, L.; Yabumoto, S.; Nakagawa, T.; Abe, M. Structural Transformation of the 2-(p-Aminophenyl)-1-Hydroxyinden-3-Ylmethyl Chromophore as a Photoremovable Protecting Group. *ChemPhotoChem* **2020**, *4* (12), 5392–5398. <https://doi.org/10.1002/cptc.202000149>.
- (56) Bassolino, G.; Nançoz, C.; Thiel, Z.; Bois, E.; Vauthey, E.; Rivera-Fuentes, P. Photolabile Coumarins with Improved Efficiency through Azetidiny Substitution. *Chem Sci* **2018**, *9* (2), 387–391. <https://doi.org/10.1039/c7sc03627b>.
- (57) Bordwell, F. G. Equilibrium Acidities in Dimethyl Sulfoxide Solution. *Acc Chem Res* **1988**, *21* (12), 456–463. <https://doi.org/10.1021/ar00156a004>.

Chapter 2

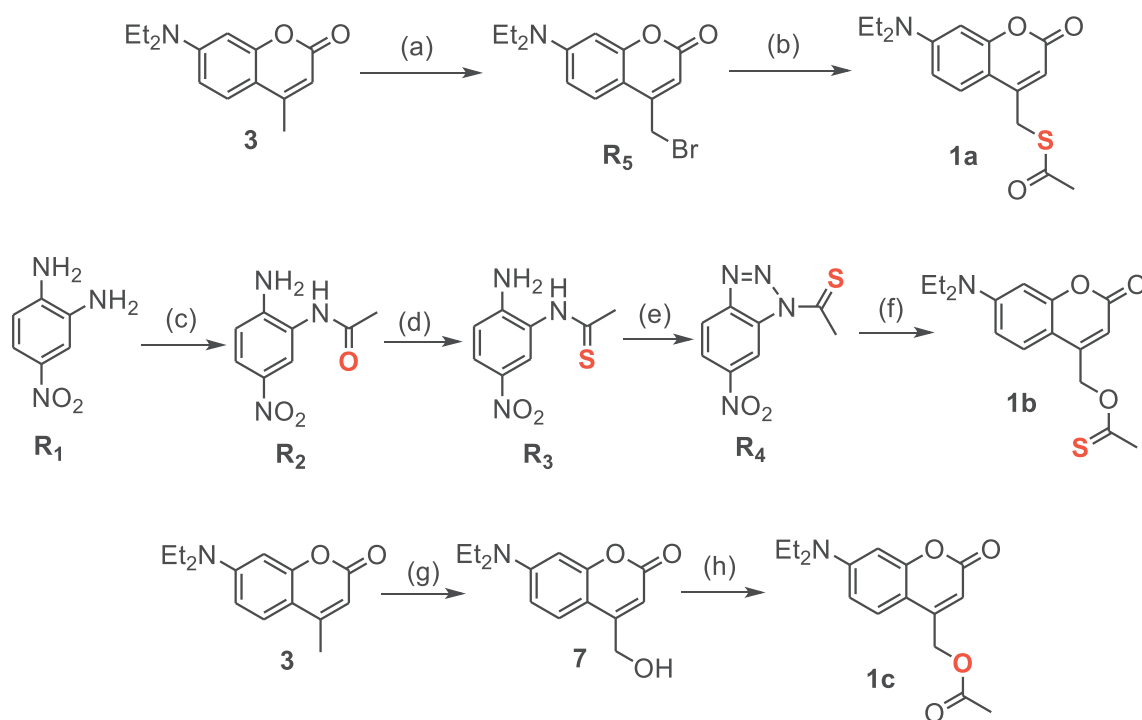
Sulfur Atom Effect on the Uncaging Reaction of DEACM-based Caged Carboxylic Acid

2-1. Introduction

In this chapter, thioester **1a**, thionoester **1b** and ester **1c** were synthesized. The photophysical properties of these three compounds were examined in DMSO. The photochemical properties of **1a**, **1b** and **1c** were studied by product analysis and laser flash photolysis (LFP) method.

2-2. Synthetic routes

Compound **1a**, **1b** and **1c** were synthesized by the following reported synthetic routes.



Scheme 1. Synthesis of **1a-c**; Reagents and conditions: (a) LiHMDS, NBS, THF $-78\text{ }^{\circ}\text{C}$ to $-30\text{ }^{\circ}\text{C}$, 77% yield. (b) AcSK, MeOH, RT, 79% yield. (c) CH_3COCl , Et_3N , THF, $-40\text{ }^{\circ}\text{C}$. (d) Lawesson's reagent, THF, $0\text{ }^{\circ}\text{C}$, 77% yield. (e) NaNO_2 , CH_3COOH , $0\text{ }^{\circ}\text{C}$, 56% yield. (f) **7**, imidazole, CH_2Cl_2 , RT, 50% yield. (g) DMA-DMF, DMF, RT; NaIO_4 , THF/ H_2O , RT; NaBH_4 , THF, $0\text{ }^{\circ}\text{C}$, 55% yield. (h) Ac_2O , NaHCO_3 , THF, RT, 99% yield.

2-3. Photophysical properties

The photophysical properties of **1a-c** were observed in DMSO, summarized in Table 2. It can be seen that all three compounds have the absorption maxima (λ_{max}) around 384 nm with relatively high extinction coefficients ($\epsilon_{\text{max}} > 22000 \text{ M}^{-1}\text{cm}^{-1}$). On the other hand, **1a** and **1b** show the emission maxima (λ_{emi}) around 465 nm, while **1c** possess an emission maxima around 472 nm, which reveals a larger Stokes shift as compared to **1a** and **1b**. Interestingly, the fluorescence quantum yields (Φ_f) of **1a** and **1b** are significantly lower than that value of **1c**, which could originate from the lower photochemical quantum yield of **1c** in comparison with **1a** and **1b**.

Table 2. Summary of photophysical properties of **1a-c** in DMSO

	Absorption		Emission		
	λ_{max} (nm)	ϵ_{max} ($\text{M}^{-1}\text{cm}^{-1}$)	λ_{emi} (nm)	Φ_f	τ (ns)
1a	386	24017 ± 516	463	0.018	1.4
1b	384	22668 ± 343	465	0.025	1.4
1c	382	25654 ± 476	472	0.41	1.9

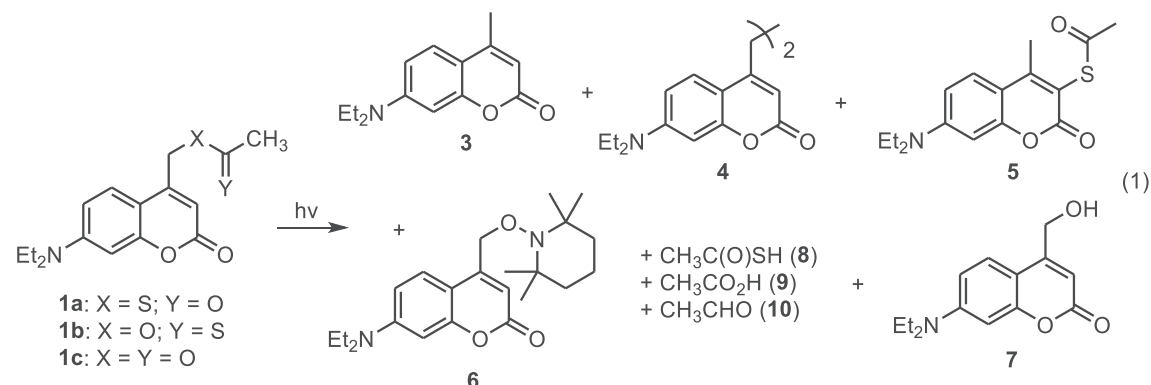
2-4. Photochemical properties

2-4-1. Photochemistry of **1a** ($\epsilon_{386} = 24,017 \pm 516 \text{ M}^{-1}\text{cm}^{-1}$)

Firstly, the photoreaction of compound **1a** (15 mM) was carried out for 2.5 hours in an Ar-saturated DMSO- d_6 solution (0.6 mL), using a 405 nm (± 20 nm) LED lamp as the light source (eq 1, Table 3, entry 1). Subsequently, the photoproducts and their chemical yields were analyzed by ^1H NMR spectroscopy (400 MHz). Thioacetic acid (**8**) and acetic acid (**9**) were obtained in yields of 33% and 20%, respectively. The formation of **9** could be explained by the conversion of **8** in DMSO, involving a single-electron transfer from **8** to DMSO.⁵⁸ Additionally, besides products derived from the leaving group, three DEACM-based products [**3** (16% yield), **4** (24% yield), **5** (14% yield)] and acetaldehyde (**10**) (8% yield) were observed. It is noteworthy that the yield of **4** dropped significantly to 14% and 5% when the photoreactions were conducted in air-saturated and O_2 -saturated DMSO, respectively (Table 3,

entries 2 and 3). The photochemical quantum yield of **1a** was determined as 0.028 in Ar-saturated DMSO and 0.026 in air-saturated (Table S3). Based on these findings, it is likely that **4** is formed through the dimerization of DEACM radical **A**, which originates from the photoinduced homolysis of the C–S bond and/or electron transfer within the ion pair (Scheme 2). To confirm the formation of **A**, the photoreaction of **1a** was performed in the presence of 45 mM TEMPO (Table 3, entry 5). DEACM-TEMPO (**6**) was obtained in 55% yield, and **4** was not detected, confirming the generation of radical **A**. Furthermore, when the photoreaction of **1a** was conducted in a DMSO/H₂O (3:2 v/v) solution (Table 1, entry 4), alcohol **7** was identified as a minor product in 6% yield, possibly through the reaction of **S-RC** with water (Scheme 2), while compound **4** was observed at a higher yield of 28%.

Table 3. Summary of Photochemistry of **1a-c**



		Products and Yields (%) ^a									
Entry	1	Conditions	3	4	5	6	7	8	9	10	1a
1	1a^f	Ar-saturated DMSO- <i>d</i> ₆	16	24	14	- ^b	- ^b	33	20	8	- ^b
2		Air-saturated DMSO- <i>d</i> ₆	19	14	4	- ^b	- ^c	48	17	12	- ^b
3		O ₂ -saturated DMSO- <i>d</i> ₆	17	5	3	- ^b	- ^c	39	22	16	- ^b
4		Ar-saturated DMSO/H ₂ O (3:2)	5 ^e	28 ^e	19 ^e	- ^b	6 ^e	- ^d	- ^d	- ^d	- ^b
5		Air-saturated DMSO- <i>d</i> ₆ with 3.0 equiv. TEMPO	- ^b	- ^b	20	55	- ^b	2	29	- ^b	- ^b
6	1b^g	Ar-saturated DMSO- <i>d</i> ₆	4	10	5	- ^b	- ^b	10	3	1	49
7		Ar-saturated DMSO/H ₂ O (3:2)	- ^b	2 ^e	6 ^e	- ^b	- ^b	- ^d	- ^d	- ^d	53 ^e
8	1c^h	Ar-saturated DMSO- <i>d</i> ₆	11	4	- ^b	- ^b	- ^c	- ^b	83	4	- ^b
9		Ar-saturated DMSO/H ₂ O (3:2)	7 ^e	11 ^e	- ^b	- ^b	39 ^e	- ^b	- ^d	- ^d	- ^b
10		Ar-saturated DMSO/H ₂ O (3:2) with 3.0 equiv. TEMPO	- ^b	- ^b	- ^b	46 ^e	20 ^e	- ^b	- ^d	- ^d	- ^b
11		Air-saturated DMSO- <i>d</i> ₆ with 3.0 equiv. TEMPO	- ^b	- ^b	- ^b	58	- ^b	- ^b	100	- ^b	- ^b

^aDetermined by ¹H NMR (400 MHz) if no additional descriptions were included. ^bNot formed. ^cTrace amount. ^dThese products could not be detected by a UV detector when HPLC was used. ^eDetermined by HPLC analysis. ^f $\Phi_{DMSO}^{Ar} = 0.028$.

^g $\Phi_{DMSO}^{Ar} = 0.68$. ^h $\Phi_{DMSO}^{Ar} = 0.0031$.

2-4-2. Photochemistry of **1b** ($\epsilon_{384} = 22,668 \pm 343 \text{ M}^{-1}\text{cm}^{-1}$)

The photoreaction of DEACM thionoester **1b** (15 mM) was conducted in the same manners to those used for **1a** (Table 1, entries 6 and 7). Interestingly, after 12 minutes of irradiation, thioester **1a** was observed as the predominant product (49%), accompanied by compounds **3** (4%), **4** (10%), and **5** (5%), revealing efficient recombination of the radical pair or ion pair.

The quantum yield of the photochemical decomposition of **1b** was found to be 0.68 in Ar-saturated DMSO and 0.60 in air-saturated DMSO (Table S3), demonstrating high efficiency in both C–S bond breaking and recombination processes. Computational analysis revealed that thioester **1a** is energetically more stable by 12.9 kcal mol⁻¹ than thionoester **1b** at the B3LYP/6-31G+(d) level of theory in DMSO, supporting the observed efficient isomerization process. It is noteworthy that this type of photoinduced isomerization of thionoesters to thioesters has not been studied. The presence of compounds **3-5** suggests the generation of radical **A** during the irradiation of **1b**. In addition, in the presence of TEMPO, ¹H NMR signals of **6** were witnessed along with those of **1a** (Figure S16), providing clear evidence for the existence of radical **A**. It is noteworthy that alcohol **7** was not detected by HPLC analysis, even in DMSO/H₂O (3:2) (Table 3, entry 7), indicating that the generated ion pair is present in small quantities.

2-4-3. Photochemistry of **1c** ($\epsilon_{382} = 25,654 \pm 476 \text{ M}^{-1}\text{cm}^{-1}$)

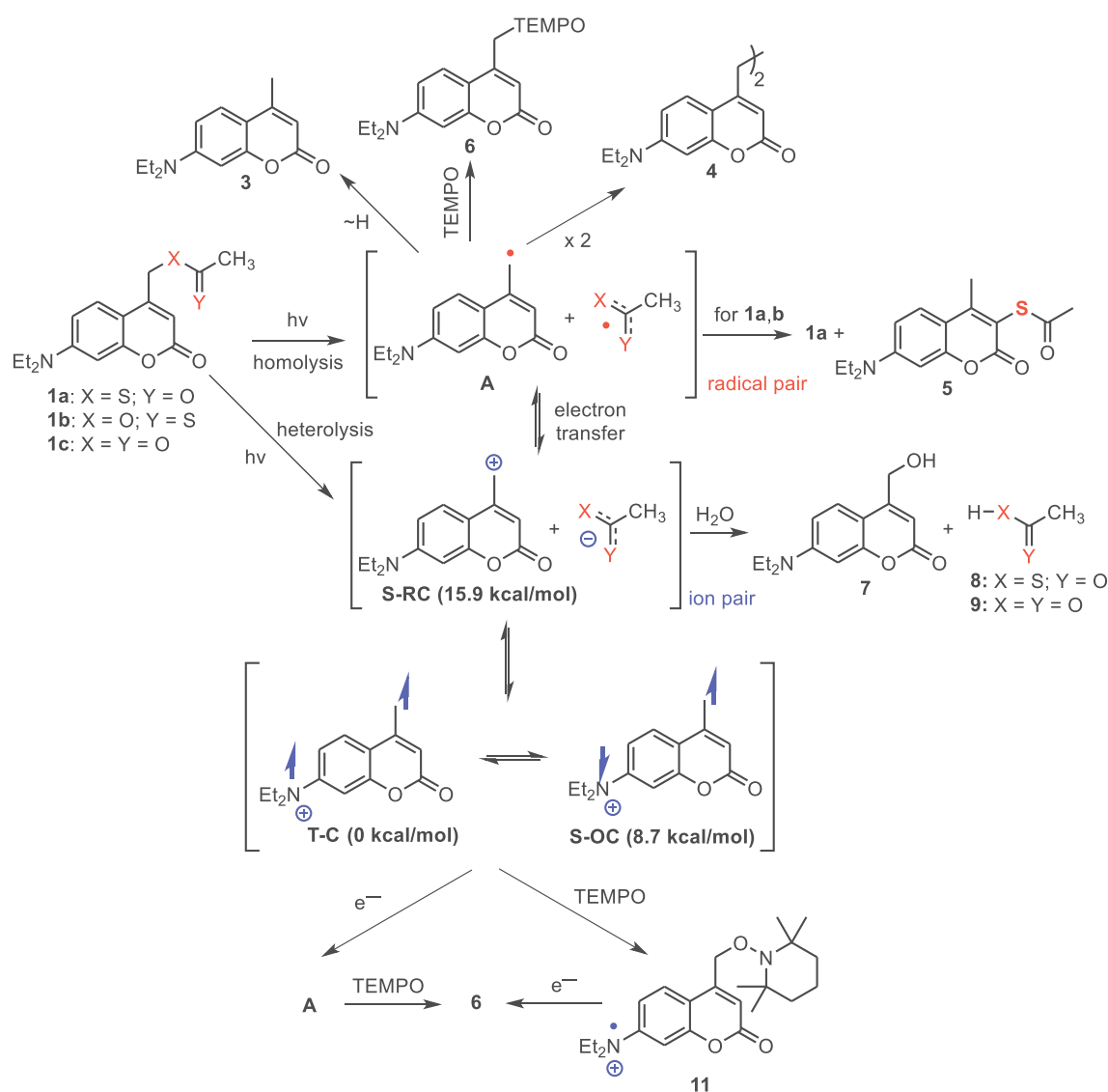
In Ar-saturated DMSO, the photoreaction of DEACM ester **1c** (15 mM) led to the release of acetic acid (**9**) with a high chemical yield of 83% (Table 3, entry 8). Other observed products included **3** (11%) and **4** (4%), both originating from radical **A**. The photochemical quantum yields of **1c** in Ar-saturated DMSO and air-saturated DMSO were determined to be 0.0031 and 0.0027, respectively.

Notably, TEMPO-adduct **6** was produced in a relatively high yield of 58% in the presence of TEMPO (45 mM), alongside the quantitative formation of **9** (Table 3, entry 11). The high chemical yield of **9** (100%) during the photolysis of **1c** (Table 3, entry 11) contrasted with the low chemical yields of **8** and **9** in the photoreaction of **1a** with TEMPO (Table 3, entry 5). This difference reveals a significant amount of the acetate anion in the reaction of **1c**. Additionally, the photoreaction of **1c** in a DMSO/H₂O (3:2) yielded **7** with the yield of 39%, which is significantly higher than the yields observed from **1a** and **1b** but lower than the 83% yield of acetic acid (**9**) (Table 3, entry 9). The formation of **7** provides strong evidence for the

presence of the DEACM cation (**S-RC**). Interestingly, in the presence of TEMPO, the photolysis of **1c** in DMSO/H₂O produced compounds **6** (46%) and **7** (20%) (Table 3, entry 10), which further supports the open-shell nature of the DEACM cation.

2-5. Mechanism

On the basis of detailed product analysis, a mechanism for the photochemical reaction of DEACM esters **1a–c** was proposed, as illustrated in Scheme 2. In the photoreactions of **1a** (X = S, Y = O) and **1b** (X = O, Y = S), the radical pair **A** containing CH₃C(O)S[•] play a crucial role. This is supported by the relatively high chemical yields of compounds **3–6**, derived from radical **A**, as compared to the low chemical yields of **8**, **9**, and **10** originating from the CH₃C(O)S[–] anion and **S-RC**. Conversely, the relatively high yields of **9** and **7** in the photoreaction of **1c** (X = Y = O) disclose that the key intermediate is the ion pair of **S-RC** with CH₃CO₂[–]. The formation of the radical-trapped product **6** during the photoreaction of **1c** in the presence of TEMPO may seem unconventional. However, it can be rationalized by the existences of **S-OC** and **T-C**, open-shell forms of the DEACM cation, which are in a thermal equilibrium with **S-RC** (Scheme 2).



Scheme 2. Proposed mechanism of Photoreaction of 7-diethylamino(coumarin-4-yl)methyl Esters

The open-shell cations **T-C** and **S-OC** were calculated to be energetically lower by 15.9 and 8.7 kcal/mol, respectively, in comparison with the closed-shell cation **S-RC**, which is in agreement with a published literature by Winter et al.⁵⁹ This calculation was performed at the B3LYP/6-31G+(d)

(SMD = DMSO) level of theory.⁶⁰ Therefore, **S-OC** and **T-C** can be trapped by TEMPO to produce cation radical **11**, followed by electron transfer to form compound **6**. On the other hand, an electron transfer from open-shell cations (**S-OC** and **T-C**) to generate radical **A**, which then undergoes a TEMPO trap to generate compound **6**. This emphasizes the crucial role of open-shell cations in photochemical reactions.⁶¹ The formation of the ion pair can be explained by photoinduced heterolytic bond breaking or single electron transfer within the radical pair released during homolysis. Another plausible pathway for the formation of **7** is the nucleophilic addition of H₂O to the open-shell cation **S-OC**,⁶² along with the reaction with **S-RC** (Scheme 2). The generation of acetaldehyde (**10**) can be rationalized by the reaction between singlet oxygen and diethylamino moiety.^{63,64}

2-6. ¹⁸O-Labeling Experiments

To gain further understanding of the uncaging mechanism, we performed the photoreaction of ¹⁸O-labeled **1c** (92% ¹⁸O) in air-saturated DMSO-*d*₆. The goal was to study the occurrence of ¹⁸O atom scrambling in **1c** (Figure 4). The ¹³C NMR signals of ¹⁸O–C (61.62 ppm) and ¹⁶O–C (61.64 ppm) in the methylene group were well-resolved at 151 MHz, allowing the detection of the scrambling reaction by ¹³C NMR method (Figure 4a). If recombination of **1c** from the radical pair and/or ion pair occurs, ¹⁸O atom scrambling in **1c** should be witnessed during the photolysis because of the relatively low quantum yield ($\Phi^{\text{air}} = 0.0027$, Table S3). It was reported that the low quantum yield of DEACM esters has been attributed to the recombination of ion pairs.^{65,66} Interestingly, the observed ¹⁸O atom scrambling was almost negligible, even though a significant amount of acetic acid **9** was detected at 12.3%, along with compounds **3** (<5%) and **4** (<5%) at 20% conversion of ¹⁸O-**1c** (Figure 4b). The negligible ¹⁸O scrambling disclosed that intermediates such as the ion pair generated after the bond-breaking reaction did not revert back to compound **1c**. In the case of **1b**, efficient isomerization of **1b** to **1a** was observed, revealing that the radical pair indeed took part in a recombination reaction. The rationale for the ¹⁸O-isotope labeling experiment

lies in the formation of the $[\text{S-RC}][\text{CH}_3\text{CO}_2^-]$ ion pair. This pair equilibrates with triplet cations **T-C**, which is the ground state of the DEACM cation. The recombination of **T-C** with acetate anions is a spin-forbidden process so that these intermediates could not revert to **1c**. Besides, the relatively low yield of **7** during the photolysis of **1c** is due to the triplet ground state of the DEACM cation.

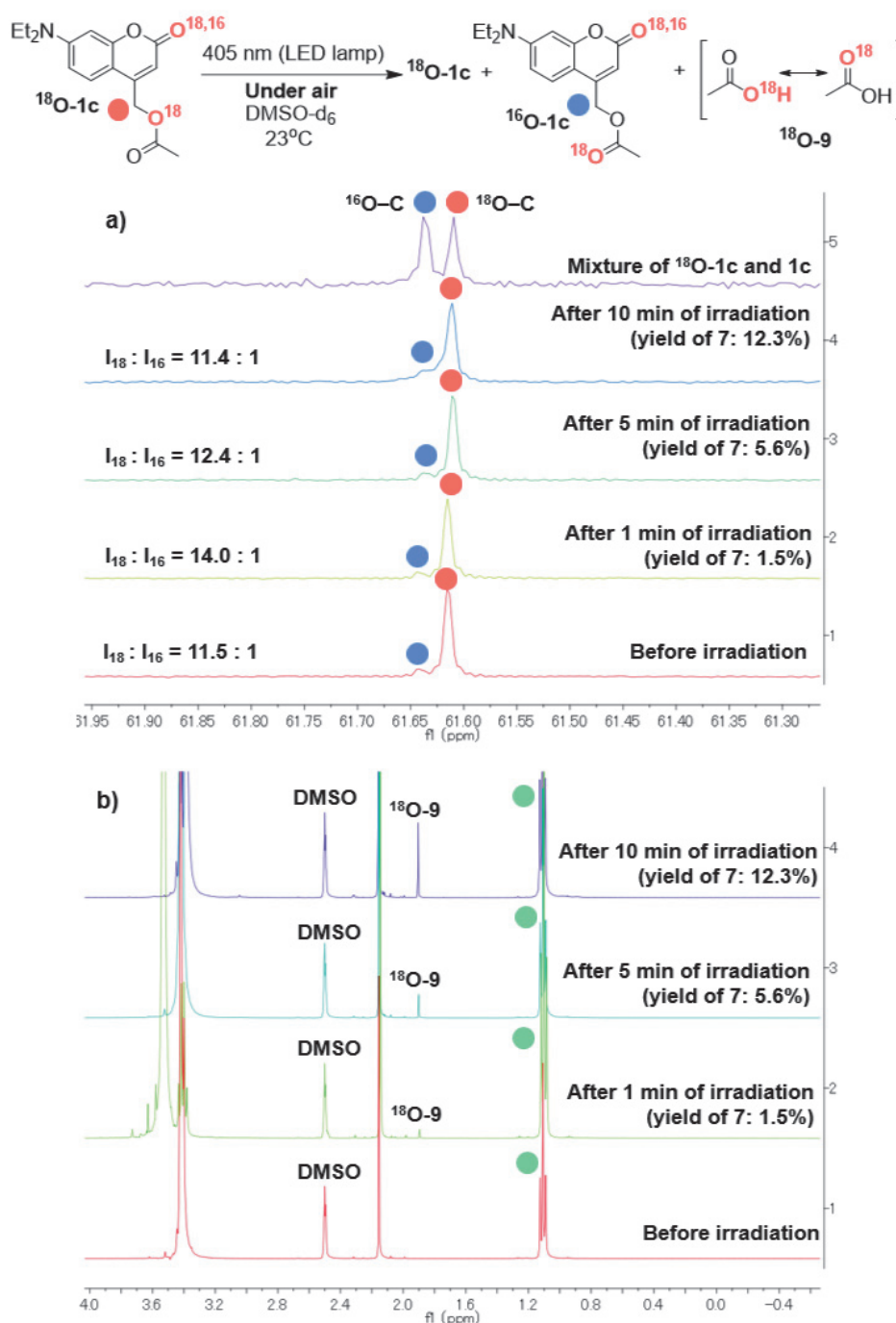


Figure 4. ^{18}O -labeling experiment in the photolysis of ^{18}O -1c; (a) ^{13}C NMR (151 MHz) spectra, $I_{18}:I_{16}$ is the ratio of intensity of ^{18}O -C and ^{16}O -C and (b) ^1H NMR (400 MHz) spectra measured in $\text{DMSO-}d_6$.

2-7. Transient Absorption Spectroscopy

The product analysis confirmed the formation of radical **A** and cationic species derived from the DEACM moiety. To directly observe the intermediates in the photolysis of **1a–c** and understand their reaction dynamics, the laser flash photolysis (LFP) experiments were carried out. The transient absorption (TA) spectra of **1a–c** (0.14 mM) and **7** (0.065 mM) were recorded on a submicrosecond time scale in air- and Ar-saturated DMSO at 293 K using a 355 nm laser (Nd, 15 mJ/pulse, 12 ns pulse width) (Figures 5 and 6). In Ar-saturated DMSO, three positive transient absorption bands at around 290 nm, 330 nm, and a broad signal over 500 nm were observed in the TA spectra of **1a–c**, while the 330 nm band disappeared in the TA spectrum of **7** (Figure 5d). The signal at around 630 nm was relatively sharp compared to the broad signals in **1a–c**. This observation suggested that the 330 nm absorption band corresponds to the transient species generated from the photoinduced bond cleavage. On the other hand, a negative signal between 350 and 420 nm was witnessed, which is attributed to the photobleaching of **1a–c** and **7**.

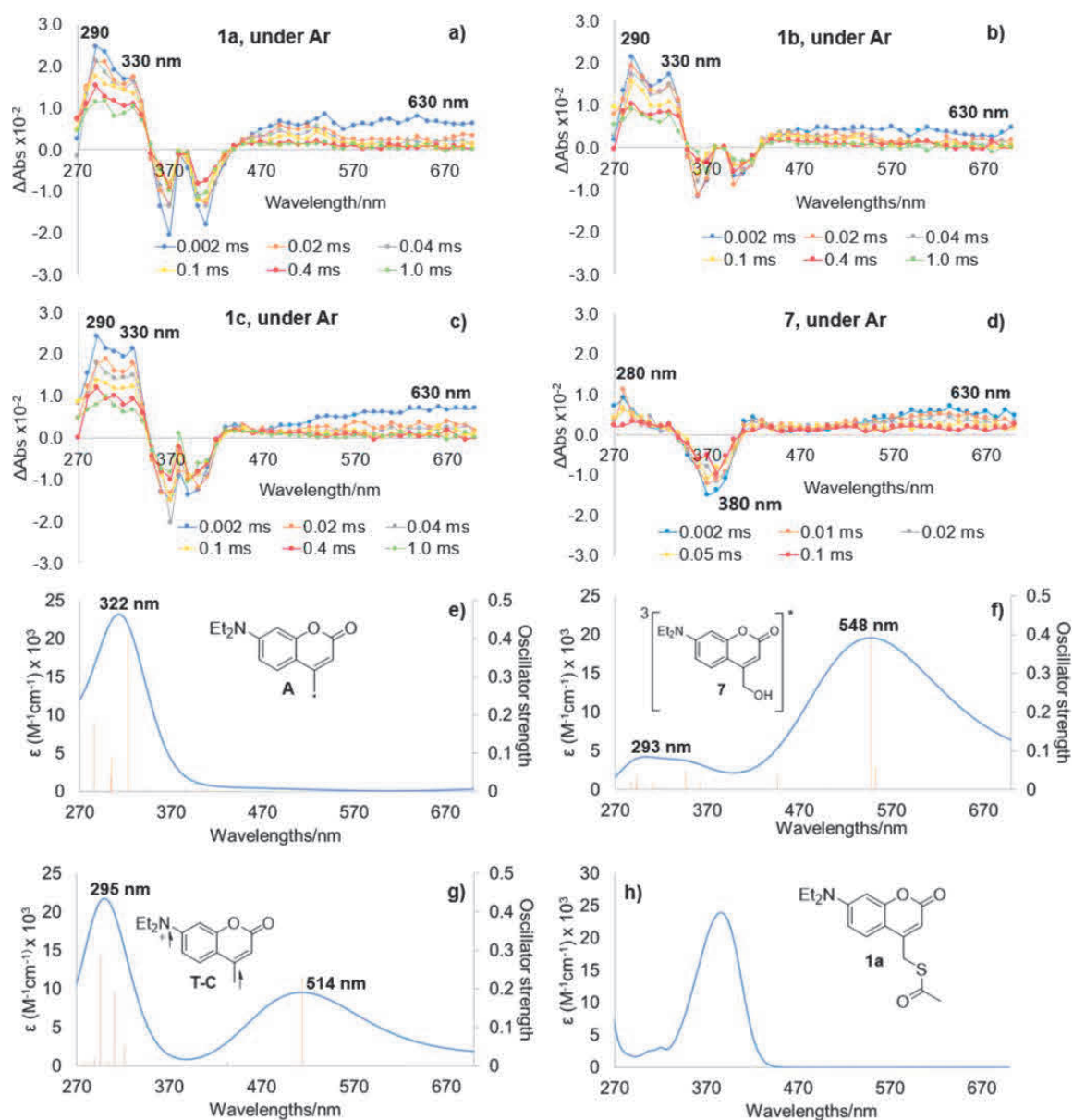


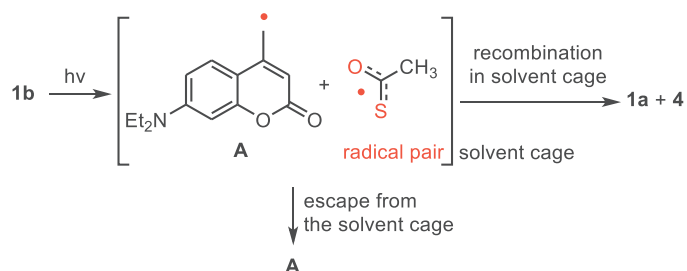
Figure 5. Transient absorption spectra of (a) **1a**, (b) **1b**, (c) **1c** and (d) **7** in an Ar-saturated DMSO solution at 293 K (laser: Nd:YAG, 355 nm, 15 mJ/pulse, 12 ns pulse width). Simulated UV-Vis spectra of (e) **A**, (f) triplet excited state of **7** and (g) **T-C** at the (R/U)B3LYP/6-31G+(d) (SMD = DMSO) level of theory. (h) Absorption spectrum of **1a** in DMSO.

The time profiles monitored at 330 nm in the transient spectra of **1a–c** showed a multicomponent decay. These signals were quenched in the presence of TEMPO (Figures S23–S25), indicating that the transient species was likely a radical. The simulated UV spectrum of radical **A**, calculated at the UB3LYP/6-31G+(d) (SMD = DMSO) level of theory, consistent with the transient signal observed during photolysis (Figure 5e). Based on these observations and the formation of compounds **4** and **6** (Table 3), the TA band at 330 nm was assigned to radical **A**.

The broad TA band around 630 nm observed in the laser flash photolysis (LFP) of **1a–c**, and **7** corresponded to the triplet-triplet (T-T) absorption of the triplet-excited state of the coumarin chromophores. This assignment was supported by the quenching of the bands in the presence of molecular oxygen. In addition, the simulated spectrum of the T-T absorption of coumarin chromophores matched the experimentally observed spectrum (Figures 5f, S29d). In the photolysis of **7**, the decay rate constant (k_{fall}) at 630 nm was $1.4 \times 10^{10} \text{ M}^{-1} \text{ s}^{-1}$, comparable with the rise rate constant (k_{rise}) at 380 nm, which was $1.3 \times 10^{10} \text{ M}^{-1} \text{ s}^{-1}$, indicating the $T_1\text{--}S_0$ transformation. It would be noted that the time profiles followed a second-order kinetic model due to the T-T annihilation originating from the high intensity of the pump laser utilized (15 mJ/pulse, 2.7×10^{16} photons/pulse). The concentration of $^3[7]^*$ was assumed to be similar to that of $^1[7]^*$, as calculated from the time profile monitored at 380 nm (Supporting Information). Besides the T-T absorption band, a weak broad signal around 500 nm was observed in the transient absorption spectra of **1a–c**.

As mentioned, the photochemical quantum yields (Φ) of **1a–c** varied significantly, ranging from $\Phi^{\text{Ar}} = 0.0031$ (for **1c**) to $\Phi^{\text{Ar}} = 0.68$ (for **1b**). However, the absorbances (~ 0.02) of the transient species at ~ 300 nm were quite similar immediately after the laser flash (355 nm, 15 mJ/pulse, 2.7×10^{16} photons/pulse, 12 ns pulse width). For instance, the absorbance at ~ 330 nm, corresponds to radical **A**, was 0.018, 0.019, and 0.021 in the LFP of **1a**, **1b**, and **1c**, respectively. The molar extinction coefficient for **A** at 322 nm was

estimated to be $22,028 \text{ M}^{-1} \text{ cm}^{-1}$. Therefore, the absorbance of **A** generated in the LFP of **1b** would be approximately 0.92 at $\Phi^{\text{Ar}} = 0.68$, which is significantly different from the observed value of 0.019. Since the absorption spectrum of **1b** ($\lambda_{\text{max}} = 384 \text{ nm}$, $\varepsilon = 22,668 \pm 343 \text{ M}^{-1} \text{ cm}^{-1}$) is accurately reproduced by the TD-DFT calculation ($\lambda_{\text{max}} = 378 \text{ nm}$, $\varepsilon = 21,684 \text{ M}^{-1} \text{ cm}^{-1}$), the discrepancy between the observed and predicted values is not due to overestimation of the computed spectrum but rather to the solvent-cage effect (Scheme 3).⁶⁵ In the submicrosecond TA experiments, the recombination process with zero-order kinetics in the solvent cage is undetectable, so only the radicals that escape from the solvent cage are detected. Based on the observed absorbance of 0.019, the escaped radical can be estimated to be $1.69 \times 10^{-7} \text{ mol}$, indicating a ratio of radicals in the solvent cage to escaped radicals of 248:1.



Scheme 3. Solvent Cage Effect in Radical Pair

In the laser flash photolysis (LFP) of **1c** (Figure 5c), the recombination process is negligible because ^{18}O -scrambling was not observed (Figure 4). When radical **A** is generated in the photolysis of **1c** ($\Phi^{\text{Ar}} = 0.0031$), the absorbance at 330 nm is estimated to be 0.0042, which is lower than the experimental value of 0.021. This significant difference can be rationalized by the overlap with triplet cation **T-C** and the triplet excited state of **1c** with radical **A**. The simulated UV spectrum of **T-C**, computed at the same level of theory, illustrates bands at approximately 290 nm with $\varepsilon \sim 22,000$ and at 512 nm with $\varepsilon \sim 10,000$ (Figure 5g). In the absence of TEMPO (Figure 6a), a broad signal over 470 nm was obtained. However, the signal at approximately 540 nm was quenched in the presence of TEMPO (Figure 6b). The band at

630 nm, corresponding to the triplet excited state of **1c**, remained. Notably, a new TA band at 430 nm emerged after 1 μ s ($k_{\text{rise}} = 6.2 \times 10^6 \text{ s}^{-1}$, Figure 6c) and decayed within 10 μ s ($k_{\text{fall}} = 7.6 \times 10^4 \text{ s}^{-1}$, Figure 6c) in the presence of TEMPO (0.42 mM) during the LFP of **1c** (0.14 mM). On the other hand, such transient bands were not detected in the TA analysis of **1a** and **1b** under similar conditions (Figures 6, S23, and S24 for **1a** and **1b**). From the rise signal, the bimolecular reaction rate was evaluated to be $1.5 \times 10^{10} \text{ M}^{-1} \text{ s}^{-1}$, roughly matching the diffusion rate constant in DMSO ($3.3 \times 10^9 \text{ M}^{-1} \text{ s}^{-1}$ at 25 $^{\circ}\text{C}$).

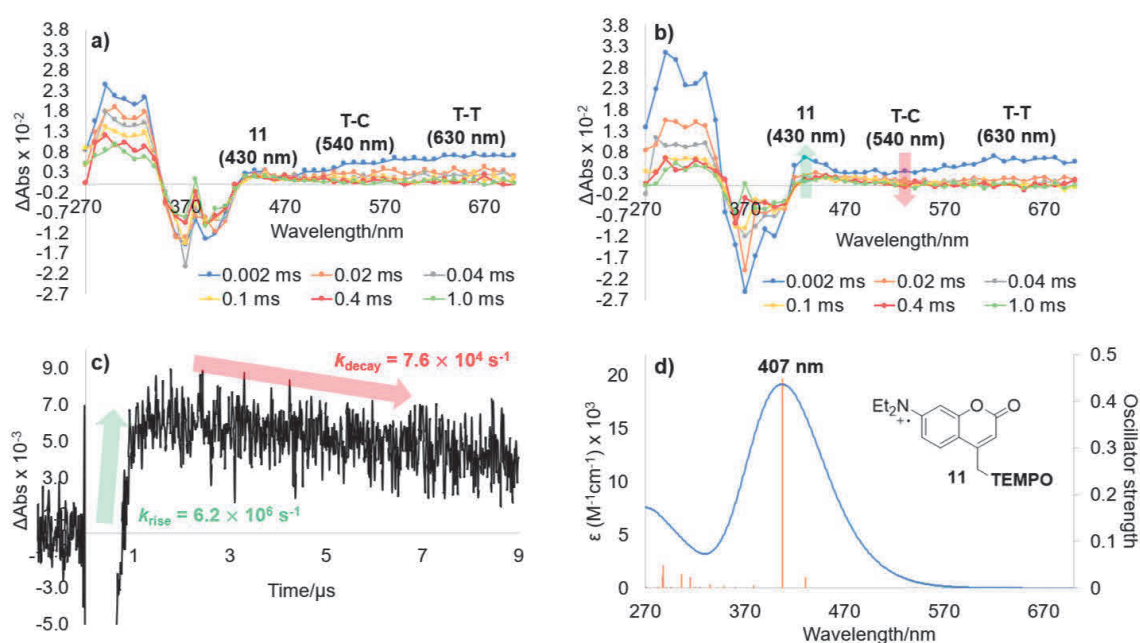


Figure 6. Transient absorption spectra of **1c** in Ar-saturated DMSO at 293 K (laser: Nd:YAG, 355 nm, 15 mJ/pulse, 12 ns pulse width), (a) without TEMPO, (b) TEMPO (0.42 mM). (c) Time profile monitored at 430 nm observed in the presence of 0.42 mM TEMPO in 10 μ s time scale (20 mJ/pulse). (d) Simulated UV spectrum of **11**.

The radical-radical coupling reaction of **T-C** with TEMPO was found to be a barrierless process at the UB3LYP/6-31G(d) level of theory (Figure S32). The absorption band at 430 nm was assigned to TEMPO-adduct **11**, a

plausible product originating from the trapping of TEMPO to **T-C** and/or **S-OC** (Scheme 2). This assignment was supported by the consistence between the computed absorption band and the observed absorption band (Figure 6d). The generation of intermediate **11** was also confirmed through product analysis. The negligible detection of **11** in the TA spectra during the photolysis of **1a** and **1b** revealed that the generation of ion pairs was a minor process in the photoreactions of **1a** and **1b**.

2-8. Chalcogen Atom Effect on Relative Energetic Stability of Radical Pair Versus Ion Pair

To further understand the experimental observations, the chalcogen atom effect on the total electronic energy of the radical pairs, DEACM radical (**A**) and $\text{CH}_3\text{C}(\text{O})\text{X}^\bullet$ ($\text{X} = \text{S}$ or O), and the ion pairs, DEACM cation and $\text{CH}_3\text{C}(\text{O})\text{X}^-$ ($\text{X} = \text{S}$ or O), were calculated at the (R/U)B3LYP/6-31G+(d) in DMSO using SMD method. For $\text{X} = \text{S}$, the radical pair was computed to be $0.7 \text{ kcal mol}^{-1}$ lower in energy than that of the corresponding ion pair (**T-C** and thioacetate anion $\text{CH}_3\text{C}(\text{O})\text{S}^-$). On the other hand, the ion pair of **T-C** and acetate anion ($\text{X} = \text{O}$, $\text{CH}_3\text{C}(\text{O})\text{O}^-$) was calculated to be lower in energy by $8.2 \text{ kcal mol}^{-1}$ than the radical pair of **A** and acetate radical in DMSO at the (R/U)B3LYP/6-31G+(d) (SMD = DMSO) level of theory. The electron transfer process from **A** to $\text{CH}_3\text{CO}_2^\bullet$ is thermodynamically favorable to form the ion pair as judged by the calculated reduction potential of acetate radical ($E^\circ = 1.22 \text{ V}$ vs SCE) and the calculated reduction potential of radical **A** ($E^\circ = 0.73 \text{ V}$ vs SCE) at the (R/U) B3LYP/6-31G+(d,p) (CPCM = DMSO) level of theory.⁶⁷

2-9. Calculated energy barriers

As mentioned, the photochemical quantum yield of **1b** ($\Phi^{\text{Ar}} = 0.68$) was much higher than those number of **1a** ($\Phi^{\text{Ar}} = 0.028$) and **1c** ($\Phi^{\text{Ar}} = 0.0034$). These observations matched well with our hypothesis in which the leaving ability of thioacetic acid is better than that of acetic acid because of the lower

pK_a of the thioacetic acid as compared to acetic acid. However, during our research studies, it was found that the photoreactions of **1a** and **1b** generated mainly the thioacetate radical, which is not related to the acidity of thioacetic acid. Therefore, the difference in photochemical quantum yields cannot be explained by the pK_a of the leaving groups. To rationalize the experimental results, the quantum chemical calculations were performed to estimate the energy barriers for the bond breaking process. C-S bond of **1a**, C-O bond of **1b** and C-O bond of **1c** were scanned from the triplet excited state of **1a**, **1b** and **1c** respectively at the UB3LYP/6-31G+(d) (SMD = DMSO) level of theory.

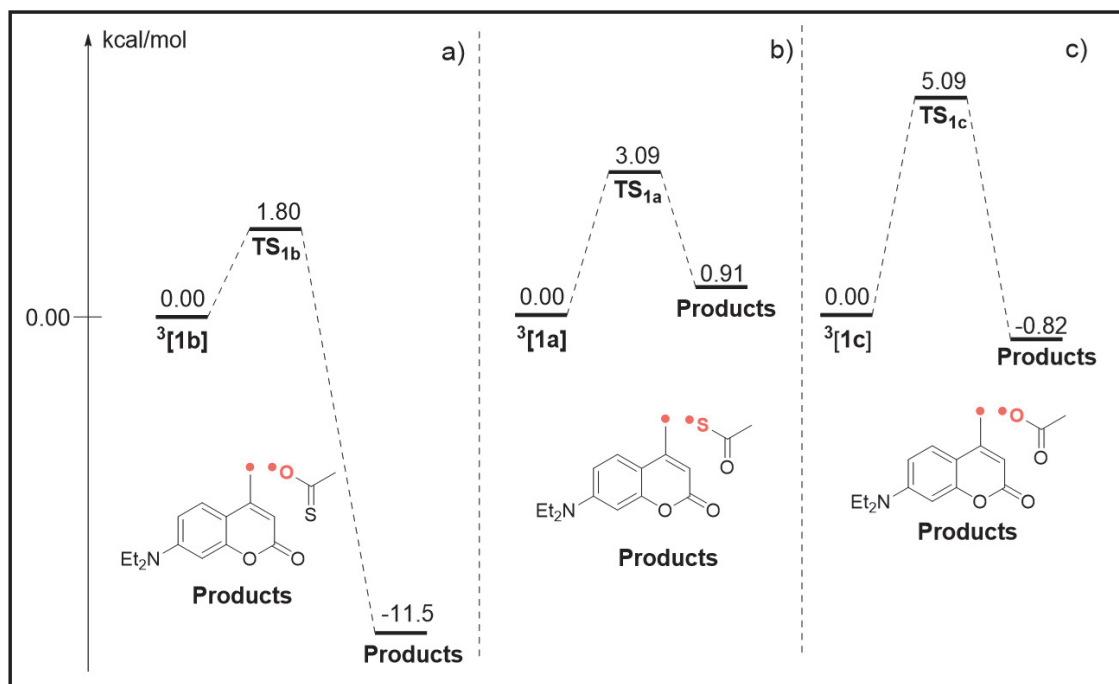


Figure 7. Computed relative energies of a) 3 [**1b**], TS_{1b}, products, b) 3 [**1a**], TS_{1a}, products and 3 [**1c**], TS_{1c}, products at UB3LYP/6-31G+(d) (SMD = DMSO) level of theory.

It was observed that the energy barrier in the case of **1b** (TS_{1b}) is the lowest, followed by the energy barriers in the case of **1a** (TS_{1a}) and **1c** (TS_{1c}),

revealing that the photoreaction of **1b** is the fastest. These observations are consistent with the trend of photochemical quantum yields. It would be noted that the energy of $^3[\mathbf{1b}]$ is significantly higher than that of $^3[\mathbf{1a}]$, which would originate from the less stable C=S bond of **1b** as compared to the C=O bond of **1a**.

2-10. References

- (58) Wang, R.; Xie, K. J.; Fu, Q.; Wu, M.; Pan, G. F.; Lou, D. W.; Liang, F. S. Transformation of Thioacids into Carboxylic Acids via a Visible-Light-Promoted Atomic Substitution Process. *Org Lett* **2022**, *24* (10), 2020–2024. <https://doi.org/10.1021/acs.orglett.2c00481>.
- (59) Albright, T. R.; Winter, A. H. A Fine Line Separates Carbocations from Diradical Ions in Donor-Unconjugated Cations. *J Am Chem Soc* **2015**, *137* (9), 3402–3410. <https://doi.org/10.1021/jacs.5b00707>.
- (60) Schade, B.; Hagen, V.; Schmidt, R.; Herbrich, R.; Krause, E.; Eckardt, T.; Bendig, J. Deactivation Behavior and Excited-State Properties of (Coumarin-4- Yl)Methyl Derivatives. 1. Photocleavage of (7-Methoxycoumarin-4-Yl)Methyl- Caged Acids with Fluorescence Enhancement. *Journal of Organic Chemistry* **1999**, *64* (25), 9109–9117. <https://doi.org/10.1021/jo9910233>.
- (61) Takano, M.; Antol, I.; Abe, M. Substituent Effects on the Electronic Ground State (Singlet versus Triplet) of Indenyl Cations: DFT and CASPT2 Studies. *European J Org Chem* **2024**. <https://doi.org/10.1002/ejoc.202301226>.
- (62) Wenthold, P. G.; Winter, A. H. Nucleophilic Addition to Singlet Diradicals: Homosymmetric Diradicals. *Journal of Organic Chemistry* **2018**, *83* (20), 12390–12396. <https://doi.org/10.1021/acs.joc.8b01413>.

- (63) Baciocchi, E.; Del Giacco, T.; Lapi, A. Oxygenation of Benzyldimethylamine by Singlet Oxygen. Products and Mechanism. *Org Lett* **2004**, *6* (25), 4791–4794. <https://doi.org/10.1021/ol047876l>.
- (64) Baciocchi, E.; Del Giacco, T.; Lanzaunga, O.; Lapi, A.; Raponi, D. The Singlet Oxygen Oxidation of Chlorpromazine and Some Phenothiazine Derivatives. Products and Reaction Mechanisms. *Journal of Organic Chemistry* **2007**, *72* (15), 5912–5915. <https://doi.org/10.1021/jo0706980>.
- (65) Schmidt, R.; Geissler, D.; Hagen, V.; Bendig, J. Kinetics Study of the Photocleavage of (Coumarin-4-Yl)Methyl Esters. *Journal of Physical Chemistry A* **2005**, *109* (23), 5000–5004. <https://doi.org/10.1021/jp050581k>.
- (66) Schmidt, R.; Geissler, D.; Hagen, V.; Bendig, J. Mechanism of Photocleavage of (Coumarin-4-Yl)Methyl Esters. *Journal of Physical Chemistry A* **2007**, *111* (26), 5768–5774. <https://doi.org/10.1021/jp071521c>.
- (67) Roth, H. G.; Romero, N. A.; Nicewicz, D. A. Experimental and Calculated Electrochemical Potentials of Common Organic Molecules for Applications to Single-Electron Redox Chemistry. *Synlett* **2016**, *27* (5), 714–723. <https://doi.org/10.1055/s-0035-1561297>.

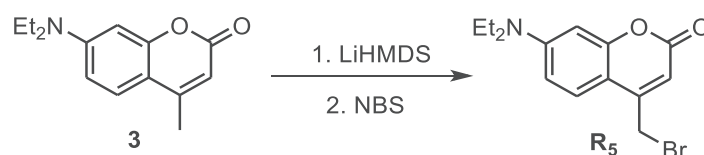
2-11. Experimental section

All commercially available chemical reagents were purchased from TCI, Wako, or Sigma-Aldrich and directly used without any further purification. NMR spectra were recorded on Bruker Ascend 400 (^1H NMR: 400 MHz, ^{13}C NMR: 100 Hz) and JEOL DELTA ECZL600G (^{13}C NMR: 150 Hz) spectrometers at 298 K. Coupling constants (J) are denoted in Hz and chemical shift (δ) in ppm. The abbreviations s, d, t, q and dd denote the resonance multiplicities singlet, doublet, triplet, quartet, and double of doublets, respectively. IR spectrum was recorded on a JASCO MCT-6000M.

Mass spectrometric data were observed with Thermo Fisher Scientific LTQ Orbitrap XL. UV-Vis spectra were recorded on a SHIMADZU UV-3600 Plus spectrometer. The spectra were observed at room temperature using a slit width of 1 nm with middle scan rate. The excitation source for sub-microsecond laser flash photolysis (LFP) was a tunable Nd:YAG laser at 355 nm. The monitoring system consisted of a 150 W Xenon arc lamp as a light source, a Unisoku MD200 monochromator detection, and a photomultiplier.

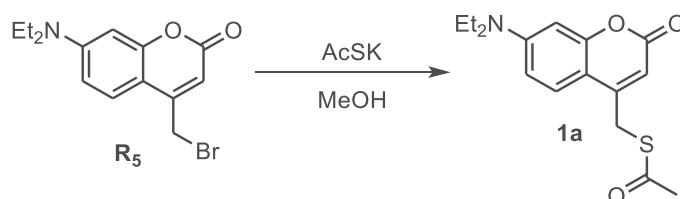
2-10-1. Synthesis of targeted compounds

Synthesis of **R**₅⁶⁸



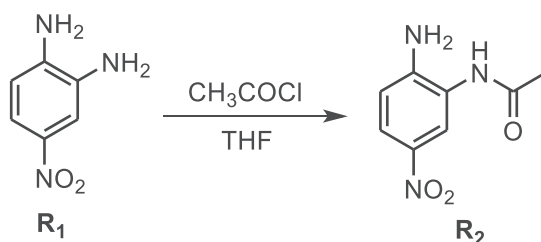
7-diethylamino-4-methylcoumarin (**3**) (2.0 g, 8.65 mmol, 1.0 equiv.) was dissolved in dry THF (150 mL) under N₂. The solution was cooled to –40 °C before adding LiHMDS (16.7 mL, 21.63 mmol, 2.5 equiv.). The solution was then warmed up to –30 °C, followed by cooling to –78 °C in a low-temperature bath. *N*-bromosuccinimide (1.7 g, 9.55 mmol, 1.1 equiv.) was added in one portion and the reaction mixture was stirred at –78 °C. After 4 hours at –78 °C, the reaction was neutralized by treating with HCl (0.1 M) at –78 °C before extracted with CH₂Cl₂. The collected organic phases were dried over Na₂SO₄ before being concentrated under reduced pressure to obtain the crude product, which was then purified by silica-gel column chromatography to afford compound **R**₅ as a yellow solid (2.1 g, 77%). ¹H NMR (400 MHz, CDCl₃) δ 7.49 (d, *J* = 9.0 Hz, 1H), 6.63 (dd, *J* = 9.0, 2.6 Hz, 1H), 6.52 (d, *J* = 2.6 Hz, 1H), 6.14 (s, 1H), 4.40 (s, 2H), 3.42 (q, *J* = 7.1 Hz, 4H), 1.22 (t, *J* = 7.1 Hz, 6H).

Synthesis of **1a**



R₅ (101.5 mg, 0.33 mmol, 1.0 equiv.) and potassium acetate (45.2 mg, 0.40 mmol, 1.2 equiv.) were dissolved in MeOH (1.0 mL). The solution was stirred under N₂ atmosphere at room temperature for 30 min before concentrated in vacuo. The crude was dissolved in CHCl₃ and then washed with water. The organic layer was dried with Na₂SO₄, concentrated under reduced pressure to obtain the crude product, which was then purified gel permeation chromatography to afford compound **1a** as a yellow solid (77.1 mg, 79%). Mp 95 °C. ¹H NMR (400 MHz, CDCl₃) δ 7.34 (d, *J* = 9.0 Hz, 1H), 6.58 (dd, *J* = 9.0, 2.6 Hz, 1H), 6.50 (d, *J* = 2.6 Hz, 1H), 6.10 (s, 1H), 4.13 (d, *J* = 0.5 Hz, 2H), 3.41 (q, *J* = 7.1 Hz, 4H), 2.39 (s, 3H), 1.21 (t, *J* = 7.1 Hz, 6H). ¹³C{¹H} NMR (101 MHz, CDCl₃) δ 193.7, 161.7, 156.4, 151.0, 150.7, 125.0, 109.0, 108.6, 107.0, 97.8, 44.7, 30.2, 29.0, 12.4. HRMS (ESI⁺) *m/z*: [M + H]⁺ calcd for C₁₆H₂₀NO₃S⁺ 306.11584, found 306.11575. IR (film, cm⁻¹): 2973, 1715, 1618, 1601, 1527, 1415, 1357, 1273, 1138.

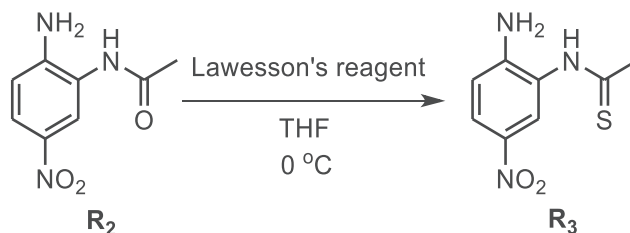
Synthesis of N-(2-amino-5-nitrophenyl)acetamide (**R₂**)⁶⁹



To a solution of **R₂** (2.0 g, 13.2 mmol, 1.0 equiv.) under N₂ atmosphere in dry THF at −40 °C was added Et₃N (2.8 mL, 19.8 mmol, 1.5 equiv.). Acetyl chloride (0.95 mL, 13.2 mmol, 1.0 equiv.) was then added dropwise into the solution. After stirred at −40 °C for 3 hours, the reaction mixture was warmed to room temperature and stirred for 15.5 hours. The precipitate was filtered off and the filtrate was concentrated under reduced pressure to afford compound **R₂** as a yellow solid (3.0 g, quant.), which was used directly to the next step

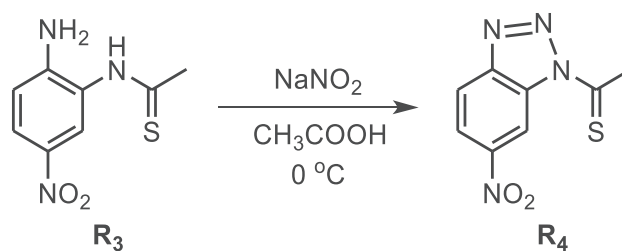
without further purification. ^1H NMR (400 MHz, CD_3CN) δ 8.24 (s, 1H), 8.18 (d, J = 2.6 Hz, 1H), 7.88 (dd, J = 9.0, 2.6 Hz, 1H), 6.78 (d, J = 9.0 Hz, 1H), 5.39 (s, 2H), 2.13 (s, 3H).

Synthesis of N-(2-amino-5-nitrophenyl)ethanethioamide (**R**₃)⁷⁰



The suspension of compound **R**₂ and Lawesson's reagent in dry THF was stirred under N_2 at 0 °C. After 14 hours, the reaction mixture was concentrated under reduced pressure to afford the crude product, which was purified by column chromatography to observe compound **R**₃ as a yellow solid.⁷⁰ ^1H NMR (400 MHz, MeOD) δ 8.03 (d, J = 2.6 Hz, 1H), 7.98 (dd, J = 9.1, 2.6 Hz, 1H), 6.81 (d, J = 9.1 Hz, 1H), 2.70 (s, 3H).

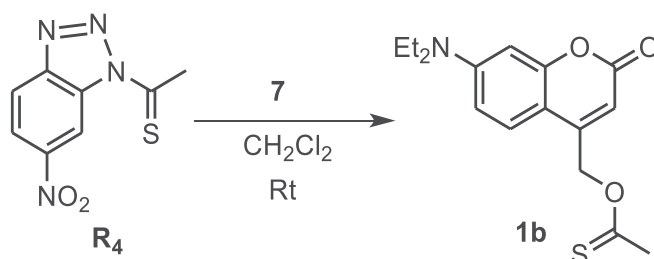
Synthesis of 1-(6-nitro-1H-benzo[d][1,2,3]triazol-1-yl)ethane-1-thione (**R**₄)⁷⁰



To a solution of compound **R**₃ (150.3 mg, 0.71 mmol, 1.0 equiv.) dissolved by gentle warming at 40 °C and then cooling to 0-5°C in 70% acetic acid (10.0 mL) was added NaNO_2 (80.0 mg, 1.07 mmol, 1.5 equiv.) in small portions with stirring. After 1 hour, ice-water was added, and the precipitate was filtered off, washed with water, and dried in vacuo to afford compound **R**₄ as an orange solid (87.5 mg, 56%). ^1H NMR (400 MHz, CDCl_3) δ 9.72 (d, J =

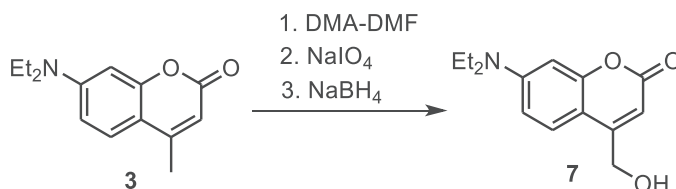
1.8 Hz, 1H), 8.44 (dd, $J = 8.9$, 1.8 Hz, 1H), 8.30 (d, $J = 8.9$ Hz, 1H), 3.46 (s, 3H).

Synthesis of 1b



A mixture of compound **R₄** (74.5 mg, 0.34 mmol, 1.0 equiv.), compound **7** (125.0 mg, 0.50 mmol, 1.5 equiv.) and imidazole (28.2 mg, 0.40 mmol, 1.2 equiv.) in dry CH₂Cl₂ (3.4 mL) was stirred under N₂ atmosphere at room temperature for 31 h. The solvent was removed in vacuo to observe the crude product, which was then purified by silica gel chromatography (Hexane/EtOAc) to afford compound **1b** as a yellow solid (52.0 mg, 50%). Mp 132 °C. ¹H NMR (400 MHz, CDCl₃) δ 7.28 (d, $J = 9.0$ Hz, 1H), 6.59 (dd, $J = 9.0$, 2.6 Hz, 1H), 6.53 (d, $J = 2.6$ Hz, 1H), 6.16 (t, $J = 1.1$ Hz, 1H), 5.56 (d, $J = 1.1$ Hz, 2H), 3.42 (q, $J = 7.1$ Hz, 4H), 2.69 (s, 3H), 1.21 (t, $J = 7.1$ Hz, 6H). ¹³C{¹H} NMR (101 MHz, CDCl₃) δ 218.8, 161.7, 156.3, 150.8, 148.4, 124.5, 108.7, 107.1, 106.0, 97.9, 68.6, 44.8, 34.1, 12.4. HRMS (ESI⁺) m/z : [M + H]⁺ calcd for C₁₆H₂₀NO₃S⁺ 306.11584, found 306.11588. IR (KBr, cm⁻¹): 2964, 1707, 1622, 1528, 1419, 1271, 1227, 1196, 1141, 1071.

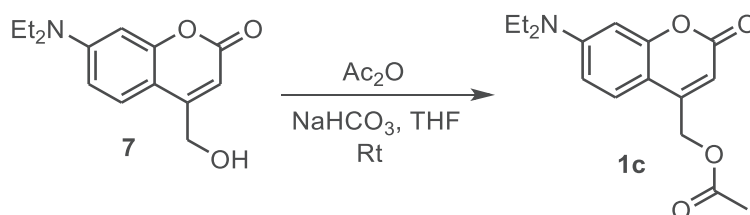
Synthesis of 7-(diethylamino)-4-(hydroxymethyl)-2H-chromen-2-one (**7**)⁷¹



To a solution of **3** (5.0 g, 0.022 mol, 1.0 equiv.) in dry DMF (25 mL), DMF-DMA (5.8 mL, 0.044 mol, 2.0 equiv.) was added under N₂. The reaction mixture was heated to reflux and stirred under N₂ atmosphere for 14 h. Conc.

NaHCO₃ solution and CH₂Cl₂ were then added. The organic layer was collected, and the aqueous layer was extracted with CH₂Cl₂ three times. The combined organic layers were dried with Na₂SO₄ before being concentrated under reduced pressure. The residue was dissolved in THF/H₂O (38.0 mL, 1:1), followed by the addition of NaIO₄ (14.0 g, 0.066 mol, 3.0 equiv.). After stirring for 2 h at room temperature, the precipitate was filtered off and then washed with EtOAc. Half of the solvent was evaporated in vacuo before conc. NaHCO₃ solution was added. The organic layer was isolated, and the aqueous layer was extracted with CH₂Cl₂. The collected organic layers were dried with Na₂SO₄ before being concentrated under reduced pressure. The residue was then dissolved in dry THF (35 mL), cooled to 0 °C and NaBH₄ (1.7 g, 0.044 mol, 2.0 equiv.) was added. The reaction mixture was then warmed up to room temperature and stirred under N₂ for 2 h before conc. NaHCO₃ solution was added. The organic layer was collected, and the aqueous layer was extracted with CH₂Cl₂. The combined organic layers were dried with Na₂SO₄ before being concentrated under reduced pressure to afford the crude product, which was then purified by silica gel chromatography (EtOAc/Hexane) to give compound **7** as a yellow solid (3.0 g, 55%). ¹H NMR (400 MHz, CDCl₃) δ 7.32 (d, *J* = 9.0, 1H), 6.56 (dd, *J* = 9.0, 2.6 Hz, 1H), 6.52 (d, *J* = 2.6 Hz, 1H), 6.25 (t, *J* = 1.2 Hz, 1H), 4.83 (s, 2H), 3.41 (q, *J* = 7.1 Hz, 4H), 2.59 (s, 1H), 1.20 (t, *J* = 7.1 Hz, 6H).

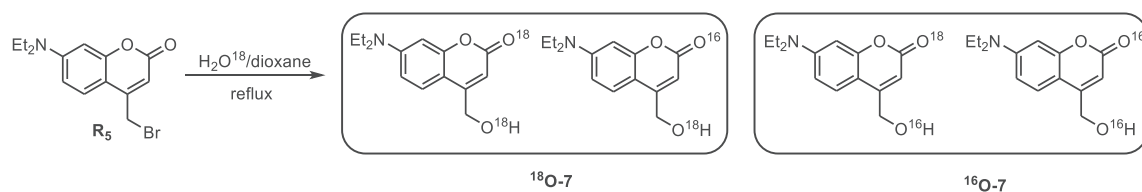
Synthesis of **1c**



A solution of **7** (50.8 mg, 0.2 mmol, 1.0 equiv.), NaHCO₃ (35.6 mg, 0.4 mmol, 2.0 equiv.) and acetic anhydride (0.1 mL, 1.0 mmol, 5.0 equiv.) in dry THF (1.2 mL) was stirred under N₂ at room temperature for 24 h. The reaction mixture was then filtered and the filtrate was concentrated under reduced

pressure. The residue was washed with H₂O, extracted with CH₂Cl₂. The organic phase was dried with Na₂SO₄ before concentrated under reduced pressure to give the crude product, which was purified by silica gel chromatography to afford compound **1c** as a yellow solid (57.3 mg, 99%). Mp 110 °C. ¹H NMR (400 MHz, CDCl₃) δ 7.28 (d, *J* = 9.0 Hz, 1H), 6.57 (dd, *J* = 9.0, 2.6 Hz, 1H), 6.51 (d, *J* = 2.6 Hz, 1H), 6.12 (t, *J* = 1.2 Hz, 1H), 5.21 (d, *J* = 1.2 Hz, 1H), 3.41 (q, *J* = 7.1 Hz, 4H), 2.18 (s, 3H), 1.20 (t, *J* = 7.1 Hz, 6H). ¹³C{¹H} NMR (101 MHz, CDCl₃) δ 170.2, 161.8, 156.3, 150.7, 149.34, 124.3, 108.6, 106.5, 106.0, 97.8, 61.3, 44.7, 20.7, 12.4. HRMS (ESI⁺) *m/z*: [M + H]⁺ calcd for C₁₆H₂₀NO₄⁺ 290.13868, found 290.13867. IR (film, cm⁻¹): 2976, 1745, 1715, 1623, 1604, 1528, 1422, 1227, 1076, 1143.

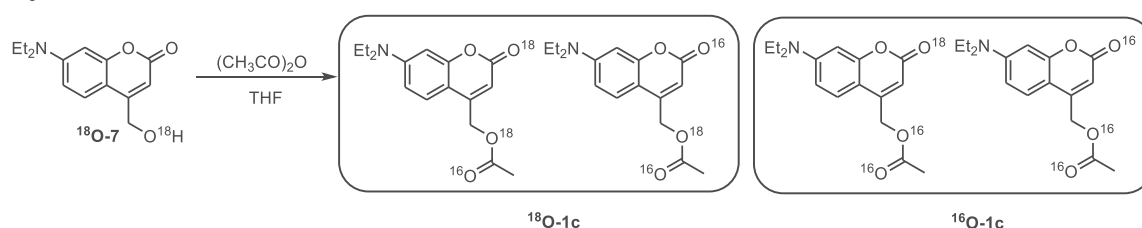
Synthesis of ¹⁸O-7



Compound **R₅** (250.5 mg, 0.81 mmol, 1.0 equiv.) was dissolved in H₂O¹⁸/Dioxane (2.5 mL, 2:3). The reaction mixture was heated to reflux and stirred for 40 h under N₂ before concentrated under reduced pressure. The residue was washed with water and extracted with EtOAc. The organic layer was concentrated in vacuo to give the crude product, which was then purified by silica gel chromatography to observe four isotopomers in which the two isotopomers in the box are denoted as ¹⁸O-7 (92% in the mixture, determined by ¹³C NMR) (147.0 mg). mp 142 °C. ¹H NMR (400 MHz, CDCl₃) δ 7.31 (d, *J* = 9.0 Hz 1H), 6.55 (dd, *J* = 9.0, 2.6 Hz, 1H), 6.47 (d, *J* = 2.6 Hz, 1H), 6.26 (s, 1H), 4.82 (d, *J* = 5.1 Hz, 2H), 3.39 (q, *J* = 7.1 Hz, 4H), 2.67 (t, *J* = 5.1 Hz, 1H), 1.19 (t, *J* = 7.1 Hz, 6H). ¹³C{¹H} NMR (101 MHz, CDCl₃) δ 162.73 (s), 162.70 (s), 156.1 (s), 154.9 (s), 150.529 (s), 124.4 (s), 108.6 (s), 106.3 (s), 105.4 (s), 97.8 (s), 60.9 (s), 44.7 (s), 12.4 (s). HRMS (ESI⁺) *m/z*: [M + Na]⁺ calcd for C₁₄H₁₇N¹⁸O₂ONa⁺ 274.11856, found 274.11841, [M + Na]⁺ calcd for C₁₄H₁₇N¹⁸OO₂Na⁺ 272.11431, found 272.11426, [M + Na]⁺ calcd for

$C_{14}H_{17}NO_3Na^+$ 270.11006, found 270.11002. **IR** (film, cm^{-1}): 3403, 2976, 1687, 1606, 1527, 1417, 1357, 1273, 1199, 1141, 1077.

Synthesis of ^{18}O -1c



A mixture of ^{18}O -7 (131.9 mg, 0.53 mmol, 1.0 equiv.), $NaHCO_3$ (92.6 mg, 1.06 mmol, 2.0 equiv.) and $(CH_3CO)_2O$ (0.25 mL, 2.65 mmol, 5.0 equiv.) in dry THF was stirred at room temperature for 24 hours under N_2 atmosphere. The mixture was then filtered, and the filtrate was concentrated. The residue was washed with H_2O , extracted with CH_2Cl_2 . The organic phase was dried by Na_2SO_4 before concentrated under reduced pressure to observe the crude product, which was purified by silica-gel column chromatography (Hexane/EtOAc) to observe four isotopomers in which the two isotopomers in the box are denoted as ^{18}O -1c (92% in the mixture, determined by ^{13}C NMR) (142.2 mg). Mp 110 °C. 1H NMR (400 MHz, $CDCl_3$) δ 7.28 (d, J = 9.0 Hz, 1H), 6.57 (dd, J = 9.0, 2.6 Hz, 1H), 6.51 (d, J = 2.6 Hz, 1H), 6.13 (t, J = 1.2 Hz, 1H), 5.21 (d, J = 1.2 Hz, 2H), 3.41 (q, J = 7.1 Hz, 4H), 2.19 (s, 3H), 1.20 (t, J = 7.1 Hz, 6H). $^{13}C\{^1H\}$ NMR (101 MHz, $CDCl_3$) δ 170.2 (s), 161.83 (s), 161.80 (s), 156.3 (s), 150.7 (s), 149.3 (s), 124.3 (s), 108.6 (s), 106.5 (s), 106.0 (s), 97.9 (s), 61.3 (s), 44.7 (s), 20.7 (s), 12.4 (s). **HRMS** (ESI $^+$ m/z): $[M + Na]^+$ calcd for $C_{16}H_{19}N^{18}O_2O_2Na^+$ 316.12912, found 316.12915, $[M + Na]^+$ calcd for $C_{16}H_{19}N^{18}OO_3Na^+$ 314.12487, found 314.12503, $[M + Na]^+$ calcd for $C_{16}H_{19}NO_4Na^+$ 312.12063, found 312.12079. **IR** (film, cm^{-1}): 2976, 1748, 1694, 1606, 1529, 1420, 1222, 1143, 1066.

2-10-2. Photophysical properties of targeted compounds

Table S1. Summary of photophysical properties of **1a**, **1b** and **1c** in DMSO

	Absorption		Emission		
	λ_{max} (nm)	ϵ_{max} ($\text{M}^{-1}\text{cm}^{-1}$)	λ_{emi} (nm)	Φ_{f}	τ (ns)
1a	386	24017 ± 516	463	0.018	1.4
1b	384	22668 ± 343	465	0.025	1.4
1c	382	25654 ± 476	472	0.41	1.9
7	375	20476 ± 262	454	0.61	3.2

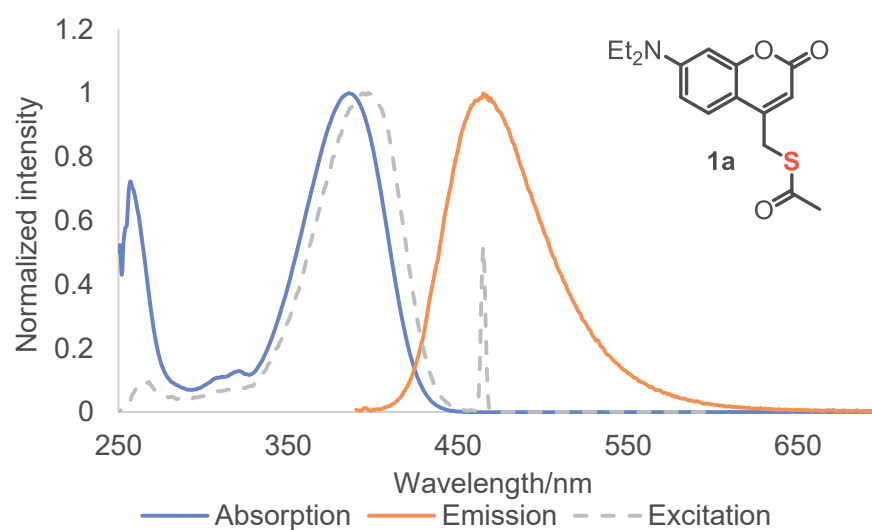


Figure S1. Absorption, emission and excitation spectra of **1a** in DMSO

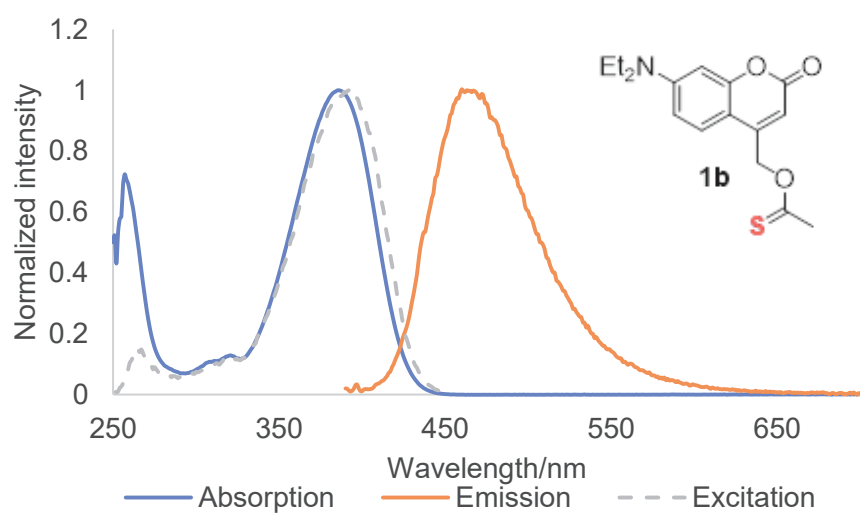


Figure S2. Absorption, emission and excitation spectra of **1b** in DMSO

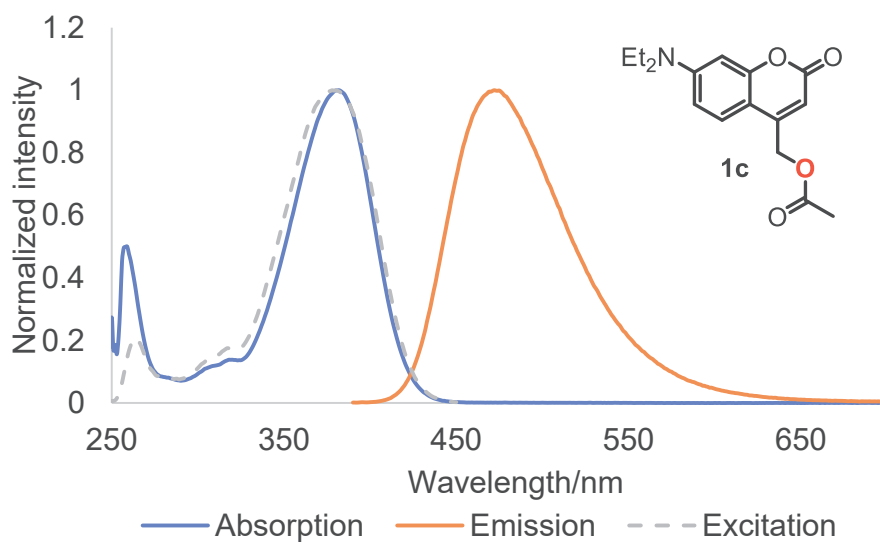


Figure S3. Absorption, emission and excitation spectra of **1c** in DMSO

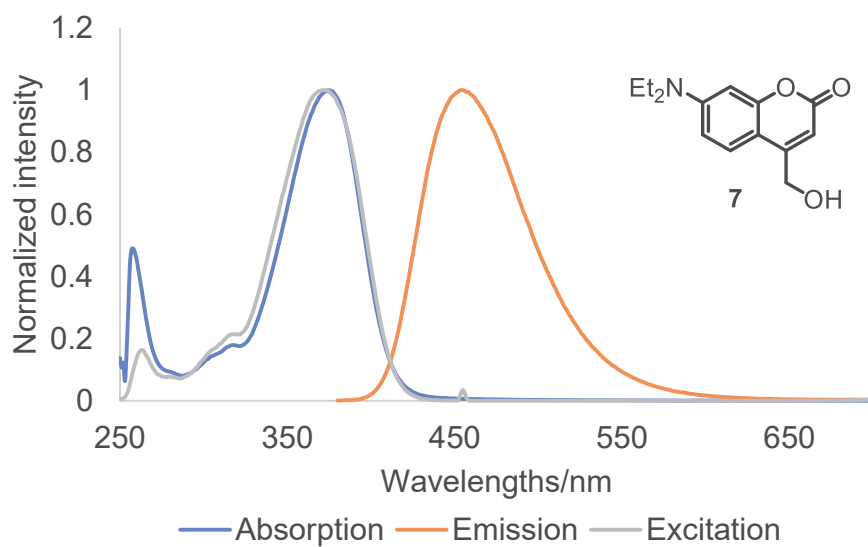


Figure S4. Absorption, emission and excitation spectra of **7** in DMSO

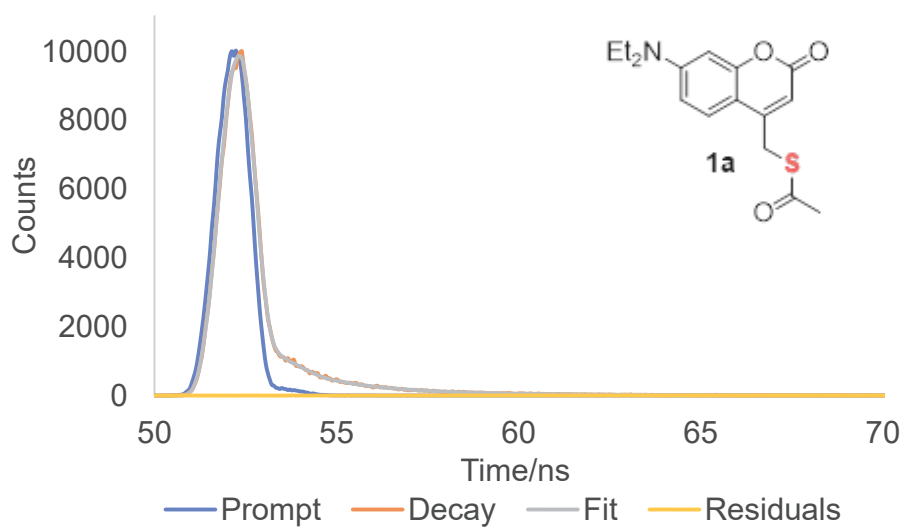


Figure S5. Time profile of the excited state **1a** in DMSO monitored at 463 nm (excited at 390 nm)

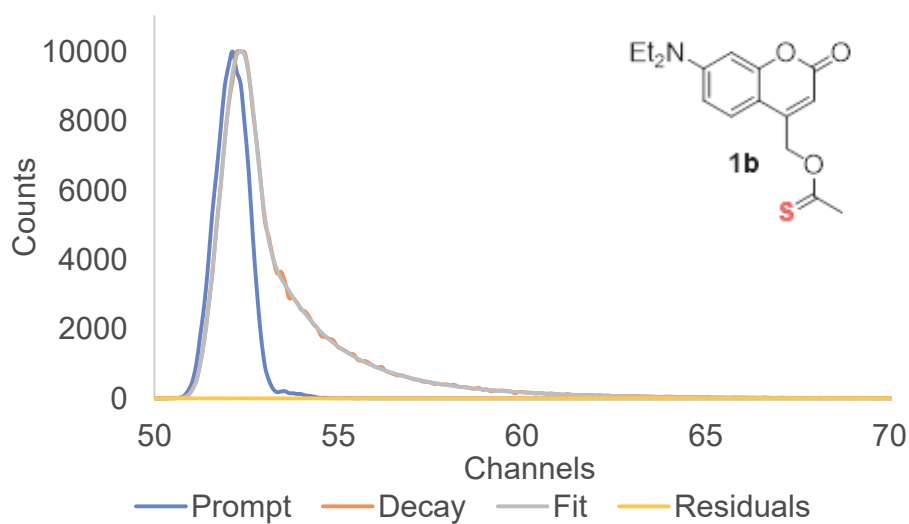


Figure S6. Time profile of the excited state of **1b** in DMSO monitored at 465 nm (excited at 390 nm)

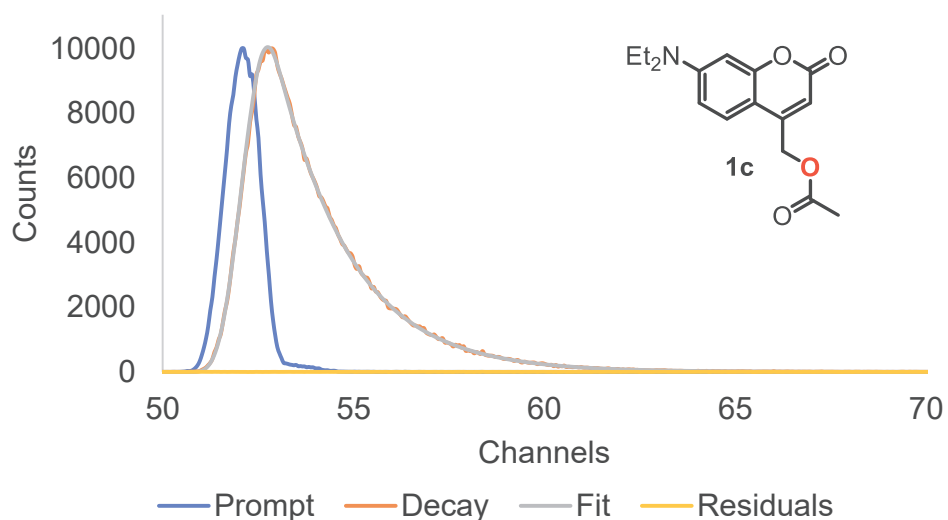


Figure S7. Time profile of the excited state of **1c** in DMSO monitored at 472 nm (excited at 390 nm)

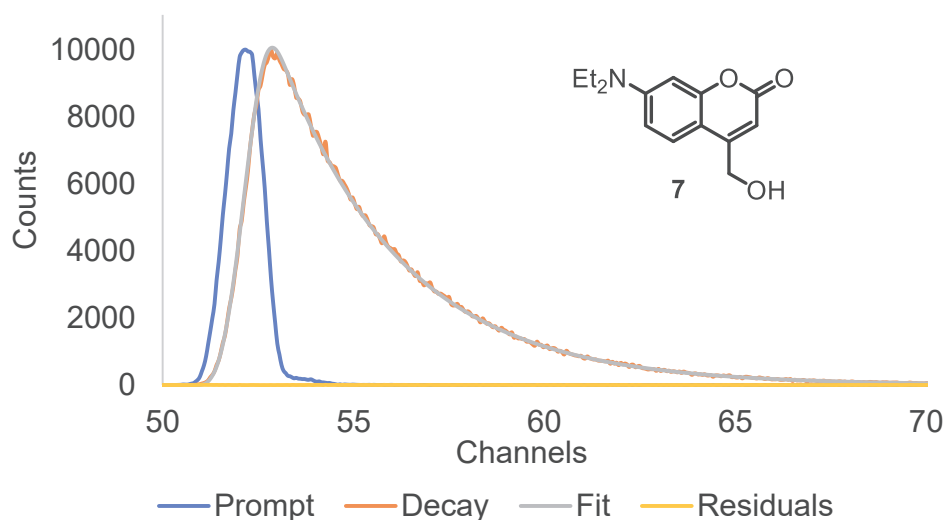


Figure S8. Time profile of the excited state of **9** in DMSO monitored at 455 nm (excited at 390 nm)

2-10-3. Photochemical properties of targeted compounds

General procedure for experiments monitored by ^1H NMR: A solution of compound **1a**, **1b**, or **1c** ($C_M = 15$ mM) in DMSO- d_6 was irradiated at $\lambda = 405$

nm (LED lamp). In the case of photoreactions proceeded in Ar-saturated and O₂-saturated DMSO-*d*₆, the solution was purged with Ar and O₂ gas by bubbling method for 10 minutes, respectively. The chemical yields of photoproducts were determined by adding triphenylmethane (TPM) as an internal standard.

General procedure for experiments monitored by HPLC: A solution of compound **1a**, **1b**, or **1c** ($C_M = 0.4$ mM) in DMSO/H₂O (3:2) was prepared. The solution was purged with Ar for 10 minutes by the bubbling method. The sample was irradiated at $\lambda = 405$ nm (LED lamp). Calibration curves for photoproducts were used to determine the chemical yields.

The conversions of starting materials (%) were calculated by using the following equation:

$$\text{Conversion (\%)} = \frac{n_S^0 (\text{mol}) - n_S^u (\text{mol})}{n_S^0 (\text{mol})} \times 100 \quad (1)$$

Whereas n_S^0 is the amount of the starting material before photoreaction (mol) and n_S^u is the amount of the unreacted starting material.

The chemical yields (%) of photoproducts were calculated by using the following equation

$$\text{Chemical yield (\%)} = \frac{n_P (\text{mol}) \times 100}{n_S^0 \times \text{Conversion}} \times 100 \quad (2)$$

Whereas n_P is the amount of photoproducts (mol).

Entry 1

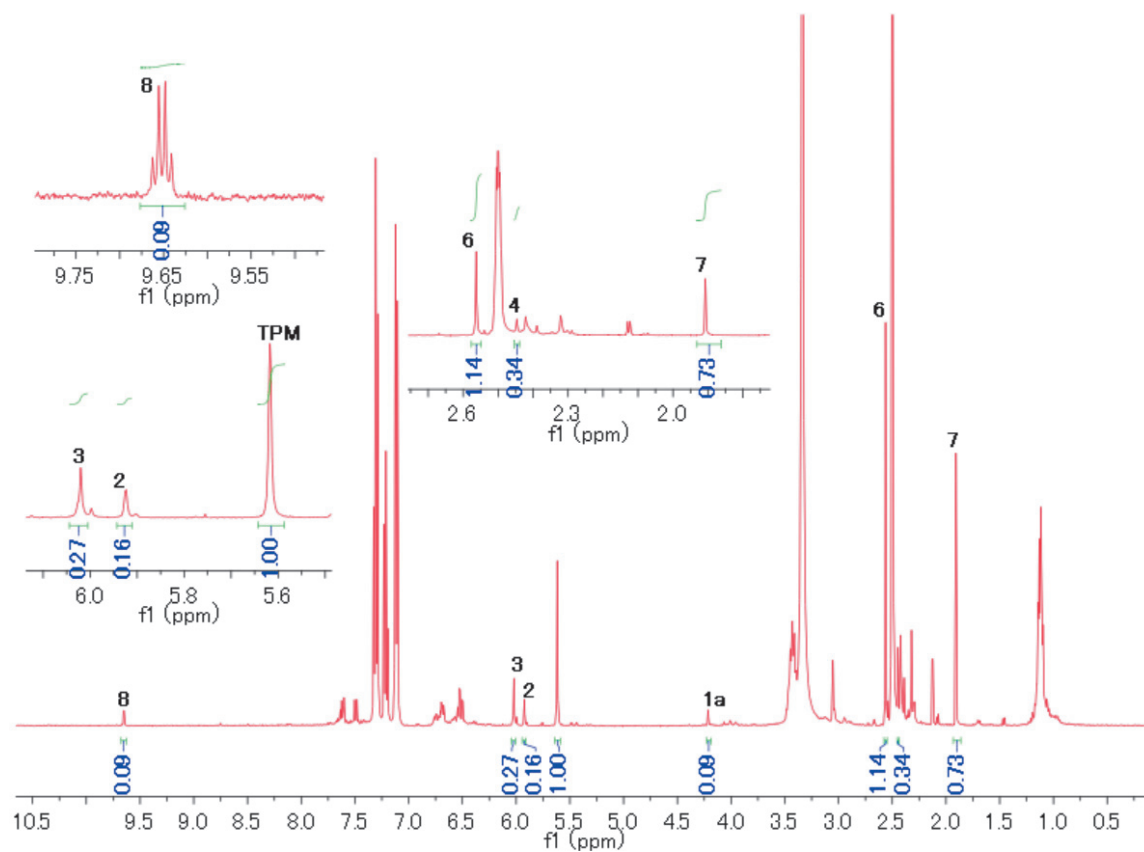


Figure S9. ^1H NMR analysis of photoreaction of **1a** (entry 1)

Entry 2

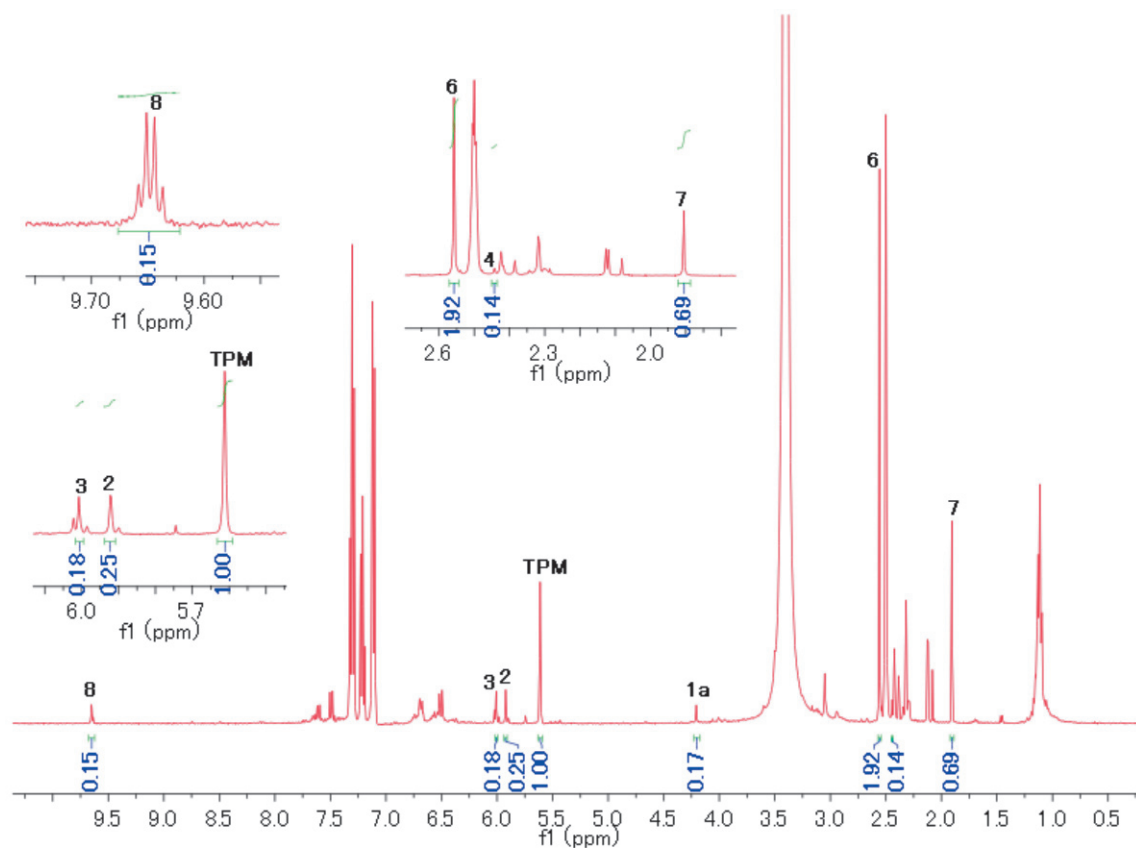


Figure S10. ^1H NMR analysis of photoreaction of **1a** (entry 2)

Entry 3

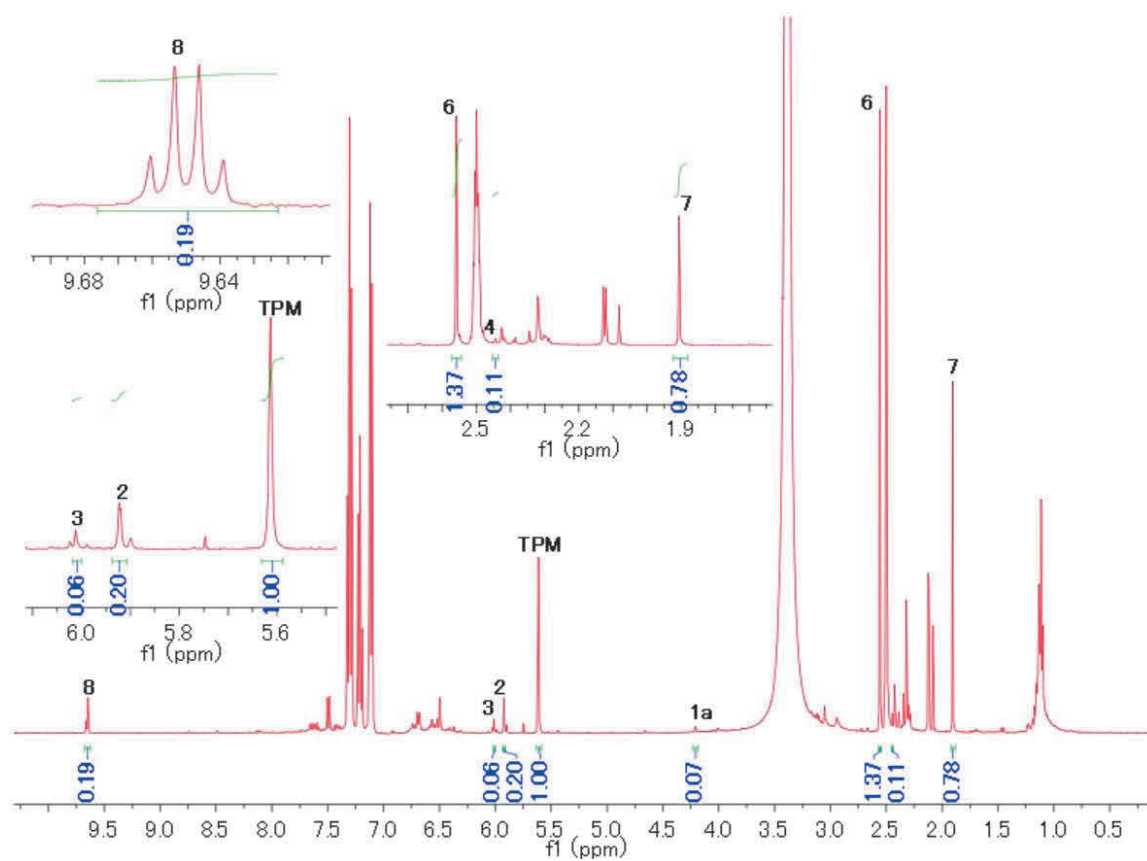


Figure S11. ^1H NMR analysis of photoreaction of **1a** (entry 3)

Entry 5

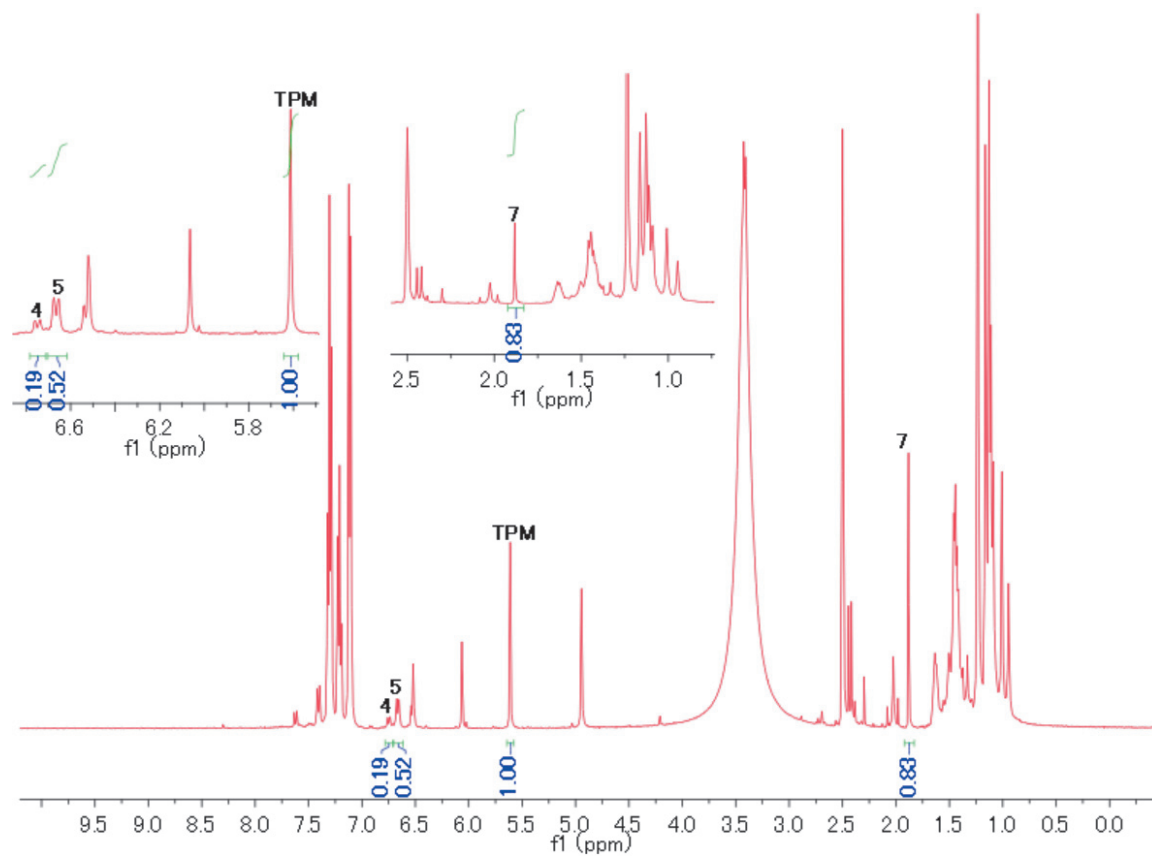


Figure S12. ^1H NMR analysis of photoreaction of **1a** (entry 5)

Entry 6

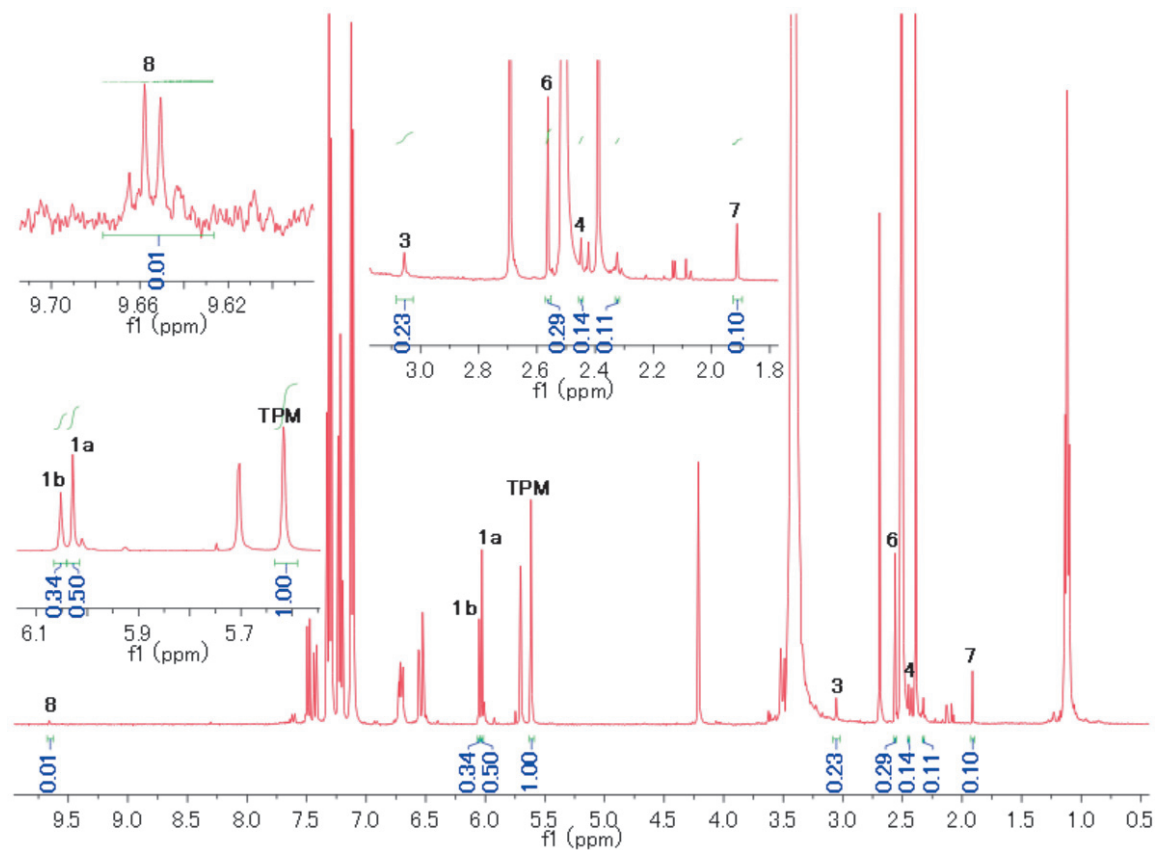


Figure S13. ^1H NMR analysis of photoreaction of **1b** (entry 6)

Entry 8

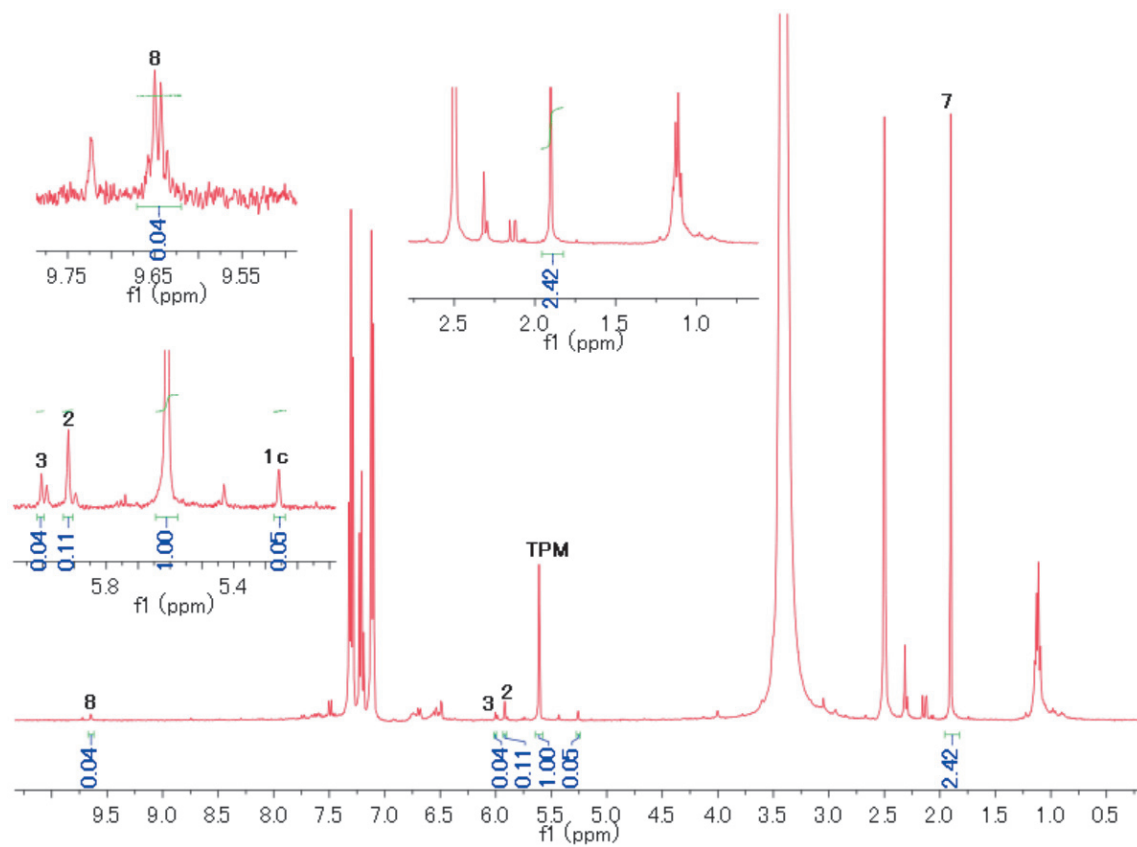


Figure S14. ^1H NMR analysis of photoreaction of **1c** (entry 8)

Entry 11

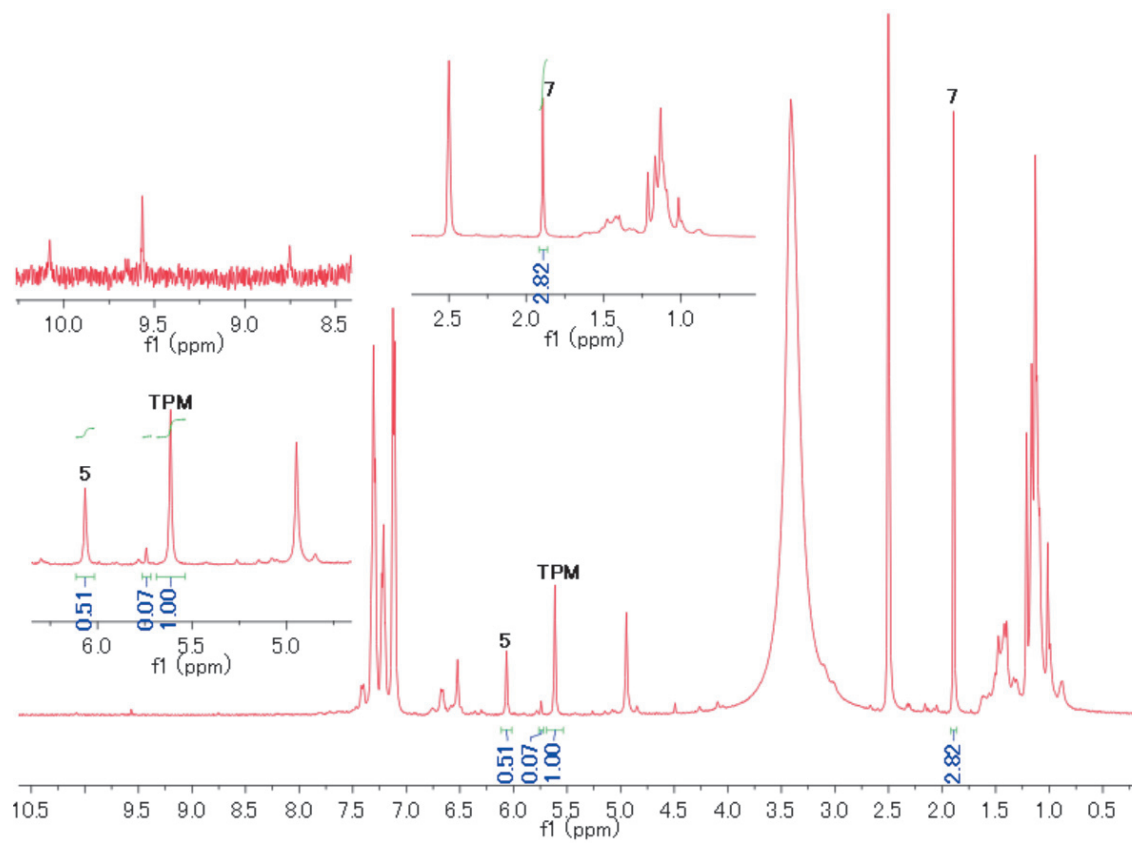


Figure S15. ^1H NMR analysis of photoreaction of **1c** (entry 11)

Photoreaction of **1b (15 mM) in air-saturated DMSO-*d*₆ in the presence of TEMPO (45 mM)**

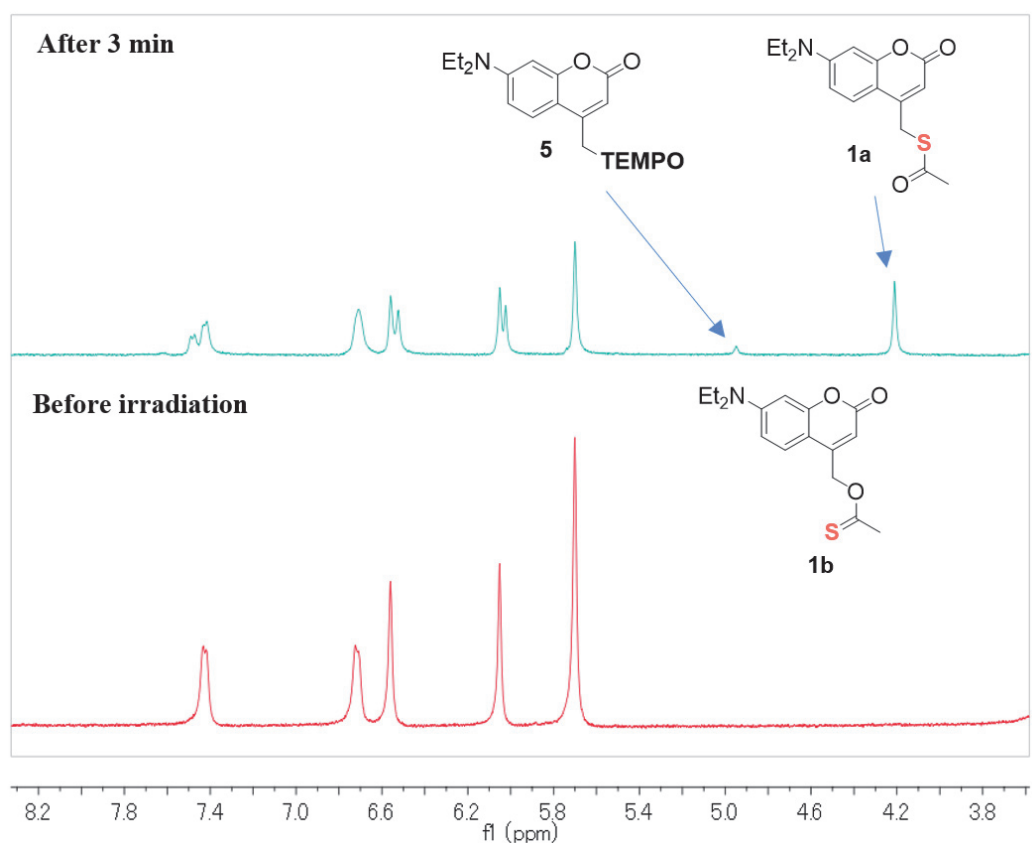


Figure S16. ¹H NMR analysis of photoreaction of **1b** in the presence of TEMPO

Determination of chemical yields by HPLC analysis

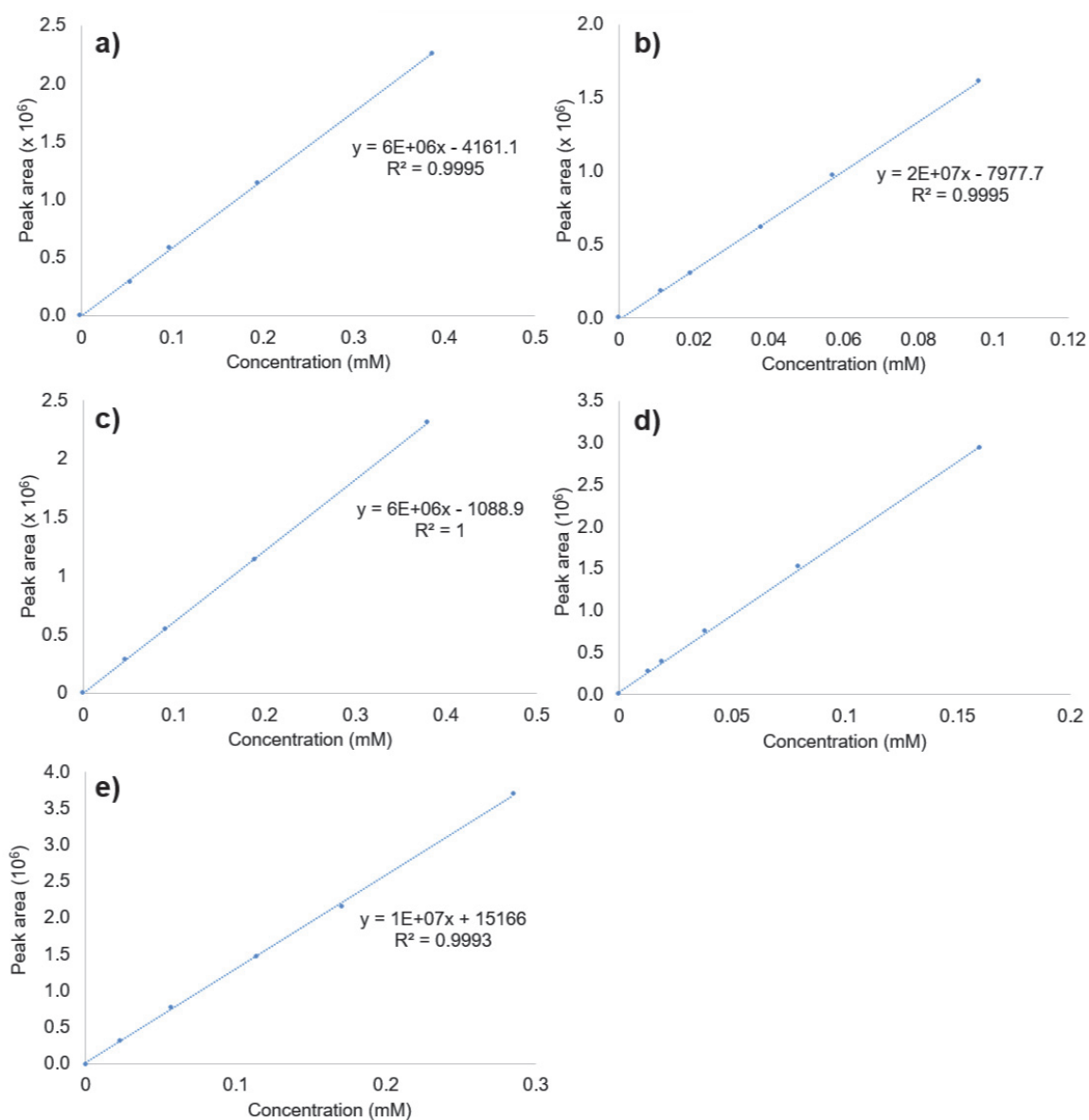


Figure S17. Calibration curves determined by HPLC analysis for compound a) 7, b) 4, c) 3, d) 5 and 6

2-10-4. Photochemical quantum yield measurements

General procedure: 3.0 mL of solution of caged compounds ($C_M = 0.28$ - 0.39 mM, $Abs_{405} = 5$) in DMSO were irradiated by using 405 nm LED lamp. The

number of photons of LED lamp was determined by using Ferrioxalate complex as the actinometer. The conversion of the starting material at a certain time was calculated by HPLC analysis. A conversion vs time graph was sketched, and the slope of the linear line was observed as the conversion rate. The photochemical quantum yield values were calculated by using the following equation:

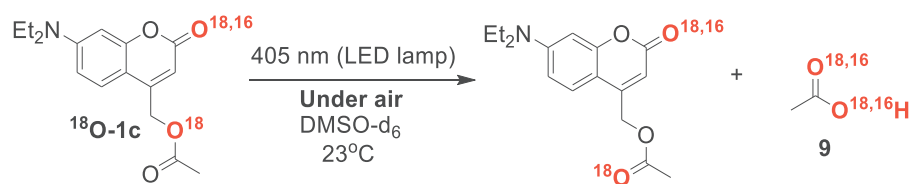
$$\Phi = \frac{\text{conversion rate (s}^{-1}) \times C_{\text{starting material (mM)}} \times V \text{ (L)}}{\text{moles of photons (mmol} \times \text{s}^{-1})}$$

Table S3. Photochemical quantum yields of photoreactions of **1a**, **1b** and **1c** measured in different conditions

Compounds Conditions	1a	1b	1c
In Ar-saturated DMSO	0.028 ± 0.002	0.68 ± 0.03	0.0031 ± 0.0002
In Air-saturated DMSO	0.026 ± 0.001	0.60 ± 0.02	0.0027 ± 0.0003
In Ar-saturated DMSO with 3.0 equiv. TEMPO	0.015 ± 0.001	0.62 ± 0.04	0.0044 ± 0.0003

2-10-5. Isotope scrambling experiment

Procedure: Three samples of **1c** dissolved in DMSO-*d*₆ (58 mM) were prepared. Sample 1, sample 2 and sample 3 were irradiated by using 405 nm (±20 nm) LED lamp for 1 minute, 5 minutes and 10 minutes, respectively. The course of photoreactions was followed by ¹H NMR (400 MHz) and ¹³C NMR (151 MHz) spectroscopy. The conversion of the starting material and the chemical yield of acetic acid (**7**) was determined by using benzene as the internal standard.



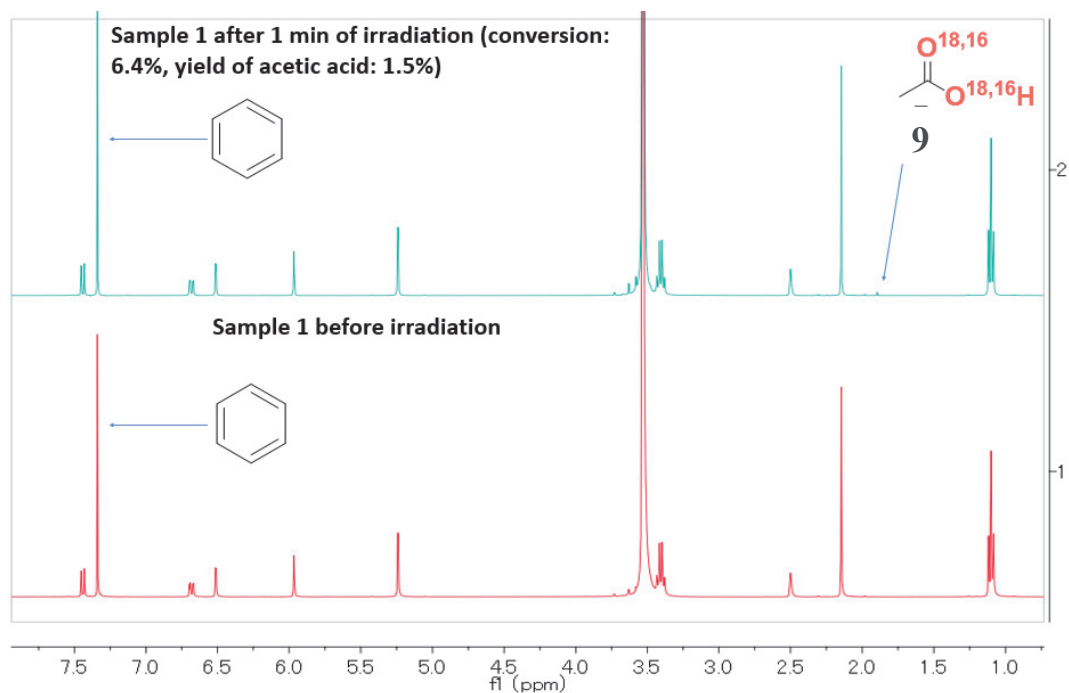


Figure S18. ^1H NMR spectra (400 MHz, $\text{DMSO}-d_6$) of irradiation of sample 1

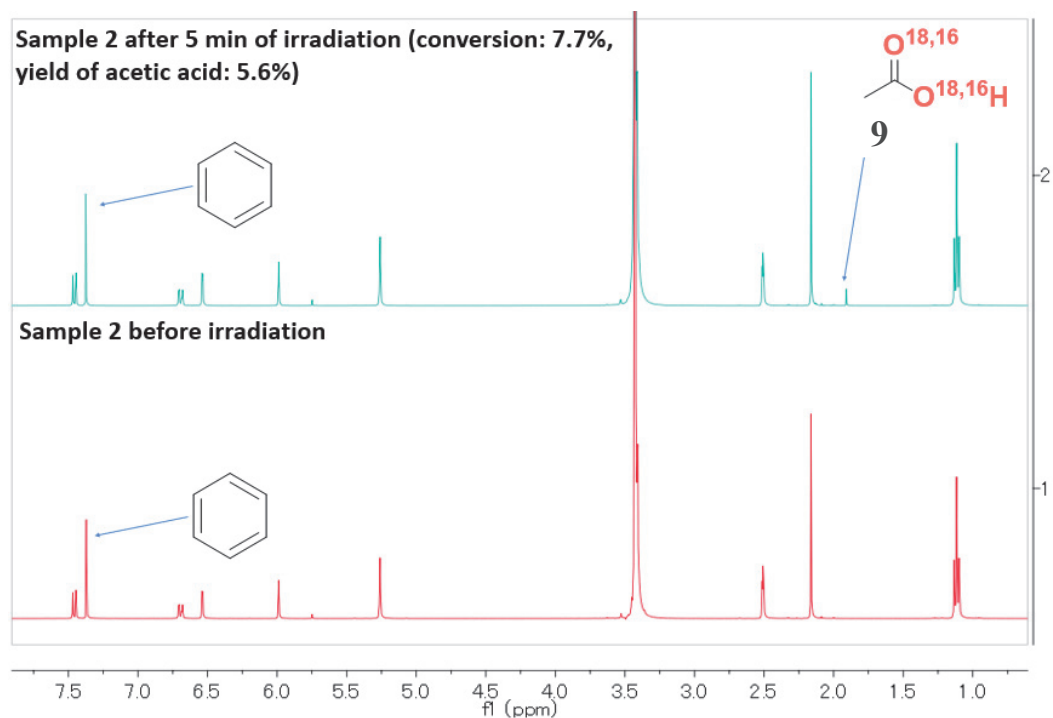


Figure S19. ^1H NMR spectra (400 MHz, $\text{DMSO}-d_6$) of irradiation of sample 2

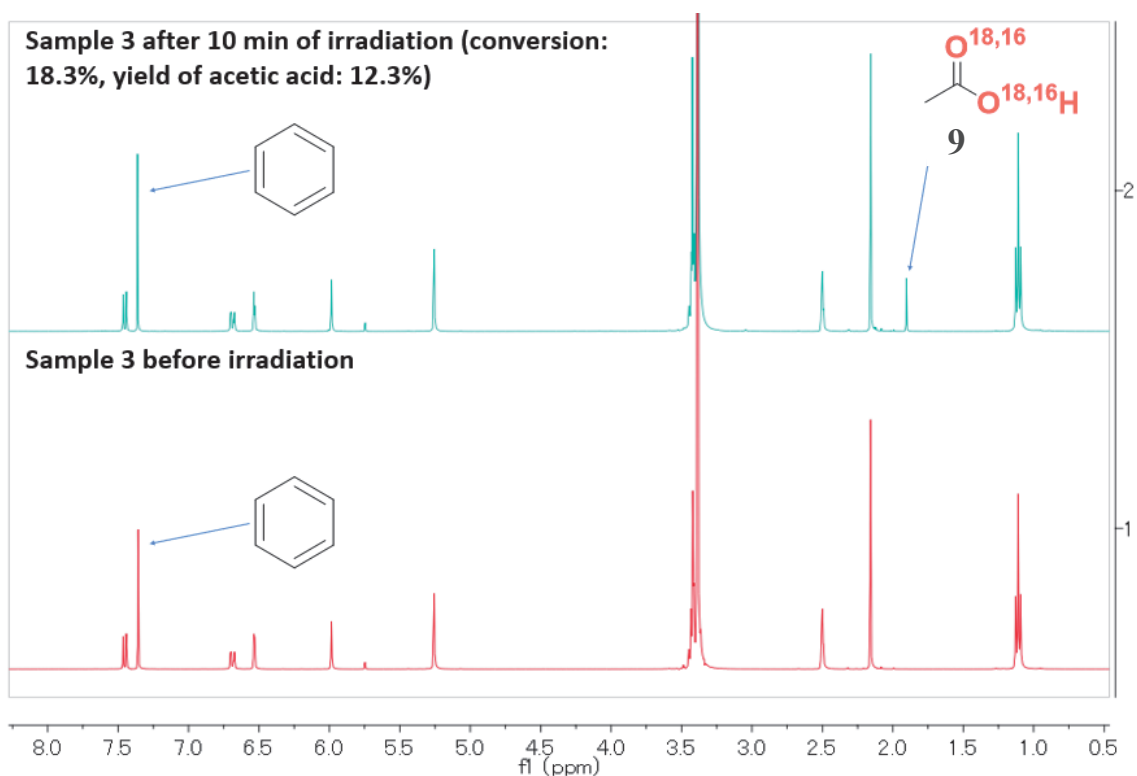


Figure S20. ^1H NMR spectra (400 MHz, $\text{DMSO}-d_6$) of irradiation of sample 3 2-10-6. **Product identification of the photoreaction of 1a in DMSO in the presence of TEMPO**

Procedure: 19.2 mg of **1a** (13.7 mM) and 27.1 mg of TEMPO (37.7 mM) were dissolved in DMSO (4.6 mL). The sample was irradiated by using a 405 nm LED lamp under Air. The course of the photoreaction was monitored by HPLC analysis. After 140 minutes of irradiation, the mixture was extracted with CH_2Cl_2 . The organic layer was dried with Na_2SO_4 , concentrated under reduced pressure to observe the crude product, which was purified by silica-gel column chromatography. Compound **6** (fraction 1, 11.2 mg, 46%) and compound **5** (fraction 4, 3.9 mg, 20%) were separated as the major byproducts.

7-(diethylamino)-4-(((2,2,6,6-tetramethylpiperidin-1-yl)oxy)methyl)-2H-chromen-2-one (6**)**⁷². ^1H NMR (400 MHz, CDCl_3) δ 7.23 (d, $J = 8.9$ Hz, 1H), 6.54 (dd, $J = 8.9, 2.6$ Hz, 1H), 6.50 (d, $J = 2.6$ Hz, 1H), 6.33 (t, $J = 1.4$ Hz,

1H), 4.96 (d, $J = 1.4$ Hz, 2H), 3.40 (q, $J = 7.1$ Hz, 4H), 1.66 – 1.32 (m, 6H), 1.23 – 1.13 (m, 18H).

S-(7-(diethylamino)-4-methyl-2-oxo-2H-chromen-3-yl) ethanethioate (5).

^1H NMR (400 MHz, CDCl_3) δ 7.45 (d, $J = 9.1$, 1H), 6.60 (dd, $J = 9.1$, 2.6 Hz, 1H), 6.48 (d, $J = 2.6$ Hz, 1H), 3.42 (q, $J = 7.1$ Hz, 4H), 2.47 (s, 3H), 2.45 (s, 3H), 1.21 (t, $J = 7.1$ Hz, 6H). **$^{13}\text{C}\{^1\text{H}\}$ NMR** (101 MHz, CDCl_3) δ 192.6 (s), 160.5 (s), 159.1 (s), 155.9 (s), 151.4 (s), 127.0 (s), 109.3 (s), 108.9 (s), 108.0 (s), 97.3 (s), 44.9 (s), 30.1 (s), 17.4 (s), 12.4 (s). **HRMS** (ESI^+) m/z : $[\text{M} + \text{H}]^+$ calcd for $\text{C}_{16}\text{H}_{20}\text{NO}_3\text{S}^+$ 306.11575, found 306.11584. Mp 118 °C. **IR** (film, cm^{-1}): 2975, 1715, 1616, 1573, 1516, 1416, 1356, 1266, 1146, 1076.

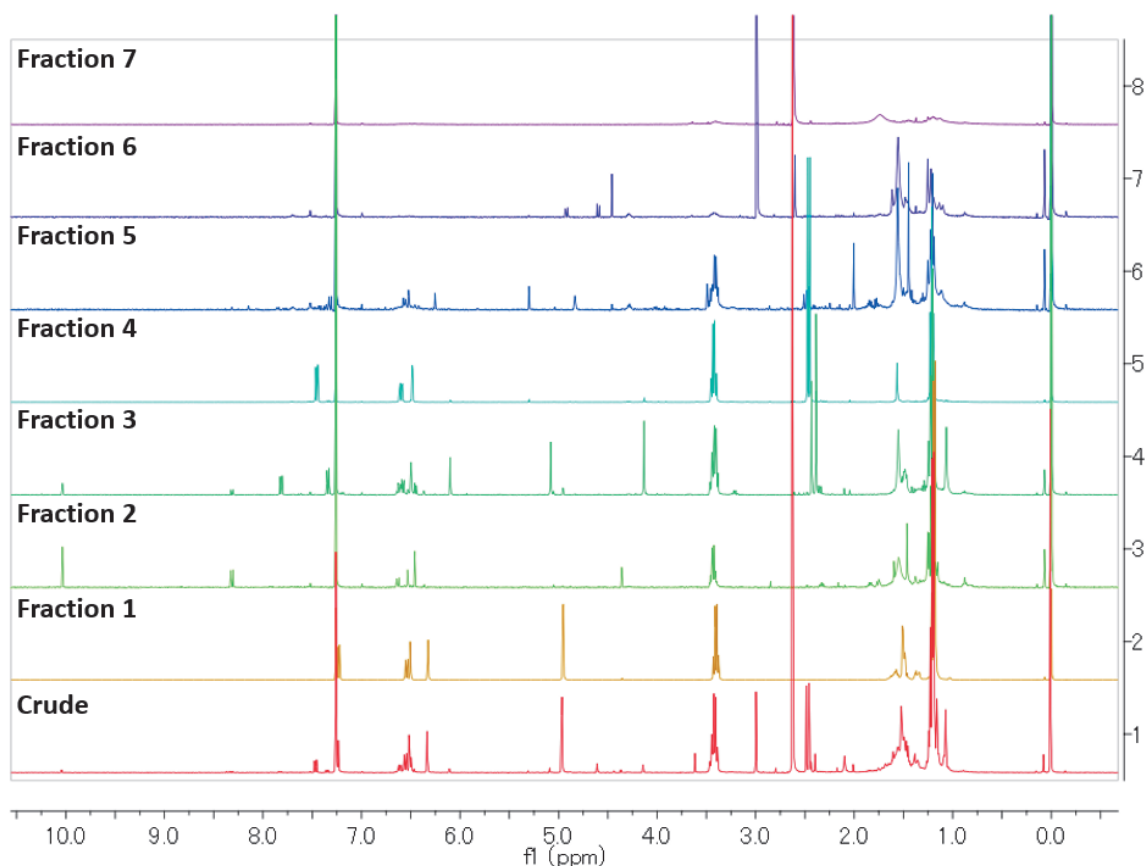


Figure S21. ^1H NMR spectra (400 MHz) of collected fractions after column chromatography measured in CDCl_3

2-10-7. Product identification of the photoreaction of **1a** in Ar-saturated DMSO

Procedure: 25.3 mg of **1a** (13.8 mM) were dissolved in DMSO (6.0 mL). The sample was irradiated by using a 405 nm LED lamp under Ar. The course of the photoreaction was monitored by HPLC analysis. After 240 minutes of irradiation, the mixture was extracted with CH₂Cl₂. The organic layer was dried with Na₂SO₄, concentrated under reduced pressure to observe the crude product, which was purified by silica-gel column chromatography. Compound **4** (fraction 3, 2.3 mg, 12%) was separated as the major byproduct as the yellow solid.

4,4'-(ethane-1,2-diyl)bis(7-(diethylamino)-2H-chromen-2-one) (4). ¹H NMR (400 MHz, CDCl₃) δ 7.38 (d, *J* = 9.0 Hz, 1H), 6.59 (dd, *J* = 9.0, 2.6 Hz, 1H), 6.53 (d, *J* = 2.6 Hz, 1H), 6.00 (s, 1H), 3.42 (q, *J* = 7.1 Hz, 4H), 3.03 (s, 2H), 1.22 (t, *J* = 7.1 Hz, 6H). ¹³C{¹H} NMR (101 MHz, CDCl₃) δ 162.1 (s), 156.4 (s), 154.7 (s), 150.7 (s), 124.9 (s), 108.7 (s), 107.8 (s), 107.7 (s), 98.0 (s), 44.8 (s), 30.3 (s), 12.5 (s). HRMS (ESI⁺) *m/z*: [M + Na]⁺ calcd for C₂₈H₃₂N₂O₄Na⁺ 483.22543, found 483.22510. Mp 188 °C. IR (film, cm⁻¹): 2972, 1713, 1616, 1604, 1525, 1416, 1356, 1271, 1140.

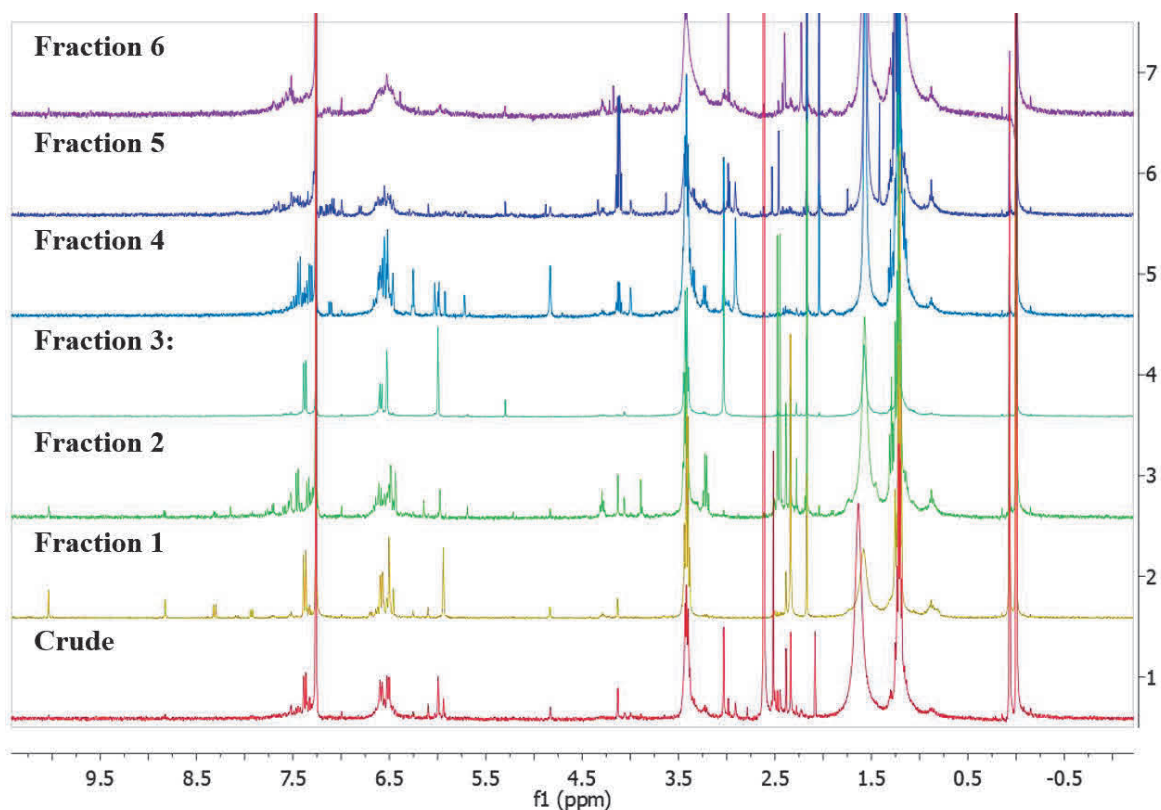


Figure S22. ^1H NMR spectra (400 MHz) of collected fractions after column chromatography measured in CDCl_3

2-10-8. Laser flash photolysis experiments

General procedure for the LFP experiments of 1a, 1b and 1c: The solutions of **1a**, **1b**, **1c** (0.14 mM) in DMSO were prepared. 1.5 mL of the stock solution was transferred to a 5.0 mm cuvette for the laser flash photolysis experiments. Transient absorption spectra were observed using a 355 nm laser (Nd-YAG, 15 mJ/pulse, 12 ns pulse width). The time profiles at 330 nm were fitted with the second order kinetic model with the assumption that the concentration of radical **A** was identical to that of the singlet excited state. The concentration of the singlet excited state was calculated from the time profiles monitored at 370 nm (absorption band of **1a**, **1b** and **1c**).

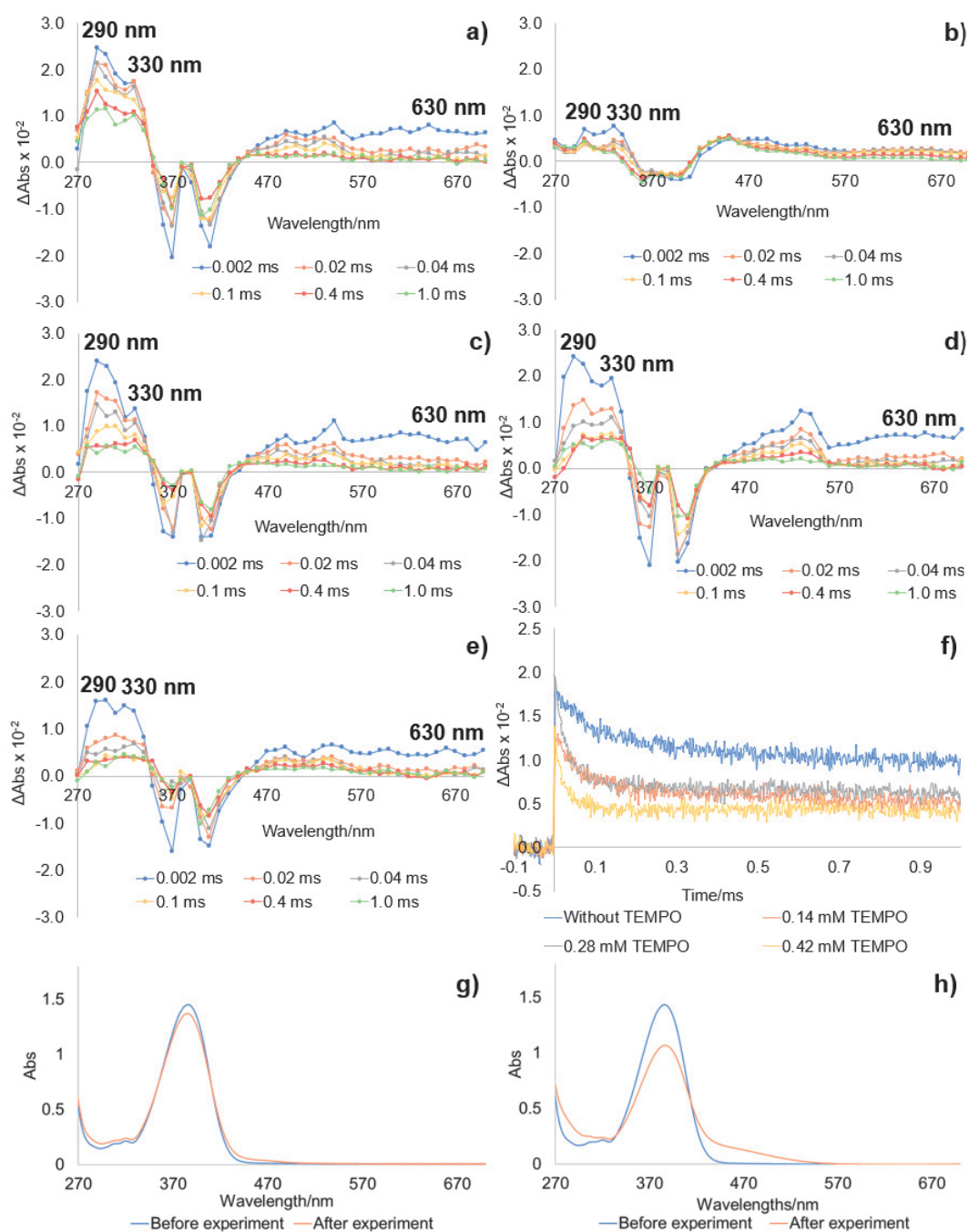


Figure S23. Transient absorption spectra of **1a** observed a) in Ar-saturated DMSO, b) in Air-saturated DMSO, c) in Ar-saturated DMSO in the presence of 0.14 mM TEMPO, d) in Ar-saturated DMSO in the presence of 0.28 mM TEMPO, e) in Ar-saturated DMSO in the presence of 0.42 mM TEMPO. f)

Time profile at 330 nm measured in the presence and in the absence of TEMPO. Absorption spectra of **1a** measured before and after LFP measurement g) under Ar and h) under Air.

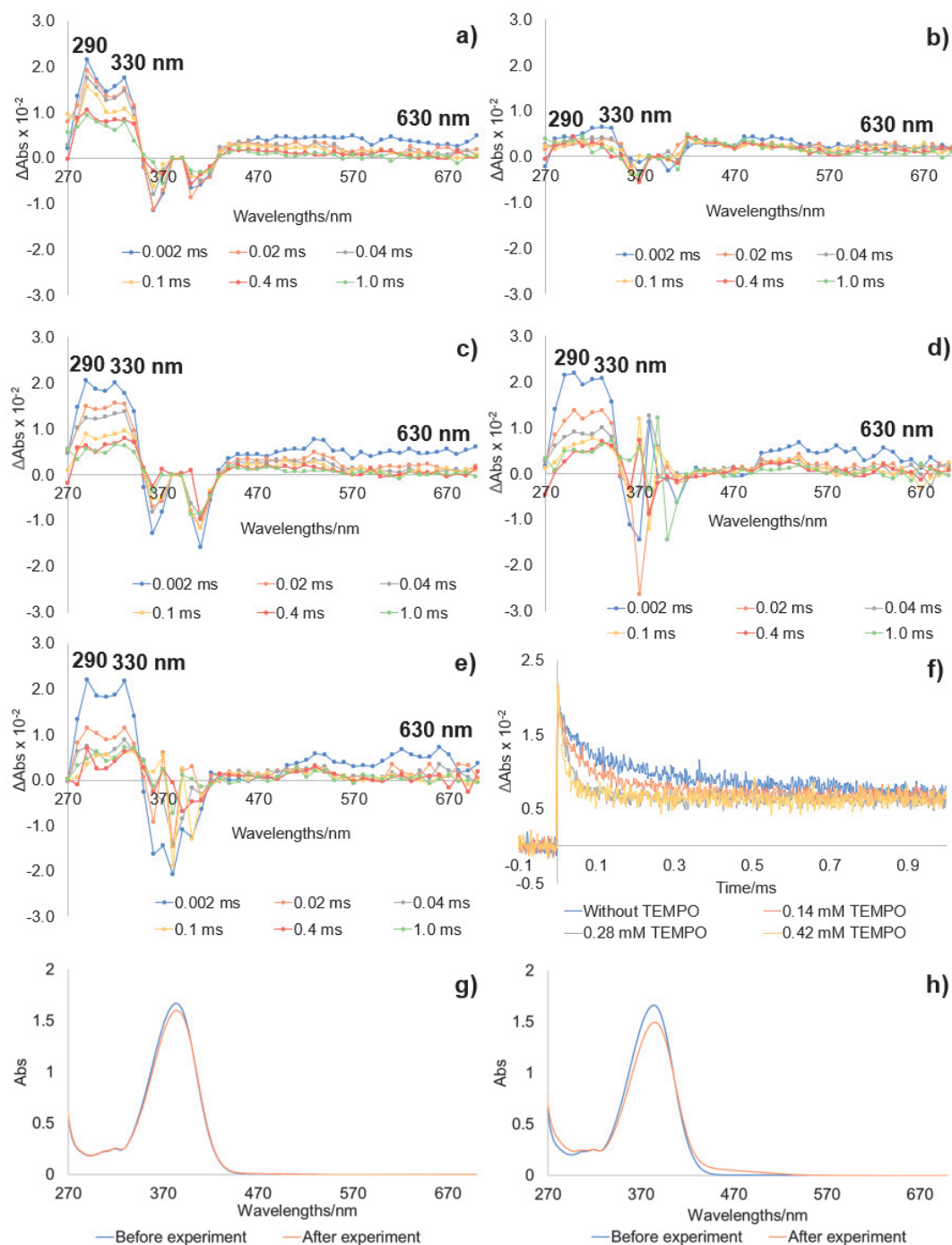


Figure S24. Transient absorption spectra of **1b** observed a) in Ar-saturated DMSO, b) in Air-saturated DMSO, c) in Ar-saturated DMSO in the presence of 0.14 mM TEMPO, d) in Ar-saturated DMSO in the presence of 0.28 mM

TEMPO, e) in Ar-saturated DMSO in the presence of 0.42 mM TEMPO. f) Time profile at 330 nm measured in the presence and in the absence of TEMPO. Absorption spectra of **1b** measured before and after LFP measurement g) under Ar and h) under Air.

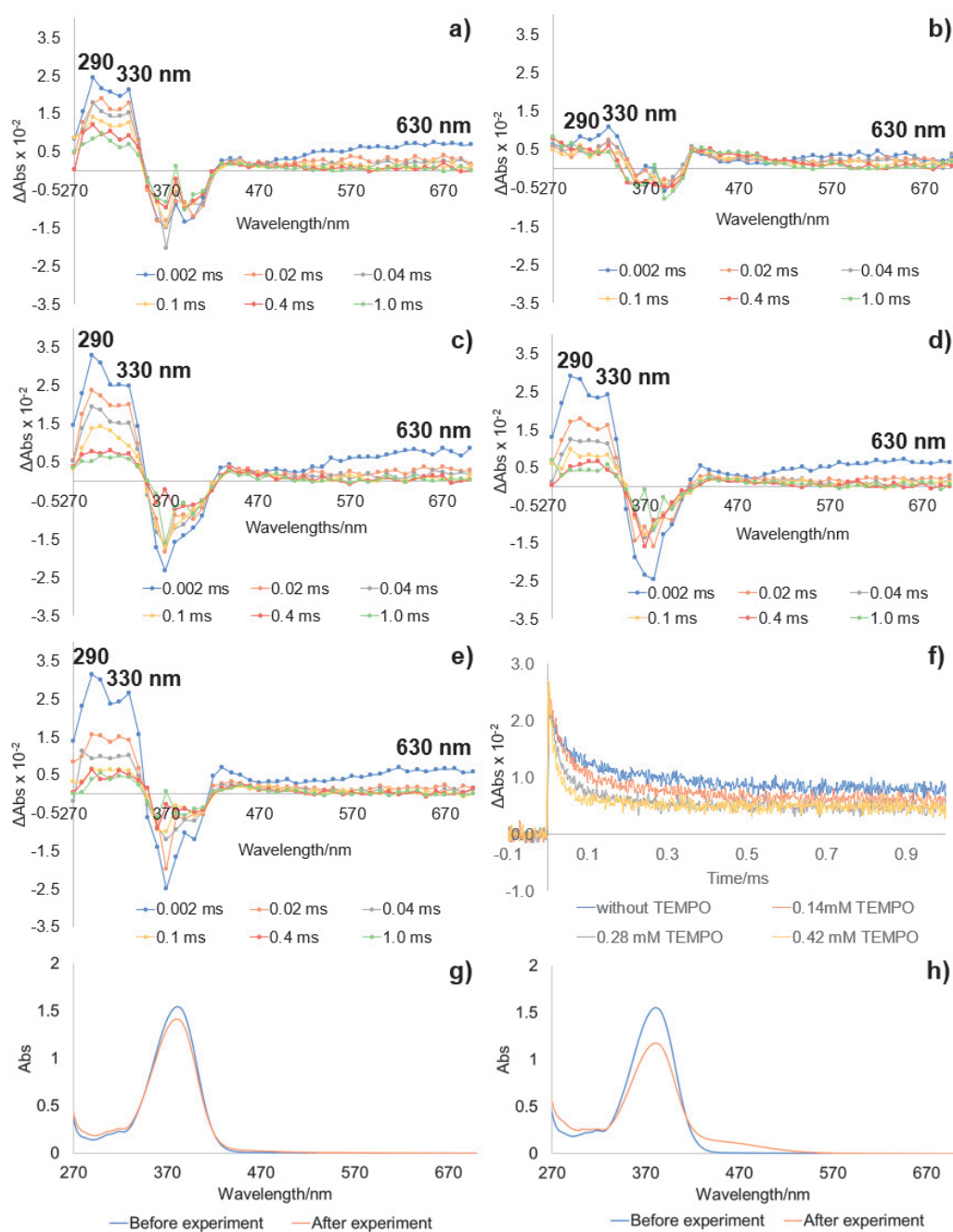


Figure S25. Transient absorption spectra of **1c** observed a) in Ar-saturated DMSO, b) in Air-saturated DMSO, c) in Ar-saturated DMSO in the presence of 0.14 mM TEMPO, d) in Ar-saturated DMSO in the presence of 0.28 mM TEMPO, e) in Ar-saturated DMSO in the presence of 0.42 mM TEMPO. f)

Time profile at 330 nm measured in the presence and in the absence of TEMPO. Absorption spectra of **1c** measured before and after LFP measurement g) under Ar and h) under Air.

Procedure for the LFP measurement of 7: The solutions of **7** (0.13 mM) in DMSO were prepared. 1.5 mL of the stock solution was transferred to a 5.0 mm cuvette for the laser flash photolysis experiments. Transient absorption spectra were observed using a 355 nm laser (Nd-YAG, 15 mJ/pulse, 12 ns pulse width). Because the absorbance at 380 nm (absorption band of **7**) is very high (Abs = 2.8), the transient signal at this band is not clear (Figure S10a). To observe an apparent time profile at 380 nm, the more diluted solution of **7** (0.065 mM) was prepared and a 10 cm cuvette was used for the measurements.

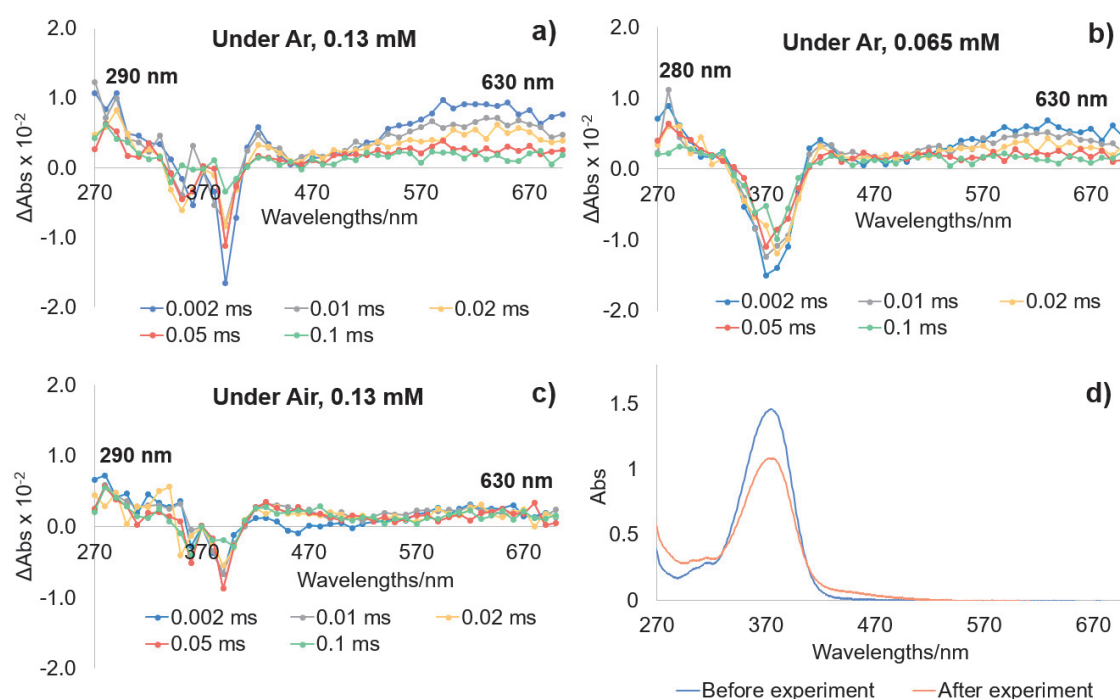


Figure S26. Transient absorption spectra of **7** observed a) in Ar-saturated DMSO ($C_M = 0.13$ mM) by using 5 mm cuvette, b) in Ar-saturated DMSO ($C_M = 0.065$ mM) by using 10 mm cuvette, c) in Air-saturated DMSO ($C_M = 0.13$ mM) by using 5 mm cuvette. d) Absorption spectrum of the sample before and after experiments under Ar.

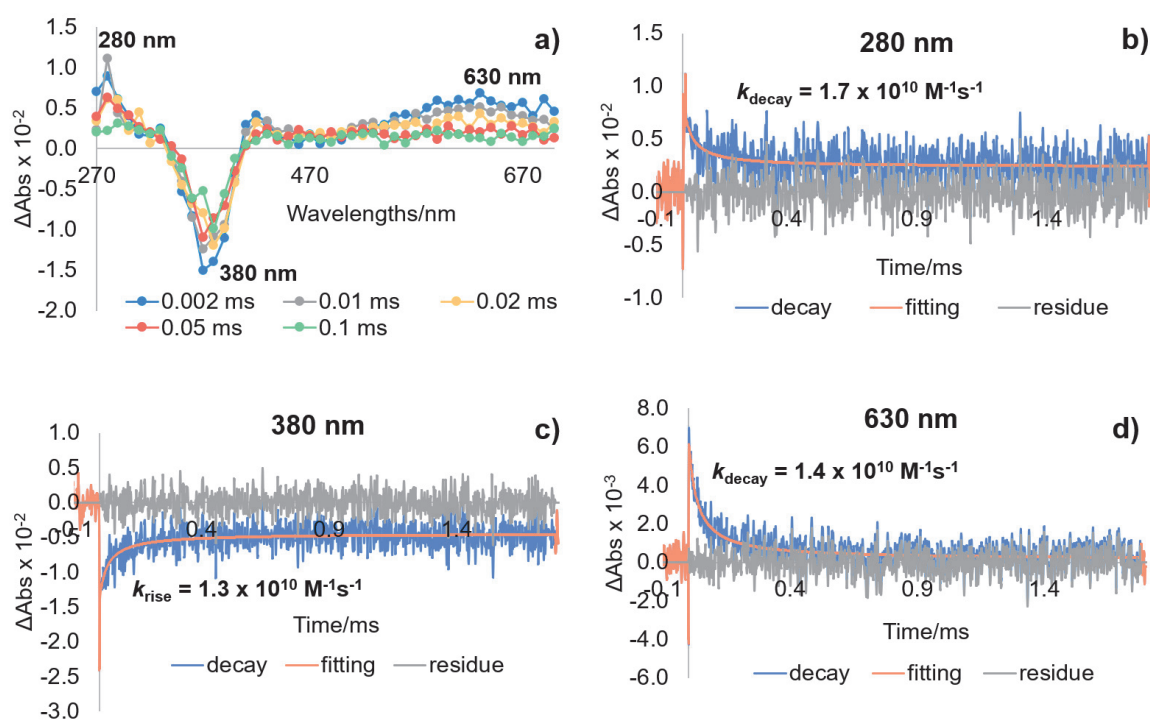


Figure S27. a) Transient absorption spectra of **7** observed in Ar-saturated DMSO ($C_M = 0.065$ mM) by using 10 mm cuvette. b) Time profiles observed in Ar-saturated DMSO ($C_M = 0.065$ mM) by using 10 mm cuvette, monitored at b) 280 nm, c) 380 nm, d) 630 nm.

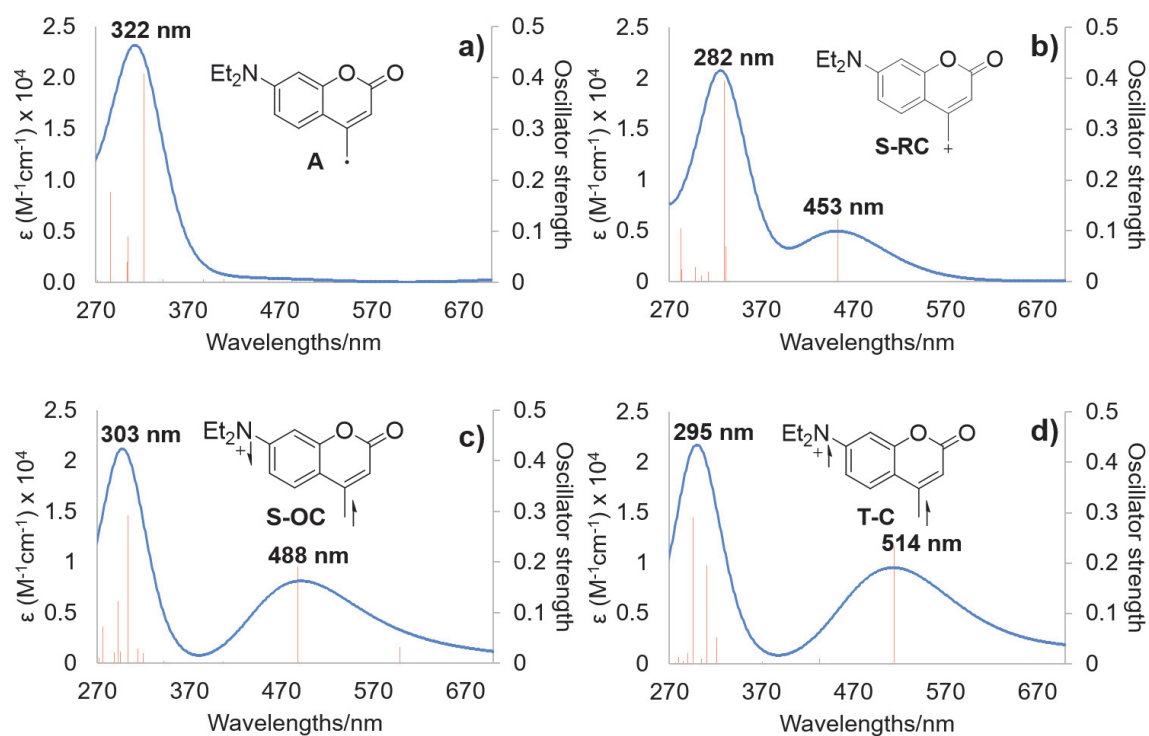


Figure S28. a) Simulated UV spectrum of a) **A**, b) **S-RC**, c) **S-OC**, d) **T-C** calculated at the (R/U)B3LYP/6-31G+(d) in DMSO.

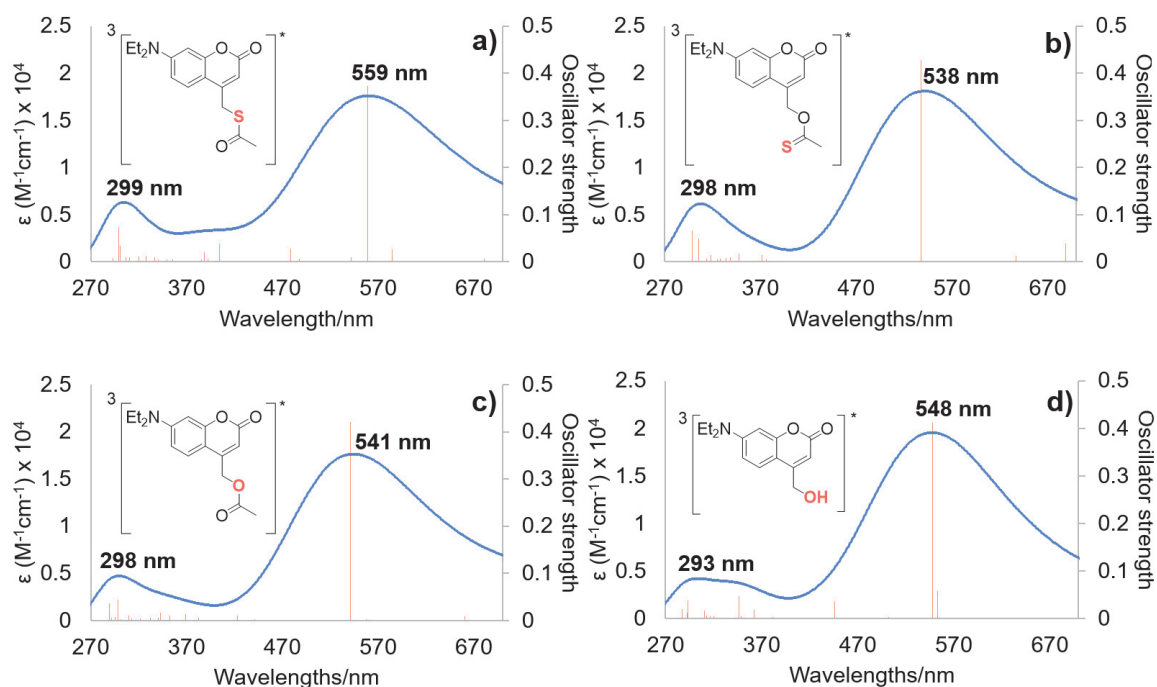


Figure S29. a) Simulated UV spectrum of the triplet excited state of a) **1a**, b) **1b**, c) **1c**, d) **7** calculated at the UB3LYP/6-31G+(d) in DMSO.

Calculation of the theoretical absorbance of radical A

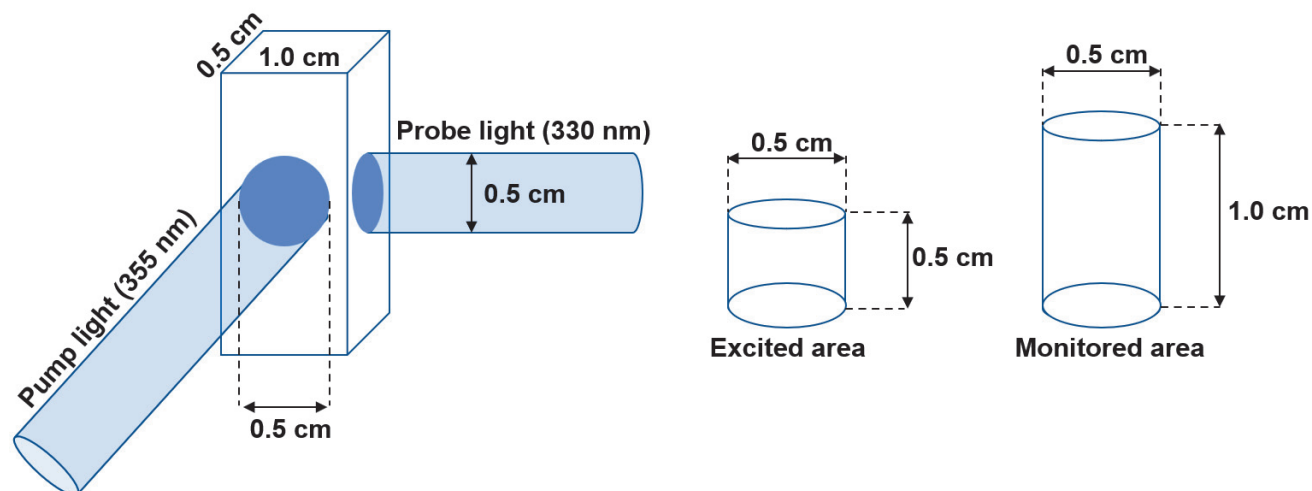


Figure 30. LFP measurement setup

Transient absorption spectra of **1a**, **1b** and **1c** ($C_M = 1.40 \times 10^{-4}$ M) were observed by using a 355 nm laser (Nd-YAG, 15 mJ/pulse, 12 ns pulse width) as the pump light. The number of photons were calculated to be 2.70×10^{16} photons/pulse ($\sim 4.48 \times 10^{-5}$ mmol/pulse). The shape of the excited area was assumed to be a cylinder, in which the radius is 0.25 cm and the height is 0.5 cm. The excited area's volume was therefore determined to be 0.098 mL (Figure S29a). The mole of starting compounds excited was estimated as followed:

$$n_{\text{starting compound in excited area}} = C_{\text{sample}} \times V_{\text{excited area}} = 1.40 \times 10^{-4} \times 0.098 = 1.37 \times 10^{-5} \text{ mmol} \quad (1)$$

The theoretical absorbance of **A** at 330 nm ($\text{Abs}_{\text{theoretical A,330 nm}}$) was estimated by using the following equation:

$$\text{Abs}_{\text{theoretical A,330 nm}} = \epsilon_{330 \text{ nm}} \times C_{\text{A at the monitored area}} \times l \quad (2)$$

Whereas the simulated extinction coefficient of **A** at 330 nm ($\epsilon_{330 \text{ nm}}$) is $22028 \text{ M}^{-1}\text{cm}^{-1}$ (Figure S). The optical path length (l) is 1.0 cm. The concentration of **A** generated at the monitored area ($C_{\text{A at the monitored area}}$) was calculated by using equation 3:

$$C_{\text{A at the monitored area}} = \frac{n_{\text{A at the monitored area}}}{V_{\text{monitored area}}} \quad (3)$$

Whereas the shape of the monitored area was assumed to be a cylinder, in which the radius is 0.25 cm and the height is 1.0 cm. The volume of the monitored area was therefore determined to be 0.20 mL. The moles of **A** at the monitored area was determined as followed:

$$n_{\text{A at the monitored area}} = n_{\text{starting compound excited}} \times \Phi^{\text{Ar}} \quad (4)$$

Whereas Φ^{Ar} is the decomposition quantum yield of starting compounds (**1a-c**) in Ar-saturated DMSO. Equation 4 was proposed on the assumption that the bond breaking generates radical **A** only. The moles of starting compound excited ($n_{\text{starting compound excited}}$) was calculated as followed:

$$n_{\text{starting compound excited}} = n_{\text{starting compound at the excited area}} - n_{\text{starting compound at the excited area}} \times 10^{-\text{Abs}_{355}} \quad (5)$$

Whereas Abs_{355} is the absorbance of **1a-c** at 355 nm.

$n_{\text{starting compound at the excited area}}$ is 1.37×10^{-5} mmol (equation 1). By using equation 2-5, the theoretical absorbance of **A** generated in the cases of **1a**, **1b** and **1c** were calculated.

1a ($\Phi = 0.028$; $\text{Abs}_{355} = 0.75$): $\text{Abs}_{\text{theoretical A}, 330 \text{ nm}} = 0.035$

1b ($\Phi = 0.68$; $\text{Abs}_{355} = 0.93$): $\text{Abs}_{\text{theoretical A}, 330 \text{ nm}} = 0.92$.

1c ($\Phi = 0.0031$; $\text{Abs}_{355} = 0.94$): $\text{Abs}_{\text{theoretical A}, 330 \text{ nm}} = 0.0042$.

2-10-9. Calculation details

All calculations were performed by using the Gaussian 16 programming package. Charge, spin multiplicity, number of imaginary frequencies, energies (in Hartree) and Cartesian coordinates (in Å) of computed geometries were simulated by each calculation. The energy minimum structures were confirmed by vibrational frequency analysis.

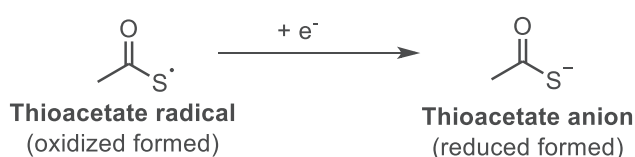
Calculations of reduction potentials

The reduction potentials were calculated by following a reported method.⁷³ The structures of intermediates were optimized at the (U)B3LYP level of theory with the 6-31+G(d,p) basis set. The CPCM model was used for all calculations to account for solvation in DMSO. Gibbs free energies at 298 K (G_{298}) were observed from the calculation output as the “Sum of electronic and thermal Free Energies.” The redox potentials (E_{calc}^0) were calculated by using the following equation:

$$E^0 = - \frac{G_{298}[\text{reduced form}] - G_{298}[\text{oxidized form}]}{n_e F} - E_{\text{SHE}}^0 - E_{\text{SCE}}^0 \quad (6)$$

Where n_e is the number of electrons transferred, \mathcal{F} is the Faraday constant (23.061 kcal mol⁻¹V⁻¹), E_{SHE}^0 is the absolute value for the standard hydrogen electrode (SHE, 4.281 V)⁷⁴ and E_{SCE}^0 is the potential of the saturated calomel electrode (SCE) relative to SHE in DMSO (-0.279 V)⁷⁴. $G_{298}[\text{reduced form}]$ and $G_{298}[\text{oxidized form}]$ are the Gibbs free energies in DMSO observed from DFT calculations.

Reduction potential of thioacetate radical



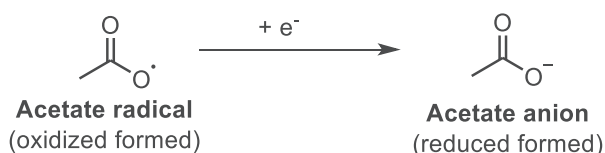
$$G_{298}[\text{Thioacetate radical}] = -551.396182 \text{ Hartree}$$

$$G_{298}[\text{Thioacetate anion}] = -551.586602 \text{ Hartree}$$

$$\begin{aligned}
 \Delta G^0 (\text{kcal mol}^{-1}) &= (G_{298}[\text{Thioacetate anion}] \\
 &\quad - G_{298}[\text{Thioacetate radical}]) \times 627.5 \\
 &= (-551.586602 + 551.396182) \times 627.5 \\
 &= -119.488550 \text{ kcal mol}^{-1}
 \end{aligned}$$

$$\begin{aligned}
 E^0 &= \frac{\Delta G^0}{n_e \mathcal{F}} - E_{\text{SHE}}^0 + E_{\text{SCE}}^0 \\
 &= -\frac{-119.488550 \text{ kcal mol}^{-1}}{23.061 \text{ kcal mol}^{-1} \text{ V}^{-1}} - 4.281 - 0.279 \\
 &= 0.62 \text{ V vs SCE}
 \end{aligned}$$

Reduction potential of acetate radical



$$G_{298}[\text{Acetate radical}] = -228.414124 \text{ Hartree}$$

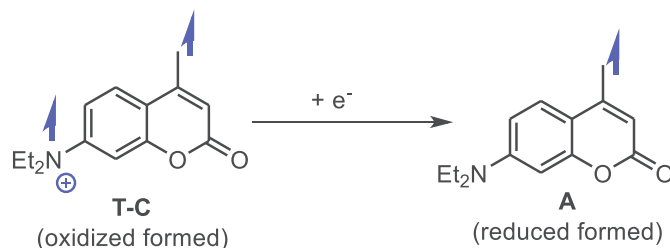
$$G_{298}[\text{Acetate anion}] = -228.626672 \text{ Hartree}$$

$$\Delta G^0(\text{kcal mol}^{-1})$$

$$\begin{aligned} &= (G_{298}[\text{Acetate anion}] \\ &- G_{298}[\text{Acetate radical}]) \times 627.5 \\ &= (-228.626672 + 228.414124) \times 627.5 \\ &= -133.375125 \text{ kcal mol}^{-1} \end{aligned}$$

$$\begin{aligned} E^o &= \frac{\Delta G^o}{n_e \mathcal{F}} - E_{\text{SHE}}^o + E_{\text{SCE}}^o \\ &= \frac{-133.375125 \text{ kcal mol}^{-1}}{23.061 \text{ kcal mol}^{-1} \text{ V}^{-1}} - 4.281 - 0.279 \\ &= 1.22 \text{ V vs SCE} \end{aligned}$$

Reduction potential of T-C



$$G_{298}[\text{A}] = -748.127819 \text{ Hartree}$$

$$G_{298}[\text{T-C}] = -747.933416 \text{ Hartree}$$

$$\begin{aligned} \Delta G^0(\text{kcal mol}^{-1}) &= (G_{298}[\text{A}] - G_{298}[\text{T-C}]) \times 627.5 \\ &= (-748.127819 + 747.933416) \times 627.5 \\ &= -121.986000 \text{ kcal mol}^{-1} \end{aligned}$$

$$\begin{aligned} E^o &= \frac{\Delta G^o}{n_e \mathcal{F}} - E_{\text{SHE}}^o + E_{\text{SCE}}^o \\ &= \frac{-121.986000 \text{ kcal mol}^{-1}}{23.061 \text{ kcal mol}^{-1} \text{ V}^{-1}} - 4.281 - 0.279 \\ &= 0.73 \text{ V vs SCE} \end{aligned}$$

Radical-radical coupling reaction

The energy profile of the radical-radical coupling reaction between triplet cation **T-C'** and TEMPO was computed at the UB3LYP/6-31G(d) level of theory to estimate the energy barrier of the coupling reaction (Figure S31).

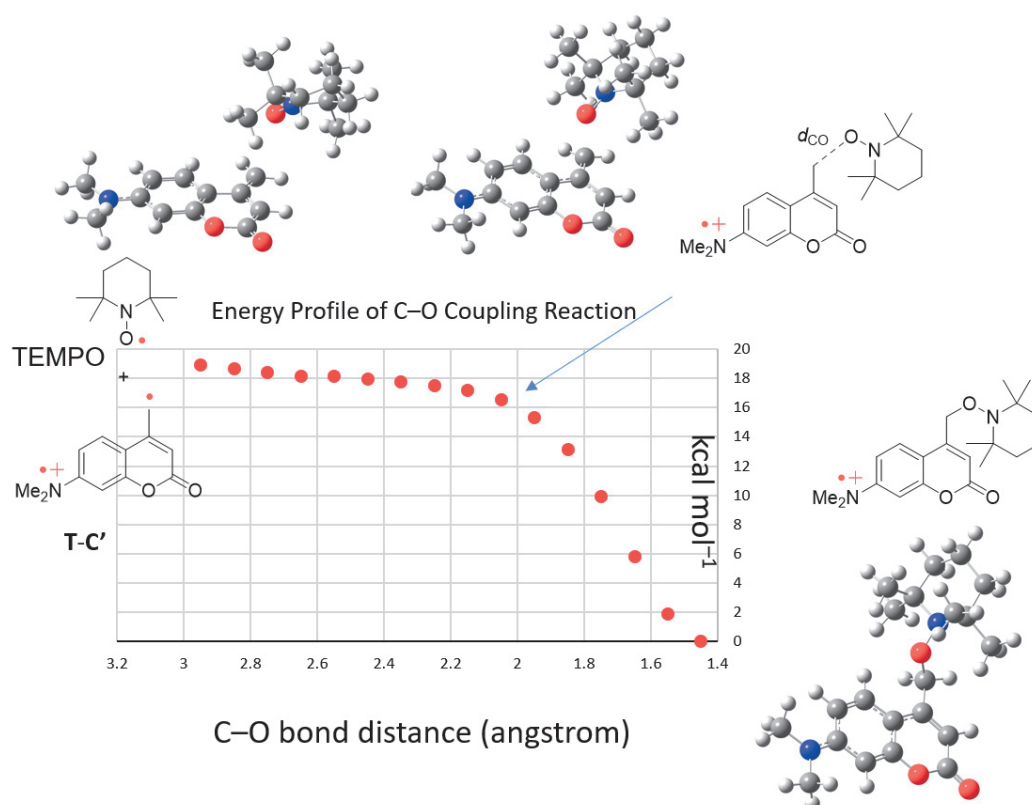


Figure S31. Energy profile of radical-radical coupling reaction of triplet cation **T-C'** with TEMPO at the UB3LYP/6-31G(d) level of theory.

Thioacetate radical

opt freq ub3lyp/6-31+g(d,p) scrf=(cpcm,solvent=dmsol); 0, 2

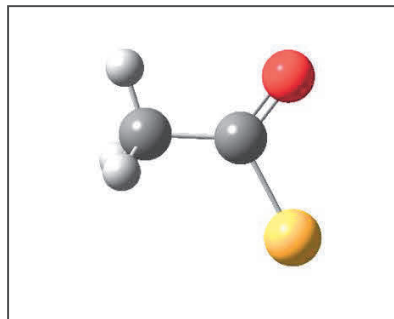
Number of Imaginary Frequencies = 0

Sum of electronic and zero-point Energies = -551.368346

Sum of electronic and thermal Energies = -551.364240

Sum of electronic and thermal Enthalpy = -551.363296

Sum of electronic and thermal Free Energy = -551.396182



Cartesian coordinate			
Atom	X	Y	Z
C	1.45478	-0.85825	-0.00001
H	2.4472	-0.39732	0.00001
H	1.34184	-1.49452	0.88637
H	1.34178	-1.49454	-0.88635
C	0.40068	0.20155	0.
S	-1.31759	-0.24669	0.
O	0.60223	1.4092	0.

Thioacetate radical

opt freq ub3lyp/6-31+g(d) scrf=(smd,solvent=dmsol); 0, 2

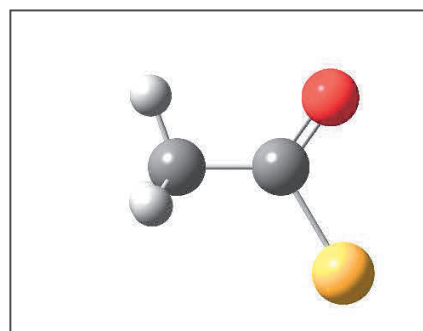
Number of Imaginary Frequencies = 0

Sum of electronic and zero-point Energies = -551.367686

Sum of electronic and thermal Energies = -551.362763

Sum of electronic and thermal Enthalpy = -551.361818

Sum of electronic and thermal Free Energy = -551.396875



Cartesian coordinate			
Atom	X	Y	Z
C	0.00057	0.00029	1.52911
H	1.01234	0.00199	1.87728
H	-0.50084	0.87564	1.88582
H	-0.50079	-0.87164	1.89419
C	-0.01239	-0.00709	-0.01081
S	-1.3548	-0.7821	-0.88585
O	0.92607	0.53478	-0.65054

Thioacetate anion

opt freq rb3lyp/6-31+g(d,p) scrf=(cpcm, solvent=dmsol); -1, 1

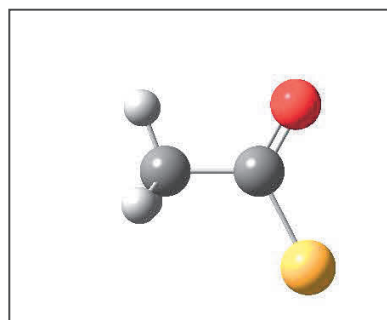
Number of Imaginary Frequencies = 0

Sum of electronic and zero-point Energies = -551.558338

Sum of electronic and thermal Energies = -551.553662

Sum of electronic and thermal Enthalpy = -551.552717

Sum of electronic and thermal Free Energy = -551.586602



Cartesian coordinate			
Atom	X	Y	Z
C	1.32878	-0.9758	0.00001
H	2.3679	-0.62708	0.00057
H	1.15926	-1.60552	0.88148
H	1.16003	-1.60481	-0.88213
C	0.36901	0.21443	0.00002
S	-1.35086	-0.15476	0.
O	0.84249	1.36023	0.

Thioacetate anion

opt freq rb3lyp/6-31+g(d) scrf=(smd, solvent=dmsol); -1, 1

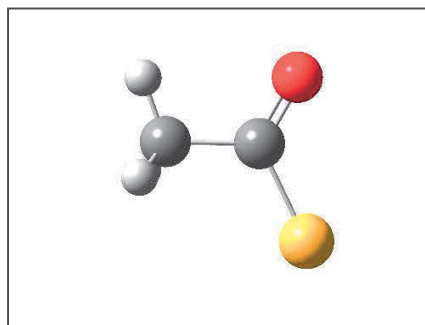
Number of Imaginary Frequencies = 0

Sum of electronic and zero-point Energies = -551.548908

Sum of electronic and thermal Energies = -551.544132

Sum of electronic and thermal Enthalpy = -551.543188

Sum of electronic and thermal Free Energy = -551.578593



Cartesian coordinate			
Atom	X	Y	Z
C	0.00057	0.00029	1.52911
H	1.01234	0.00199	1.87728
H	-0.50084	0.87564	1.88582
H	-0.50079	-0.87164	1.89419
C	-0.01239	-0.00709	-0.01081
S	-1.3548	-0.7821	-0.88585
O	0.92607	0.53478	-0.65054

Acetate radical

opt freq ub3lyp/6-31+g(d,p) scrf=(cpcm,solvent=dmsol); 0, 2

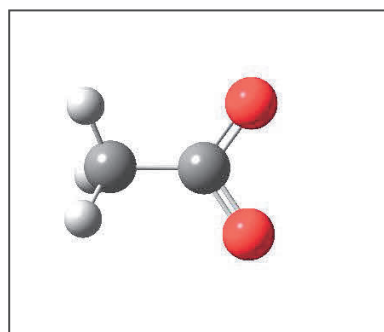
Number of Imaginary Frequencies = 0

Sum of electronic and zero-point Energies = -228.387560

Sum of electronic and thermal Energies = -228.383876

Sum of electronic and thermal Enthalpy = -228.382932

Sum of electronic and thermal Free Energy = -228.414124



Cartesian coordinate			
Atom	X	Y	Z
C	-0.09211	0.00017	-0.00951

C	1.39223	0.00107	-0.00271
H	1.77505	0.91237	-0.47262
H	1.7355	-0.02824	1.0395
H	1.77522	-0.88366	-0.52116
O	-0.81687	-1.03987	0.00172
O	-0.81893	1.03888	0.00173

Acetate radical

opt freq ub3lyp/6-31+g(d) scrf=(smd,solvent=dmsol); 0, 2

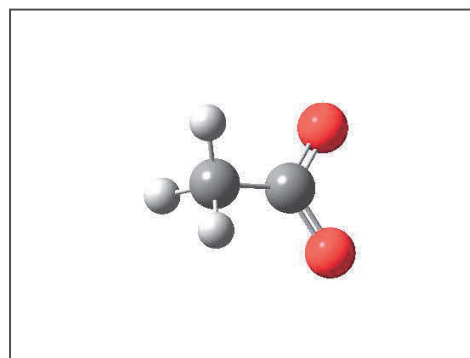
Number of Imaginary Frequencies = 0

Sum of electronic and zero-point Energies = -228.387626

Sum of electronic and thermal Energies = -228.383079

Sum of electronic and thermal Enthalpy = -228.382135

Sum of electronic and thermal Free Energy = -228.416175



Cartesian coordinate			
Atom	X	Y	Z
C	0.	0.	0.
C	0.	0.	1.54
H	1.00881	0.	1.89667
H	-0.5044	0.87365	1.89667
H	-0.5044	-0.87365	1.89667
O	-1.0725	-0.61921	-0.715
O	0.9438	0.5449	0.6292

Acetate anion

opt freq rb3lyp/6-31+g(d,p) scrf=(cpcm,solvent=dmsol); -1, 1

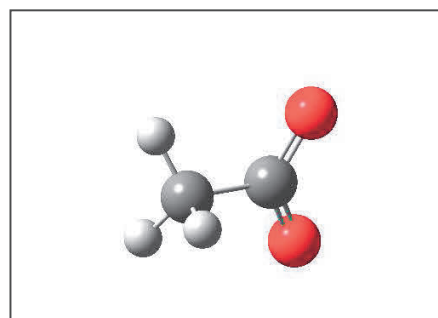
Number of Imaginary Frequencies = 0

Sum of electronic and zero-point Energies = -228.599074

Sum of electronic and thermal Energies = -228.594666

Sum of electronic and thermal Enthalpy = -228.593722

Sum of electronic and thermal Free Energy = -228.626672



Cartesian coordinate			
Atom	X	Y	Z
C	-0.19249	0.00004	-0.01112
C	1.35184	0.00401	-0.00416
H	1.7565	0.90525	-0.47938
H	1.70462	-0.00777	1.03735
H	1.75844	-0.88487	-0.5002
O	-0.75648	-1.13326	0.00214
O	-0.76548	1.12864	0.0021

Acetate anion

opt freq rb3lyp/6-31+g(d) scrf=(smd,solvent=dms0); -1, 1

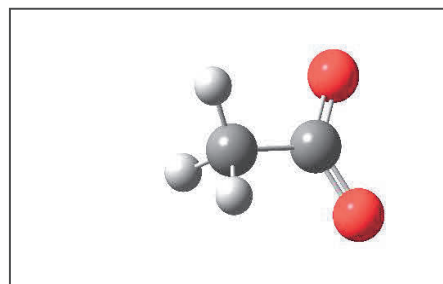
Number of Imaginary Frequencies = 0

Sum of electronic and zero-point Energies = -228.584644

Sum of electronic and thermal Energies = -228.580253

Sum of electronic and thermal Enthalpy = -228.579309

Sum of electronic and thermal Free Energy = -228.612105



Cartesian coordinate			
Atom	X	Y	Z
C	0.	0.	0.
C	0.	0.	1.54
H	1.00881	0.	1.89667
H	-0.5044	0.87365	1.89667
H	-0.5044	-0.87365	1.89667
O	-1.0725	-0.61921	-0.715
O	0.9438	0.5449	0.6292

Radical A

opt freq ub3lyp/6-31+g(d,p) scrf=(cpcm, solvent=dmsol); 0, 2

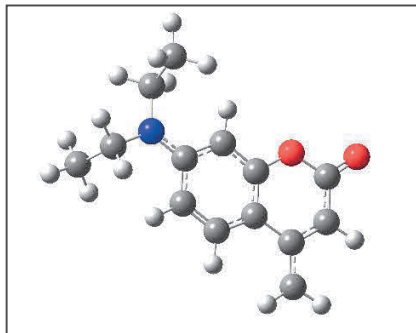
Number of Imaginary Frequencies = 0

Sum of electronic and zero-point Energies = -748.083723

Sum of electronic and thermal Energies = -748.067695

Sum of electronic and thermal Enthalpy = -748.066751

Sum of electronic and thermal Free Energy = -748.127819



Cartesian coordinate			
Atom	X	Y	Z
H	-0.54921	1.83537	-0.24451
C	-0.31433	0.78684	-0.11165
C	0.45179	-1.86307	0.28182
C	1.02696	0.42628	-0.07618
C	-1.32627	-0.19203	0.04632
C	-0.89243	-1.53902	0.24539
C	1.46623	-0.89619	0.12135
H	-1.61557	-2.33751	0.35565
H	0.72302	-2.90389	0.43206
N	-2.65786	0.13707	0.00788
C	-3.11195	1.49664	-0.30373
H	-2.45104	1.93803	-1.05642
H	-4.09581	1.40605	-0.7758
C	-3.71343	-0.84699	0.27411
H	-4.55942	-0.30038	0.70403
H	-3.37629	-1.54426	1.04678
C	-4.17364	-1.60719	-0.97379
H	-4.98212	-2.30204	-0.71254
H	-3.35463	-2.18633	-1.41554
H	-4.55376	-0.91532	-1.73526
C	-3.21364	2.40767	0.92417
H	-2.24019	2.53768	1.41068
H	-3.91249	1.99347	1.66108
H	-3.58133	3.39798	0.62625

O	1.92152	1.46549	-0.23985
C	3.29164	1.27222	-0.22572
O	3.99208	2.26835	-0.38099
C	3.7643	-0.06912	-0.0321
H	4.84023	-0.20646	-0.02556
C	2.90219	-1.16141	0.14263
C	3.44925	-2.43962	0.32741
H	4.5275	-2.56877	0.33339
H	2.83744	-3.32388	0.46714

Radical A

opt freq ub3lyp/6-31+g(d) scrf=(smd, solvent=dmsol); 0, 2

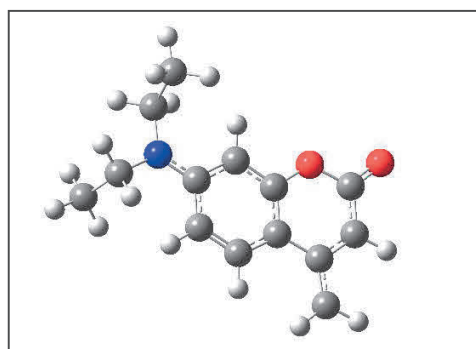
Number of Imaginary Frequencies = 0

Sum of electronic and zero-point Energies = -748.066553

Sum of electronic and thermal Energies = -748.050587

Sum of electronic and thermal Enthalpy = -748.049642

Sum of electronic and thermal Free Energy = -748.110507



Cartesian coordinate			
Atom	X	Y	Z
H	3.68602	-0.89771	-2.27424
C	3.45938	0.14911	-2.12409
C	2.84556	2.85249	-1.96602
C	3.75585	1.01039	-3.17725
C	2.85578	0.63171	-0.94772
C	2.55035	2.01938	-0.90281
C	3.46111	2.38374	-3.13991
H	2.10599	2.4507	-0.01443
H	2.59901	3.90605	-1.87552
N	2.57097	-0.18991	0.13733
C	2.9819	-1.59504	0.12139

H	4.05398	-1.68808	-0.12548
H	2.85246	-1.99116	1.13016
C	1.46403	0.16774	1.03375
H	0.9315	-0.75423	1.29692
H	0.74428	0.77794	0.47715
C	1.8859	0.89831	2.31464
H	1.00266	1.1453	2.91624
H	2.4145	1.82945	2.08648
H	2.55198	0.28111	2.92462
C	2.15957	-2.47469	-0.82423
H	2.26563	-2.18447	-1.8742
H	1.09682	-2.44271	-0.56277
H	2.50264	-3.51148	-0.73624
O	4.34062	0.41669	-4.2681
C	4.68878	1.13687	-5.4067
O	5.20075	0.53068	-6.32489
C	4.40555	2.55418	-5.3863
H	4.68804	3.09887	-6.28003
C	3.80707	3.20705	-4.30181
C	3.57029	4.58145	-4.37227
H	3.84893	5.13679	-5.26147
H	3.1115	5.14008	-3.56534

T-C

opt freq ub3lyp/6-31+g(d,p) scrf=(cpcm, solvent=dmsol); 1, 3

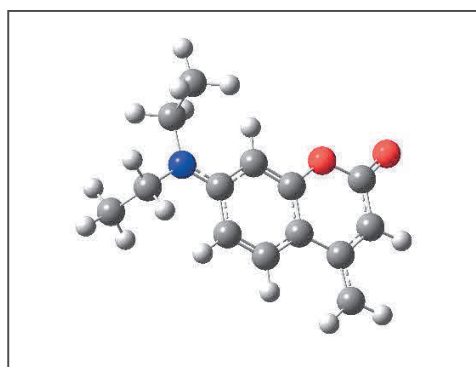
Number of Imaginary Frequencies = 0

Sum of electronic and zero-point Energies = -747.889110

Sum of electronic and thermal Energies = -747.873154

Sum of electronic and thermal Enthalpy = -747.872210

Sum of electronic and thermal Free Energy = -747.933416



Cartesian coordinate			
Atom	X	Y	Z
H	0.55464	1.84507	0.26603
C	0.30623	0.80204	0.12247
C	-0.44616	-1.87047	-0.28955
C	-1.02455	0.45058	0.08172
C	1.31191	-0.19513	-0.04962
C	0.88881	-1.55336	-0.26273
C	-1.45523	-0.88857	-0.12098
H	1.61503	-2.34555	-0.38432
H	-0.72735	-2.90587	-0.4428
N	2.62489	0.12895	-0.00932
C	3.09909	1.4951	0.29657
H	2.42948	1.95276	1.025
H	4.07427	1.37695	0.77477
C	3.69747	-0.85505	-0.26562
H	4.52341	-0.29431	-0.70985
H	3.35316	-1.57578	-1.00639
C	4.1566	-1.54749	1.02141
H	4.98333	-2.22359	0.77673
H	3.34611	-2.13286	1.46767
H	4.51349	-0.81887	1.75699
C	3.22777	2.35158	-0.96742
H	2.25596	2.5007	-1.44908
H	3.91268	1.89082	-1.68708
H	3.63102	3.33027	-0.6846
O	-1.91409	1.48159	0.2463
C	-3.28416	1.27848	0.22781
O	-3.99304	2.26018	0.3803
C	-3.74988	-0.07048	0.03165
H	-4.82523	-0.21042	0.02406
C	-2.88614	-1.16961	-0.14401
C	-3.4183	-2.44705	-0.32766
H	-2.80235	-3.32813	-0.46385
H	-4.49557	-2.58133	-0.33507

T-C

opt freq ub3lyp/6-31+g(d) scrf=(smd,solvent=dmsd); 1, 3

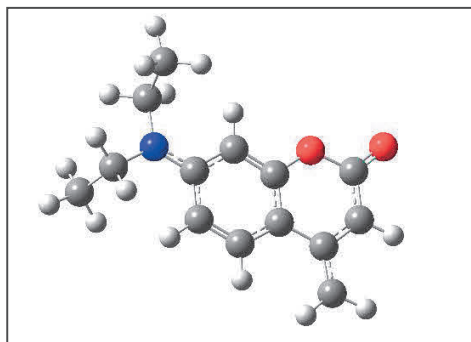
Number of Imaginary Frequencies = 0

Sum of electronic and zero-point Energies = -747.884200

Sum of electronic and thermal Energies = -747.868523

Sum of electronic and thermal Enthalpy = -747.867580

Sum of electronic and thermal Free Energy = -747.927701



Cartesian coordinate			
Atom	X	Y	Z
H	0.55391	-1.84576	-0.26389
C	0.30589	-0.80303	-0.12143
C	-0.44483	1.86871	0.28707
C	-1.02519	-0.45431	-0.08125
C	1.31123	0.19326	0.04948
C	0.88877	1.5517	0.26125
C	-1.45365	0.88762	0.12008
H	1.61597	2.34265	0.38176
H	-0.72637	2.90377	0.43895
N	2.62321	-0.12958	0.00914
C	3.09656	-1.49489	-0.29914
H	2.42635	-1.94891	-1.02903
H	4.07125	-1.37671	-0.77779
C	3.69514	0.85392	0.26795
H	4.52084	0.29257	0.71122
H	3.35027	1.571	1.01185
C	4.1527	1.55074	-1.01596
H	4.97914	2.22619	-0.77148
H	3.3413	2.13645	-1.45911
H	4.50794	0.8251	-1.75467
C	3.22331	-2.35398	0.96192
H	2.25128	-2.50186	1.44253
H	3.90733	-1.89553	1.68327

H	3.62525	-3.33239	0.67885
O	-1.9111	-1.48253	-0.24385
C	-3.28596	-1.27912	-0.22672
O	-3.99332	-2.2553	-0.3787
C	-3.74643	0.07298	-0.03109
H	-4.82122	0.21351	-0.02365
C	-2.88272	1.1712	0.14338
C	-3.41014	2.44914	0.3263
H	-2.79225	3.32844	0.46141
H	-4.48634	2.58758	0.33504

S-OC

opt freq ub3lyp/6-31+g(d) scrf=(smd,solvent=dmsol) guess=(mix,always); 1, 1

Number of Imaginary Frequencies = 0

$\langle S^2 \rangle = 1.016$

Sum of electronic and zero-point Energies (broken-symmetry) = -747.879147

Sum of electronic and thermal Energies (broken-symmetry) = -747.863500

Sum of electronic and thermal Enthalpy (broken-symmetry) = -747.862556

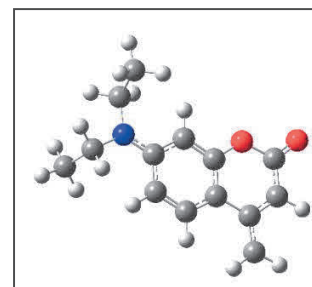
Sum of electronic and thermal Free Energy (broken-symmetry) = -747.921566

Sum of electronic and zero-point Energies (after corrected) = -747.873831

Sum of electronic and thermal Energies (after corrected) = -747.858183

Sum of electronic and thermal Enthalpy (after corrected) = -747.857239

Sum of electronic and thermal Free Energy (after corrected) = -747.916249



The correction method: the spin contamination was removed by using the following equation:

$$E_{\text{singlet}} = \frac{2E_{\langle S_z \rangle = 0} - \langle S^2 \rangle E_{\langle S_z \rangle = 1}}{2 - \langle S^2 \rangle} \quad (6)$$

Where E_{singlet} is the corrected singlet energy, $E_{\langle S_z \rangle = 0}$ is the broken-symmetry energy, $\langle S^2 \rangle$ is the expectation value of the total-spin operator for the broken-symmetry calculation and $E_{\langle S_z \rangle = 1}$ is the energy of the triplet state at the singlet geometry.⁵⁹

Cartesian coordinate			
Atom	X	Y	Z
H	-0.54678	1.84323	-0.2545
C	-0.30982	0.79678	-0.11563
C	0.43448	-1.88263	0.29387
C	1.01936	0.43102	-0.078
C	-1.32277	-0.18843	0.05052
C	-0.89899	-1.54676	0.25995
C	1.4438	-0.90863	0.12544
H	-1.62982	-2.33577	0.37735
H	0.70047	-2.92256	0.44972
N	-2.63869	0.13754	0.009
C	-3.09944	1.50168	-0.29912
H	-2.43166	1.95103	-1.03753
H	-4.07767	1.39937	-0.7772
C	-3.70827	-0.84262	0.26464
H	-4.54139	-0.28555	0.70277
H	-3.37397	-1.55606	1.01993
C	-4.16969	-1.56141	-1.00644
H	-4.99272	-2.24249	-0.75904
H	-3.35703	-2.14729	-1.44986
H	-4.5309	-0.8458	-1.75382
C	-3.21686	2.38408	0.94768
H	-2.24532	2.52024	1.43514
H	-3.9123	1.94652	1.67294
H	-3.5989	3.37029	0.65814
O	1.93441	1.44407	-0.24262
C	3.31018	1.26405	-0.22898
O	4.00776	2.25534	-0.38565
C	3.77899	-0.08036	-0.03165
H	4.84917	-0.24881	-0.0221
C	2.87564	-1.14704	0.14215
C	3.41651	-2.41282	0.32593
H	4.49595	-2.5447	0.33449
H	2.80765	-3.3012	0.46468

S-RC

opt freq rb3lyp/6-31+g(d) scrf=(smd,solvent=dmsd); 1, 1

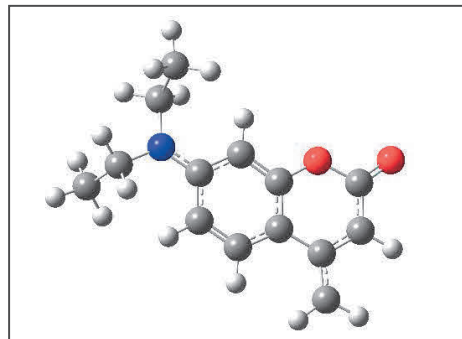
Number of Imaginary Frequencies = 0

Sum of electronic and zero-point Energies = -747.859694

Sum of electronic and thermal Energies = -747.843970

Sum of electronic and thermal Enthalpy = -747.843026

Sum of electronic and thermal Free Energy = -747.902339



Cartesian coordinate			
Atom	X	Y	Z
H	3.68602	-0.89771	-2.27424
C	3.45938	0.14911	-2.12409
C	2.84556	2.85249	-1.96602
C	3.75585	1.01039	-3.17725
C	2.85578	0.63171	-0.94772
C	2.55035	2.01938	-0.90281
C	3.46111	2.38374	-3.13991
H	2.10599	2.4507	-0.01443
H	2.59901	3.90605	-1.87552
N	2.57097	-0.18991	0.13733
C	2.9819	-1.59504	0.12139
H	4.05398	-1.68808	-0.12548
H	2.85246	-1.99116	1.13016
C	1.46403	0.16774	1.03375
H	0.9315	-0.75423	1.29692
H	0.74428	0.77794	0.47715
C	1.8859	0.89831	2.31464
H	1.00266	1.1453	2.91624
H	2.4145	1.82945	2.08648
H	2.55198	0.28111	2.92462
C	2.15957	-2.47469	-0.82423
H	2.26563	-2.18447	-1.8742
H	1.09682	-2.44271	-0.56277
H	2.50264	-3.51148	-0.73624

O	4.34062	0.41669	-4.2681
C	4.68878	1.13687	-5.4067
O	5.20075	0.53068	-6.32489
C	4.40555	2.55418	-5.3863
H	4.68804	3.09887	-6.28003
C	3.80707	3.20705	-4.30181
C	3.57029	4.58145	-4.37227
H	3.84893	5.13679	-5.26147
H	3.1115	5.14008	-3.56534

Intermediate 10

opt freq ub3lyp/6-31+g(d) scrf=(smd,solvent=dms0); 1, 3

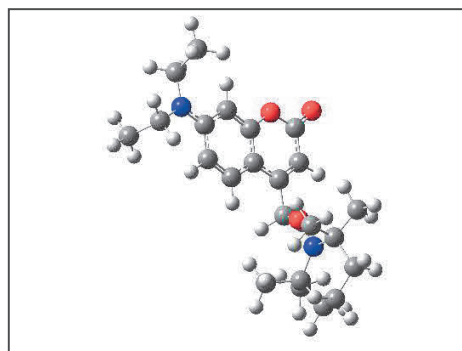
Number of Imaginary Frequencies = 0

Sum of electronic and zero-point Energies = -1231.387281

Sum of electronic and thermal Energies = -1231.358751

Sum of electronic and thermal Enthalpy = -1231.357807

Sum of electronic and thermal Free Energy = -1231.446850



Cartesian coordinate			
Atom	X	Y	Z
H	0.92305	1.66297	0.40635
C	0.5594	0.70223	0.10783
C	-0.42022	-1.89391	-0.71293
C	-0.92142	0.34183	0.33048
C	1.40448	-0.19233	-0.45713
C	0.88964	-1.58415	-0.86864
C	-1.39207	-0.85789	-0.1164
H	1.56567	-2.30472	-1.28197
H	-0.78048	-2.85743	-1.01015
N	2.81316	0.16983	-0.67593
C	3.20447	1.19536	0.30202

H	2.395	1.36789	0.97973
H	4.06163	0.86143	0.84747
C	3.80686	-0.91309	-0.66661
H	4.77336	-0.51225	-0.89275
H	3.54236	-1.64326	-1.4021
C	3.84041	-1.57247	0.72505
H	4.5644	-2.36035	0.72836
H	2.87506	-1.97389	0.95345
H	4.10532	-0.84107	1.46016
C	3.54468	2.50438	-0.43657
H	2.68815	2.83742	-0.98444
H	4.3562	2.33198	-1.11294
H	3.82632	3.25209	0.27507
O	-1.75628	1.28973	1.02797
C	-3.16599	1.1236	0.81703
O	-3.94329	2.09208	1.02135
C	-3.73682	-0.2236	0.35878
H	-4.7942	-0.39111	0.35188
C	-2.88955	-1.18335	-0.04408
C	-3.4201	-2.57286	-0.44197
H	-2.67155	-3.31103	-0.24577
H	-4.29728	-2.7913	0.12989
O	-3.74948	-2.587	-1.83611
C	-4.65977	-3.83446	-3.56737
C	-3.24377	-4.84124	-1.87491
C	-5.27629	-5.20489	-3.90778
C	-3.82447	-6.23464	-2.16921
C	-4.23685	-6.30029	-3.64347
H	-5.56557	-5.22595	-4.93698
H	-6.13698	-5.371	-3.29335
H	-3.08776	-6.98287	-1.96895
H	-4.67966	-6.40313	-1.54771
H	-4.65645	-7.25944	-3.8607
H	-3.37943	-6.14002	-4.26421
C	-3.42024	-3.59207	-4.44948
H	-3.70642	-3.61057	-5.48054
H	-2.99576	-2.63854	-4.21391

H	-2.69696	-4.3595	-4.26657
C	-5.70151	-2.73069	-3.83206
H	-6.56317	-2.89956	-3.22056
H	-5.27897	-1.77613	-3.59713
H	-5.98674	-2.75025	-4.86347
C	-2.82215	-4.76852	-0.39602
H	-2.41458	-3.80076	-0.18778
H	-3.67556	-4.93718	0.22674
H	-2.08306	-5.51653	-0.19936
C	-2.01651	-4.59562	-2.77276
H	-1.27459	-5.3415	-2.5755
H	-2.31031	-4.64864	-3.8005
H	-1.61183	-3.62693	-2.56681
N	-4.26402	-3.80769	-2.14318

Compound 1a

opt freq rb3lyp/6-31+g(d) scrf=(smd,solvent=dmsol); 0, 1

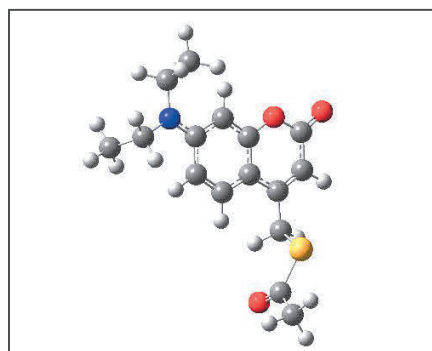
Number of Imaginary Frequencies = 0

Sum of electronic and zero-point Energies = -1299.515925

Sum of electronic and thermal Energies = -1299.494580

Sum of electronic and thermal Enthalpy = -1299.493636

Sum of electronic and thermal Free Energy = -1299.568395



Cartesian coordinate			
Atom	X	Y	Z
H	-2.61156	1.7971	0.29259
C	-1.86515	1.05309	0.04728
C	0.18924	-0.74033	-0.54001
C	-0.55918	1.49744	-0.11801
C	-2.17919	-0.31806	-0.08277
C	-1.10384	-1.20452	-0.38712
C	0.51376	0.62718	-0.40888
H	-1.28651	-2.26252	-0.527
H	0.9674	-1.45781	-0.78063

O	-0.36577	2.84466	0.0248
C	0.88399	3.44398	-0.1269
O	0.94962	4.64817	0.00959
C	1.82971	1.20281	-0.56025
C	1.98702	2.5521	-0.43109
H	2.95379	3.03144	-0.54264
C	3.03418	0.34487	-0.85643
H	2.81237	-0.48017	-1.53988
H	3.83079	0.95284	-1.29084
S	3.73369	-0.43986	0.6636
C	3.64166	-2.18567	0.24082
O	3.16994	-2.60286	-0.79857
C	4.21523	-3.09185	1.31072
H	5.06688	-3.63518	0.88588
H	3.45439	-3.82804	1.59167
H	4.54226	-2.54541	2.19922
N	-3.46968	-0.77814	0.07126
C	-3.7909	-2.20581	0.06377
H	-2.98254	-2.76251	0.54903
H	-4.67167	-2.34379	0.70184
C	-4.07485	-2.7742	-1.3335
H	-3.20607	-2.66866	-1.99161
H	-4.91722	-2.25407	-1.80426
H	-4.32887	-3.83939	-1.2667
C	-4.59654	0.13756	0.25578
H	-5.48467	-0.35133	-0.16132
H	-4.43621	1.03405	-0.35222
C	-4.85793	0.51759	1.71981
H	-5.07275	-0.37224	2.32316
H	-5.72129	1.19068	1.78911
H	-3.99335	1.0229	2.1623

Compound 1b

opt freq rb3lyp/6-31+g(d) scrf=(smd,solvent=dmsd); 0, 1

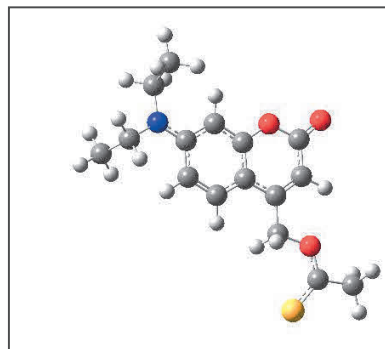
Number of Imaginary Frequencies = 0

Sum of electronic and zero-point Energies = -1299.495666

Sum of electronic and thermal Energies = -1299.474615

Sum of electronic and thermal Enthalpy = -1299.473671

Sum of electronic and thermal Free Energy = -1299.547840



Cartesian coordinate			
Atom	X	Y	Z
H	-2.86727	1.79911	-0.1292
C	-2.20678	0.94333	-0.08273
C	-0.36762	-1.14389	0.09051
C	-0.84078	1.19705	-0.10118
C	-2.6918	-0.37977	0.01934
C	-1.72185	-1.42249	0.10462
C	0.12617	0.17389	-0.01365
H	-2.03175	-2.45811	0.16337
H	0.32637	-1.9775	0.15343
N	-4.04287	-0.65178	0.03305
C	-5.04139	0.3976	-0.17935
H	-4.66471	1.10847	-0.92219
H	-5.91797	-0.07588	-0.63655
C	-4.56138	-1.99988	0.26955
H	-5.53886	-1.89123	0.75363
H	-3.92472	-2.51151	0.99884
C	-4.71021	-2.84337	-1.00409
H	-5.12149	-3.83081	-0.76058
H	-3.74644	-2.98625	-1.50396
H	-5.38873	-2.36033	-1.71674
C	-5.46122	1.12823	1.10355
H	-4.60942	1.6266	1.5776
H	-5.88907	0.42846	1.83095
H	-6.21985	1.88731	0.87682

O	-0.47539	2.51074	-0.19905
C	0.85959	2.9187	-0.22229
O	1.07769	4.10866	-0.31038
C	1.85844	1.86809	-0.13764
H	2.88867	2.19739	-0.15851
C	1.52015	0.55391	-0.03773
C	2.55013	-0.54254	0.05137
H	2.4408	-1.11499	0.98004
H	2.44733	-1.25167	-0.7785
O	3.86632	0.02453	0.01217
C	4.93928	-0.77864	0.0779
S	4.88847	-2.42086	0.20449
C	6.19295	0.05235	0.01836
H	7.07754	-0.58171	0.07064
H	6.20333	0.76916	0.84893
H	6.2099	0.63307	-0.91236

Compound 1c

opt freq rb3lyp/6-31+g(d) scrf=(smd,solvent=dmsol); 0, 1

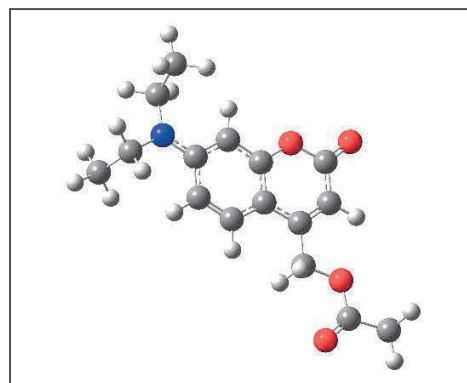
Number of Imaginary Frequencies = 0

Sum of electronic and zero-point Energies = -976.552177

Sum of electronic and thermal Energies = -976.531417

Sum of electronic and thermal Enthalpy = -976.530473

Sum of electronic and thermal Free Energy = -976.603439



Cartesian coordinate			
Atom	X	Y	Z
H	-2.86665	1.79764	-0.12837
C	-2.20594	0.94247	-0.08194
C	-0.36964	-1.1441	0.08878
C	-0.84064	1.19752	-0.10053
C	-2.69027	-0.37933	0.01925
C	-1.72268	-1.42192	0.10357
C	0.12372	0.17222	-0.01408

H	-2.03515	-2.45656	0.16128
H	0.32515	-1.97679	0.15084
N	-4.04177	-0.65088	0.03299
C	-5.03848	0.39802	-0.18181
H	-4.66045	1.10642	-0.92588
H	-5.91575	-0.07465	-0.63788
C	-4.5589	-1.99786	0.27164
H	-5.53784	-1.89024	0.75231
H	-3.92339	-2.50593	1.00401
C	-4.70025	-2.84408	-0.99992
H	-5.11121	-3.83139	-0.75877
H	-3.73316	-2.98507	-1.49293
H	-5.37429	-2.36243	-1.71702
C	-5.45526	1.13207	1.099
H	-4.601	1.62998	1.56812
H	-5.88009	0.43422	1.8293
H	-6.21381	1.8907	0.87405
O	-0.47627	2.50918	-0.19791
C	0.86129	2.91733	-0.22136
O	1.08123	4.1033	-0.30937
C	1.85671	1.86242	-0.13677
H	2.88758	2.18835	-0.1571
C	1.51772	0.55091	-0.03765
C	2.54793	-0.54488	0.05145
H	2.43808	-1.11965	0.97865
H	2.4445	-1.25618	-0.77652
O	3.85933	0.02395	0.01194
C	4.83455	-1.01837	0.09806
O	4.41372	-2.38098	0.20344
C	6.33644	-0.67849	0.0777
H	6.57606	-0.17605	-0.83611
H	6.56948	-0.04259	0.90608
H	6.90729	-1.58068	0.14897

Compound 5

opt freq rb3lyp/6-31+g(d) scrf=(smd,solvent=dmsd); 0, 1

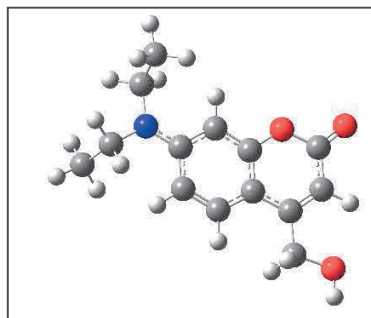
Number of Imaginary Frequencies = 0

Sum of electronic and zero-point Energies = -823.914533

Sum of electronic and thermal Energies = -823.897118

Sum of electronic and thermal Enthalpy = -823.896174

Sum of electronic and thermal Free Energy = -823.959885



Cartesian coordinate			
Atom	X	Y	Z
H	-2.48752	1.84644	-0.1417
C	-1.88392	0.94936	-0.08872
C	-0.19948	-1.27147	0.10849
C	-0.50471	1.09646	-0.10679
C	-2.46587	-0.33873	0.02594
C	-1.56816	-1.44997	0.12446
C	0.39014	0.00957	-0.00814
H	-1.95229	-2.45985	0.19518
H	0.43463	-2.15049	0.17864
N	-3.82349	-0.51292	0.03877
C	-4.7522	0.6009	-0.18841
H	-4.32169	1.28837	-0.92308
H	-5.64984	0.17907	-0.65219
C	-4.44393	-1.8214	0.28316
H	-5.40722	-1.63089	0.76762
H	-3.84349	-2.38031	1.00669
C	-4.66139	-2.645	-0.98956
H	-5.15754	-3.59199	-0.74149
H	-3.71176	-2.87629	-1.48541
H	-5.2973	-2.10508	-1.70159
C	-5.13784	1.34952	1.09138
H	-4.26383	1.80606	1.56965
H	-5.60916	0.67189	1.81353

H	-5.85397	2.14711	0.85603
O	-0.03633	2.38357	-0.21718
C	1.31666	2.68334	-0.24272
O	1.61498	3.86686	-0.34607
C	2.23619	1.5777	-0.14538
H	3.28856	1.82926	-0.16648
C	1.80285	0.28589	-0.03155
C	2.75746	-0.87418	0.07241
H	2.58733	-1.42642	1.00287
H	2.60609	-1.56943	-0.76068
O	4.10462	-0.39518	0.04751
H	4.70992	-1.13755	0.11152

Triplet state of 1a

opt freq ub3lyp/6-31+g(d) scrf=(smd,solvent=dmsol); 0, 3

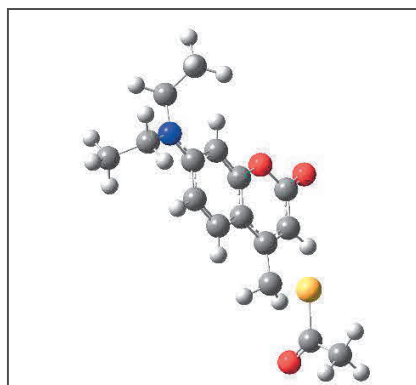
Number of Imaginary Frequencies = 0

Sum of electronic and zero-point Energies = -1299.439243

Sum of electronic and thermal Energies = -1299.417305

Sum of electronic and thermal Enthalpy = -1299.416361

Sum of electronic and thermal Free Energy = -1299.494476



Cartesian coordinate			
Atom	X	Y	Z
H	-2.79854	1.68884	0.21933
C	-2.01783	0.96731	0.01518
C	0.10475	-0.78323	-0.47062
C	-0.72339	1.44111	-0.13745
C	-2.28787	-0.42207	-0.07399
C	-1.17282	-1.2843	-0.32767
C	0.38619	0.60049	-0.37979
H	-1.31915	-2.35209	-0.43078
H	0.91114	-1.48286	-0.66702
O	-0.56543	2.80253	-0.03267

C	0.66648	3.4238	-0.16589
O	0.6835	4.64356	-0.05641
C	1.68252	1.2097	-0.51897
C	1.80022	2.57099	-0.41686
H	2.76034	3.06535	-0.52039
C	2.91816	0.38604	-0.77419
H	2.73824	-0.43309	-1.47501
H	3.71421	1.01566	-1.17718
S	3.5319	-0.37794	0.79353
C	4.2903	-1.88945	0.17112
O	4.30007	-2.1867	-1.00909
C	4.91488	-2.73753	1.25151
H	5.99318	-2.80382	1.0619
H	4.49722	-3.74915	1.18948
H	4.75252	-2.33872	2.25654
N	-3.55516	-0.91703	0.0707
C	-3.83471	-2.35892	0.09731
H	-3.01651	-2.87993	0.60282
H	-4.72094	-2.49952	0.72463
C	-4.08456	-2.9603	-1.289
H	-3.20489	-2.85975	-1.93497
H	-4.93077	-2.4674	-1.78282
H	-4.32035	-4.02808	-1.19578
C	-4.72126	-0.03707	0.21819
H	-5.57986	-0.57216	-0.20009
H	-4.58398	0.85453	-0.40103
C	-5.01559	0.35267	1.67006
H	-5.20052	-0.53733	2.28366
H	-5.91074	0.98618	1.7118
H	-4.18287	0.90894	2.1151

Triplet state of 1b

opt freq ub3lyp/6-31+g(d) scrf=(smd,solvent=dmsol); 0, 3

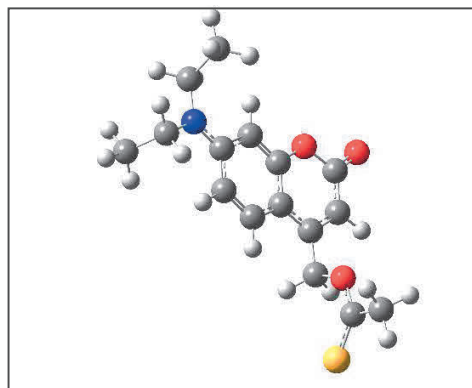
Number of Imaginary Frequencies = 0

Sum of electronic and zero-point Energies = -1299.420076

Sum of electronic and thermal Energies = -1299.398642

Sum of electronic and thermal Enthalpy = -1299.397698

Sum of electronic and thermal Free Energy = -1299.474141



Cartesian coordinate			
Atom	X	Y	Z
H	-2.86294	1.70597	0.10372
C	-2.11012	0.94086	-0.03485
C	-0.06422	-0.94163	-0.3323
C	-0.81186	1.36734	-0.17337
C	-2.44203	-0.4485	-0.04842
C	-1.3652	-1.37307	-0.19953
C	0.29258	0.44941	-0.34646
H	-1.55542	-2.43921	-0.22162
H	0.72171	-1.6825	-0.43193
N	-3.7455	-0.86992	0.08236
C	-4.8689	0.07303	0.12137
H	-4.6578	0.91105	-0.54833
H	-5.73685	-0.44455	-0.30185
C	-4.09921	-2.28899	0.19008
H	-5.01422	-2.34685	0.78976
H	-3.32776	-2.81035	0.76365
C	-4.32414	-2.96964	-1.16692
H	-4.60999	-4.01756	-1.01749
H	-3.41816	-2.94329	-1.7808
H	-5.12623	-2.47627	-1.72742
C	-5.19984	0.57336	1.53396
H	-4.3552	1.11286	1.9738
H	-5.45306	-0.26045	2.19866
H	-6.06042	1.25162	1.49771

C	0.58949	0.34429	-0.3689
H	-1.45405	-2.40834	-0.33486
H	0.87079	-1.80146	-0.55862
N	-3.51046	-0.70144	0.08079
C	-4.57171	0.31079	0.18813
H	-4.31282	1.17198	-0.43068
H	-5.47184	-0.13325	-0.24596
C	-3.96793	-2.09825	0.12995
H	-4.8705	-2.10963	0.74708
H	-3.22256	-2.70409	0.64861
C	-4.27573	-2.67036	-1.25656
H	-4.65229	-3.69412	-1.15206
H	-3.37955	-2.69402	-1.88518
H	-5.0411	-2.07485	-1.76622
C	-4.84299	0.73464	1.63433
H	-3.96289	1.20783	2.08193
H	-5.12487	-0.12611	2.25063
H	-5.66961	1.45383	1.65294
O	-0.14114	2.66873	-0.04812
C	1.19295	3.13548	-0.14996
O	1.33582	4.35001	-0.02289
C	2.19545	2.16752	-0.38651
H	3.21069	2.5421	-0.46584
C	1.92674	0.76434	-0.53477
C	3.03562	-0.18533	-0.80788
H	2.75106	-0.98553	-1.49746
H	3.90328	0.33028	-1.2277
O	3.46445	-0.8283	0.45305
C	4.48622	-1.69842	0.35452
O	5.04982	-1.96571	-0.69112
C	4.83648	-2.28328	1.70142
H	5.14966	-1.48711	2.38609
H	3.96099	-2.7712	2.14333
H	5.64489	-3.00811	1.59083

Triplet state of 7

opt freq ub3lyp/6-31+g(d) scrf=(smd,solvent=dmsol); 0, 3

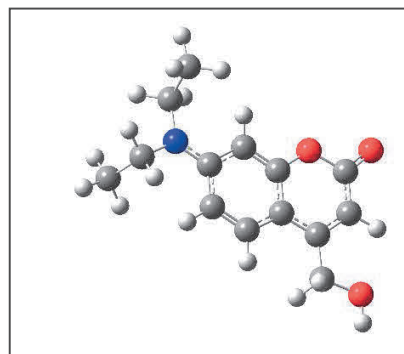
Number of Imaginary Frequencies = 0

Sum of electronic and zero-point Energies = -823.831758

Sum of electronic and thermal Energies = -823.813757

Sum of electronic and thermal Enthalpy = -823.812813

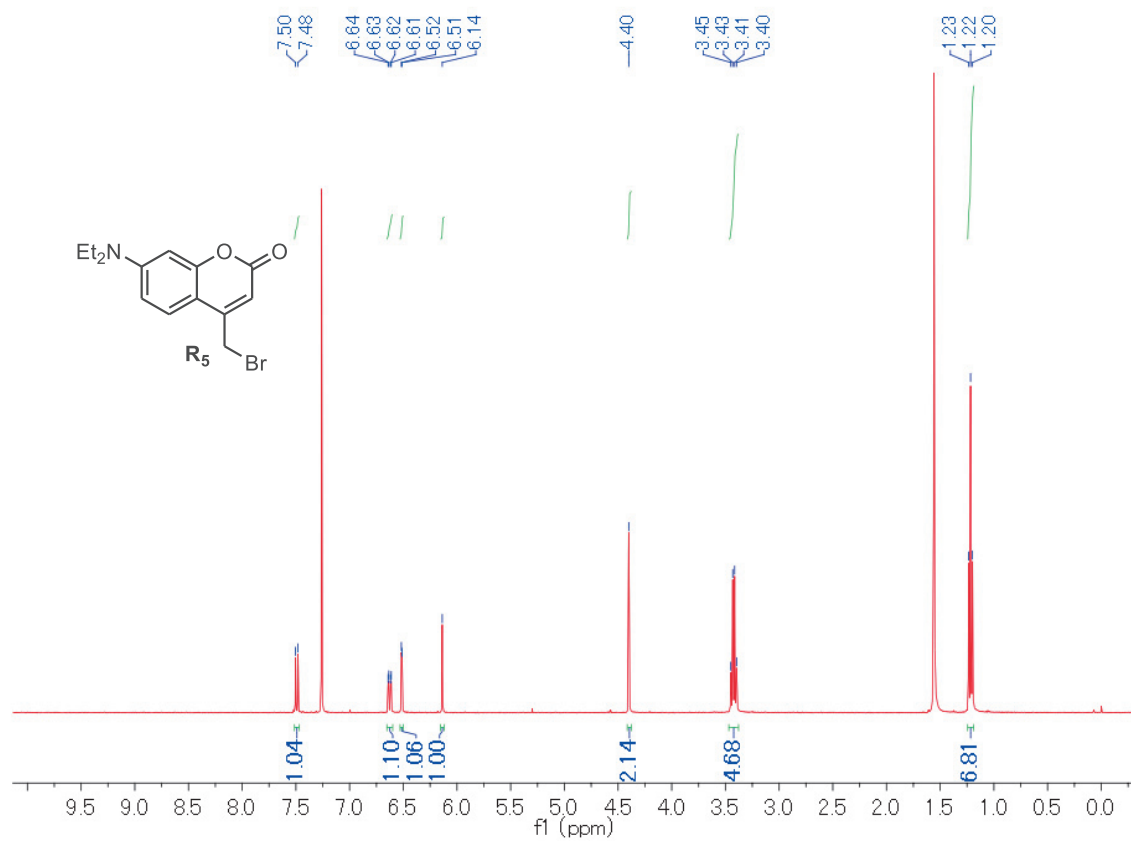
Sum of electronic and thermal Free Energy = -823.879484

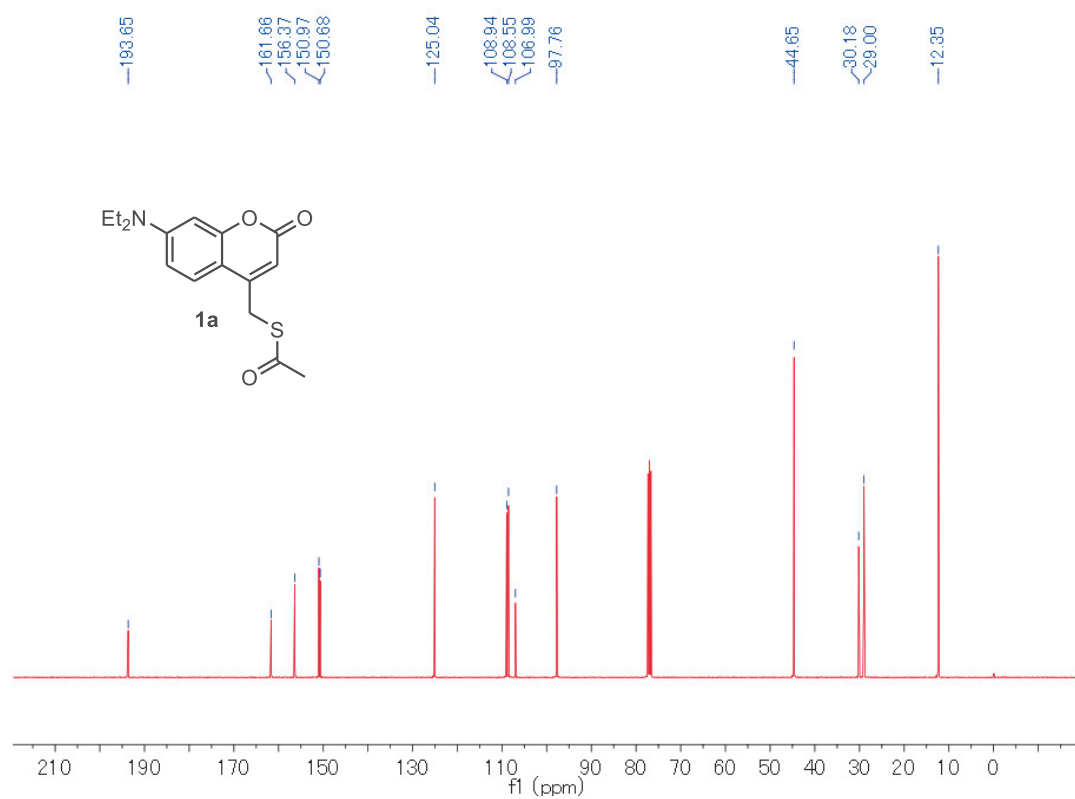
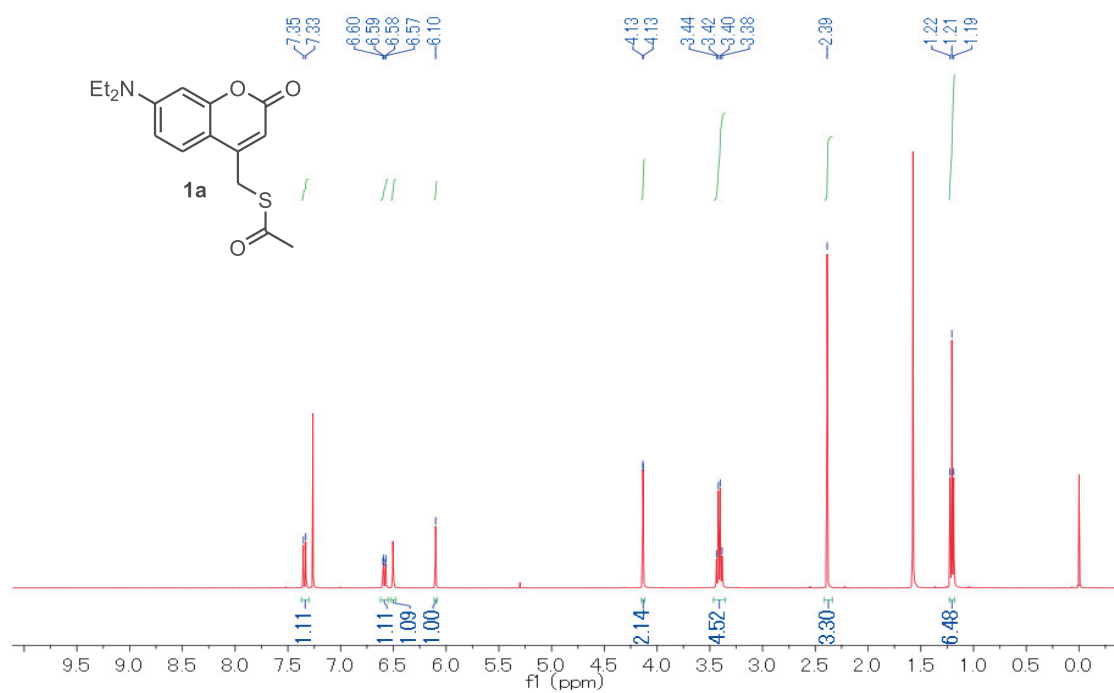


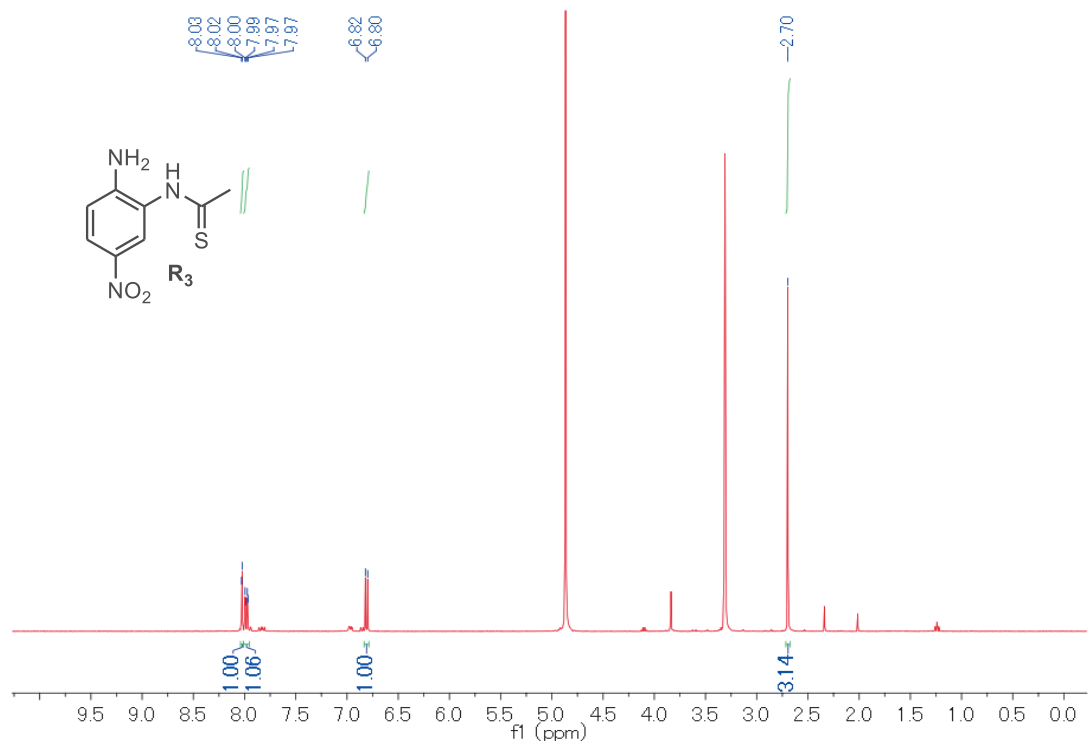
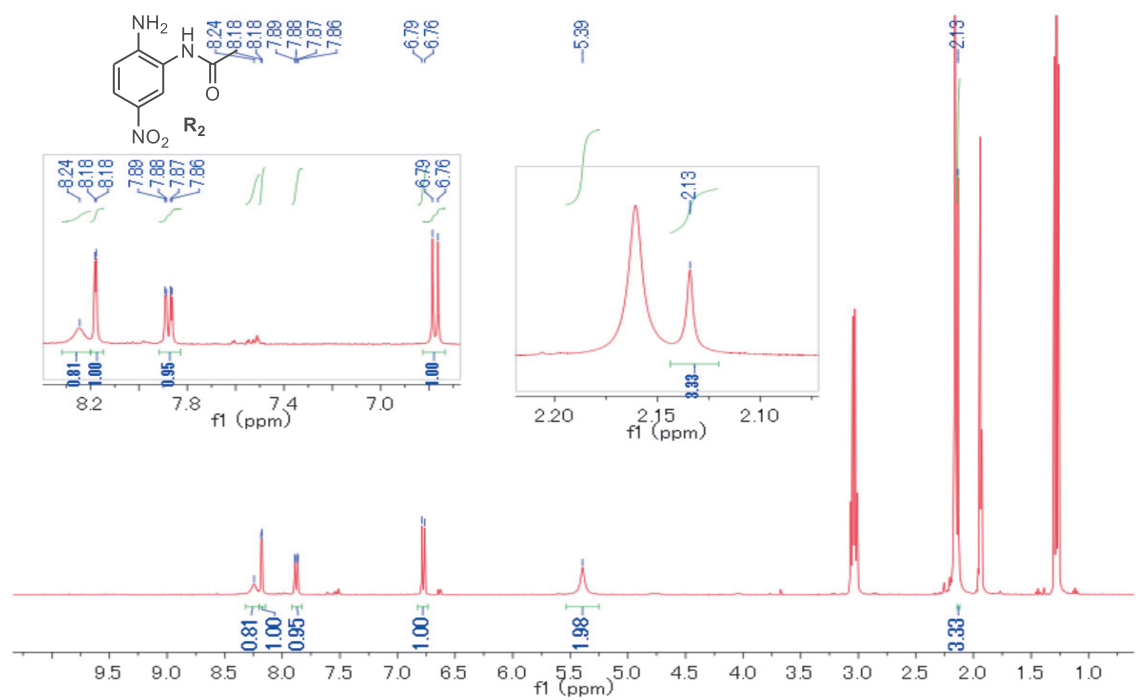
Cartesian coordinate			
Atom	X	Y	Z
H	-1.12088	1.91569	-0.21865
C	-0.75081	0.90361	-0.11395
C	0.34924	-1.64458	0.20778
C	0.62434	0.71627	-0.09724
C	-1.62606	-0.20236	0.03068
C	-1.02282	-1.49071	0.19025
C	1.2305	-0.54736	0.06519
H	-1.6395	-2.37605	0.28027
H	0.75346	-2.64573	0.3258
N	-2.98699	-0.04775	0.01519
C	-3.61822	1.2452	-0.27419
H	-3.02654	1.77748	-1.02523
H	-4.58541	1.03185	-0.74107
C	-3.90474	-1.15956	0.29438
H	-4.80181	-0.72593	0.74861
H	-3.46496	-1.81439	1.05256
C	-4.29557	-1.96144	-0.95084
H	-5.00676	-2.75177	-0.67857
H	-3.42218	-2.43317	-1.4155
H	-4.77432	-1.31639	-1.69757
C	-3.82788	2.11898	0.96652
H	-2.87582	2.37228	1.44651
H	-4.45779	1.60652	1.70375
H	-4.3278	3.05436	0.6844

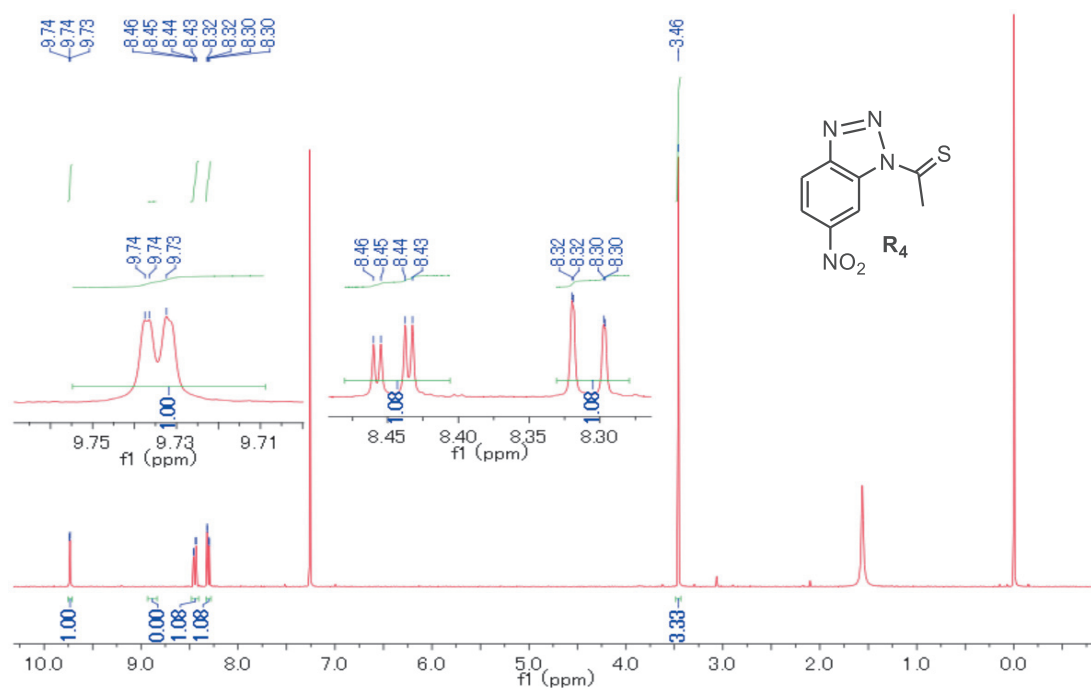
O	1.38949	1.84901	-0.2394
C	2.77623	1.81514	-0.23672
O	3.35008	2.88941	-0.37208
C	3.40028	0.52688	-0.07735
H	4.48265	0.51082	-0.07864
C	2.66899	-0.61928	0.06946
C	3.33758	-1.95841	0.23736
H	3.02147	-2.39998	1.19386
H	2.99646	-2.63259	-0.56185
O	4.75621	-1.81307	0.1984
H	5.14615	-2.69584	0.31162

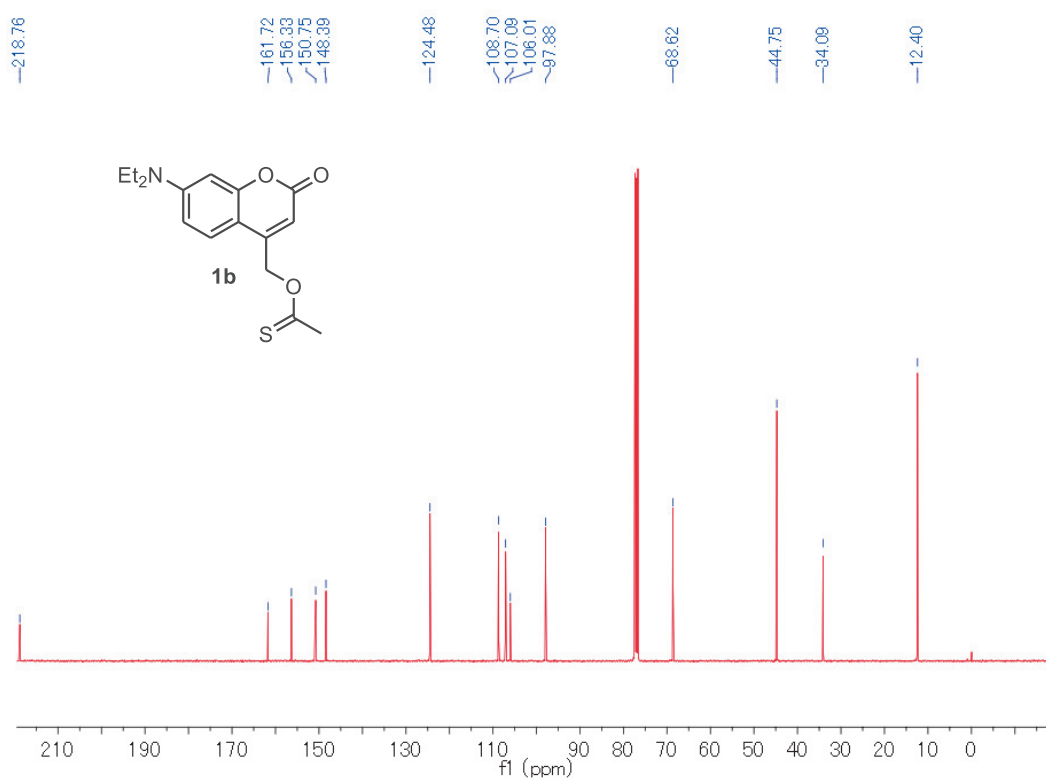
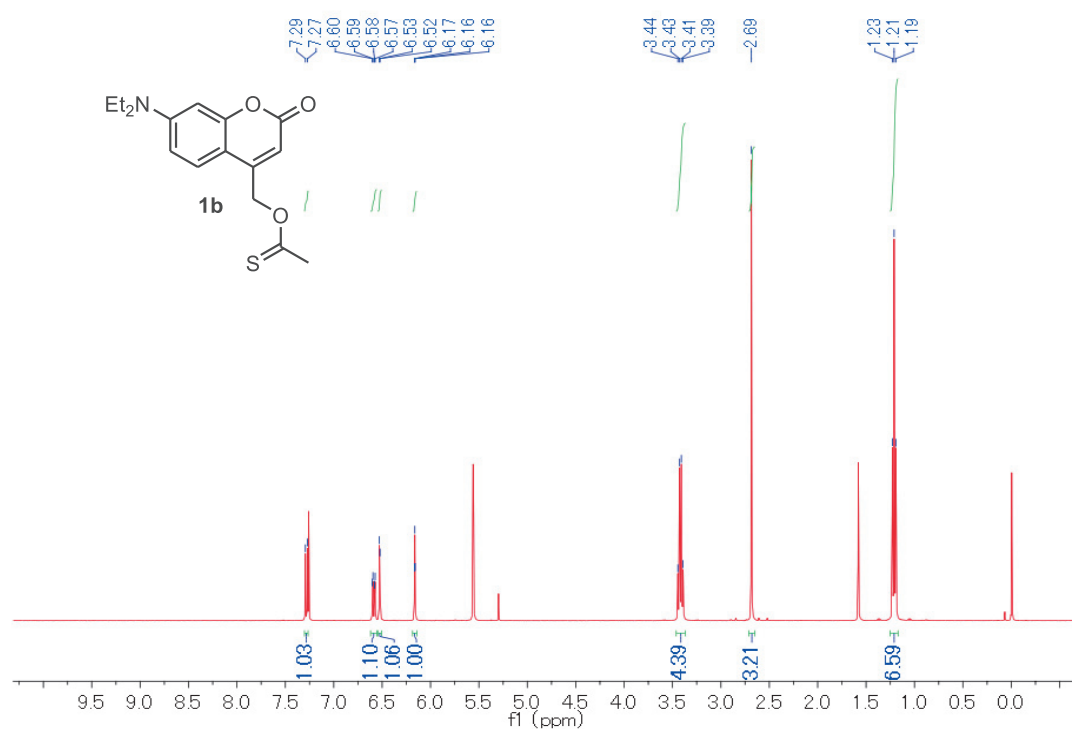
2-12. Spectra

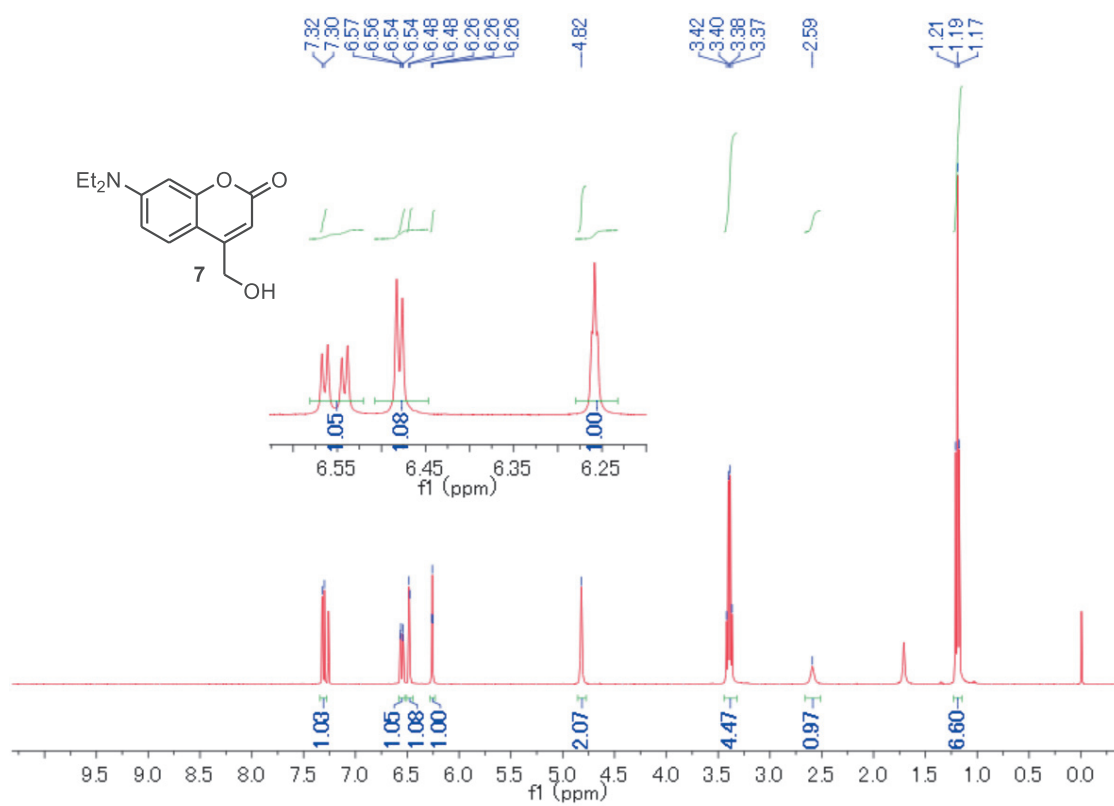


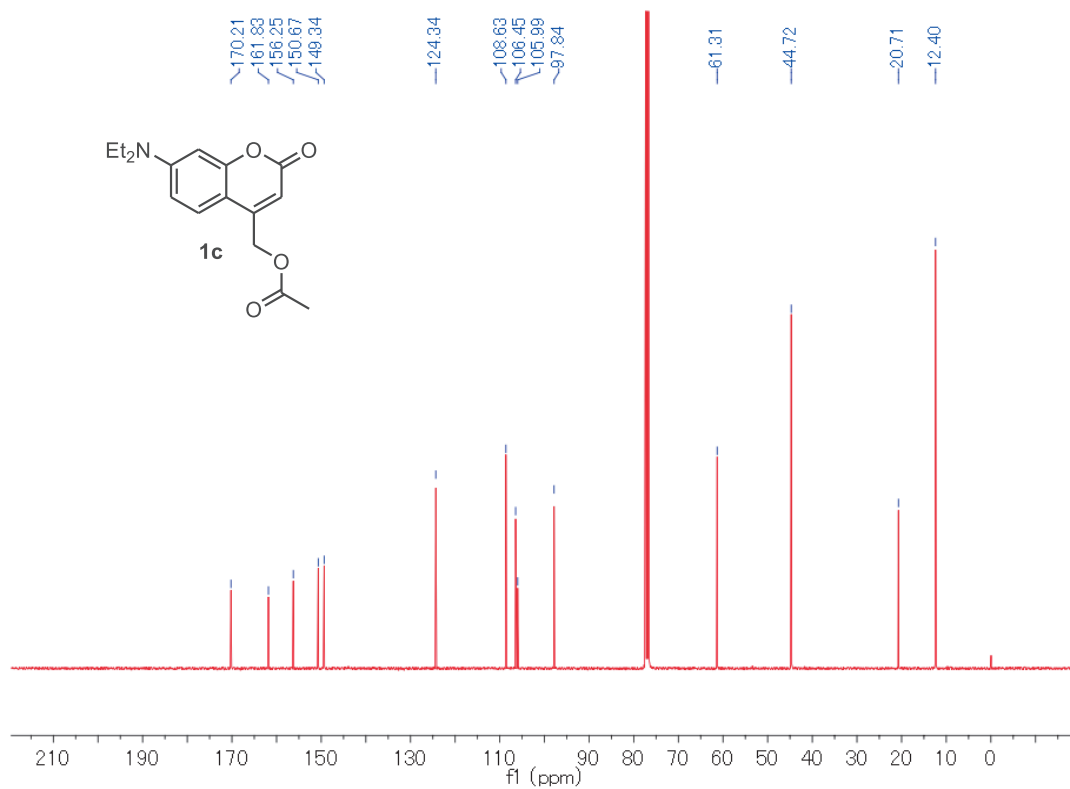
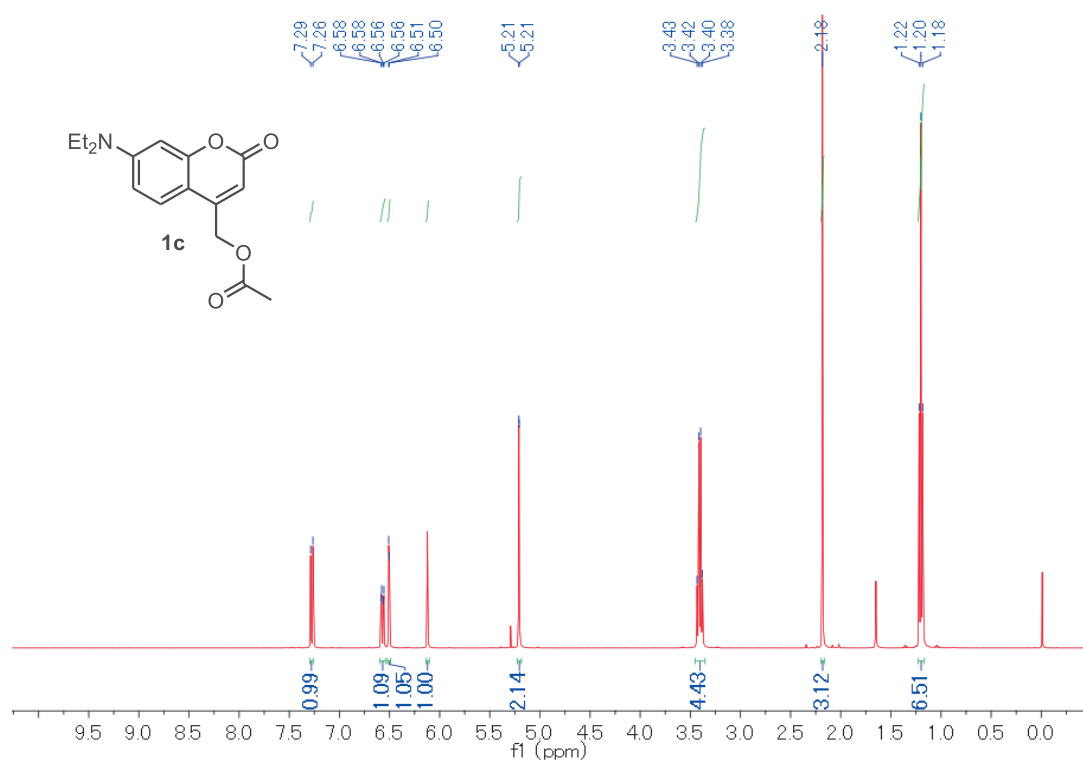


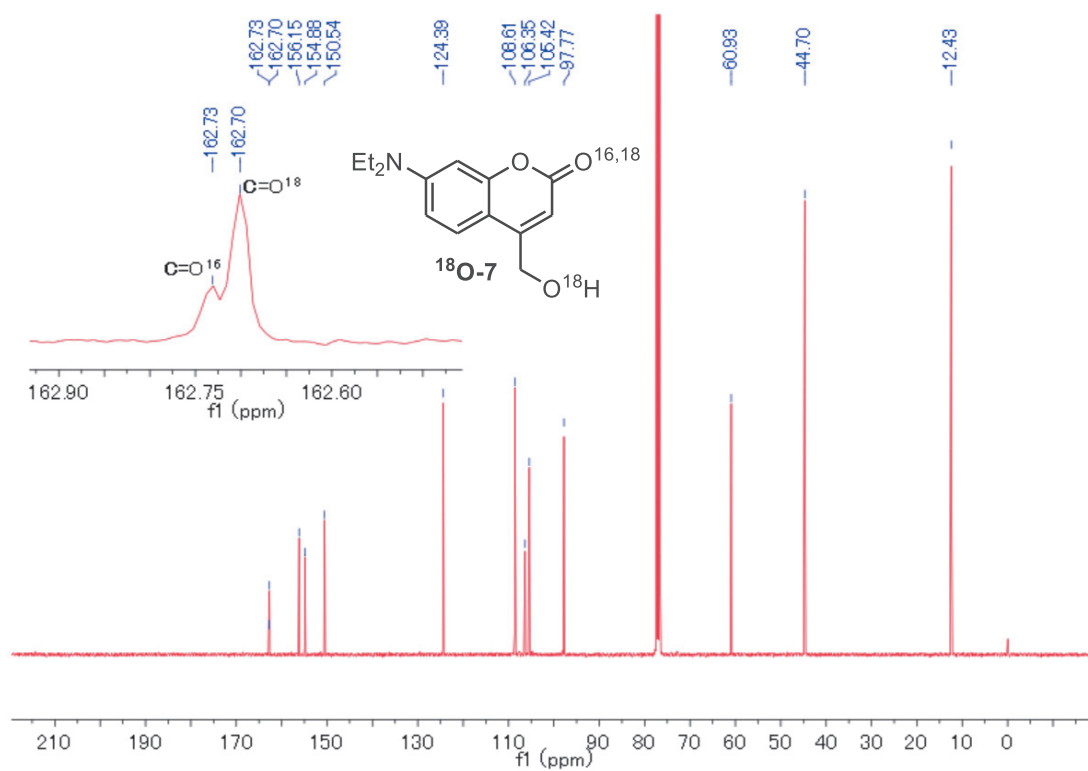
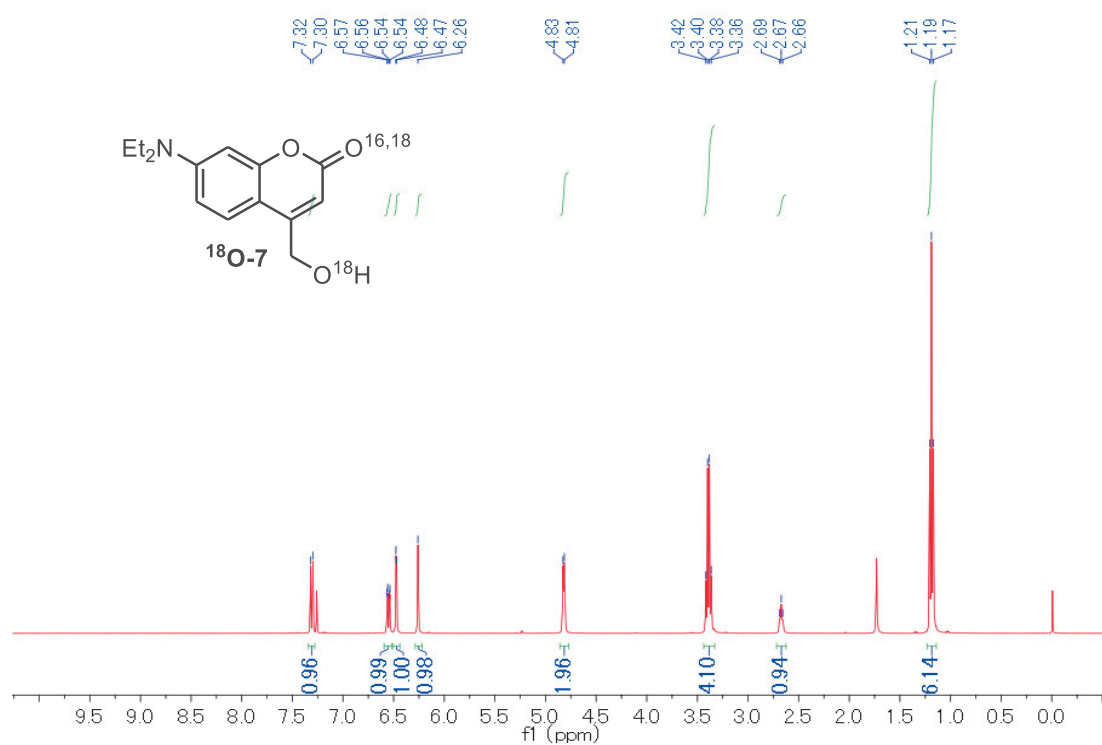


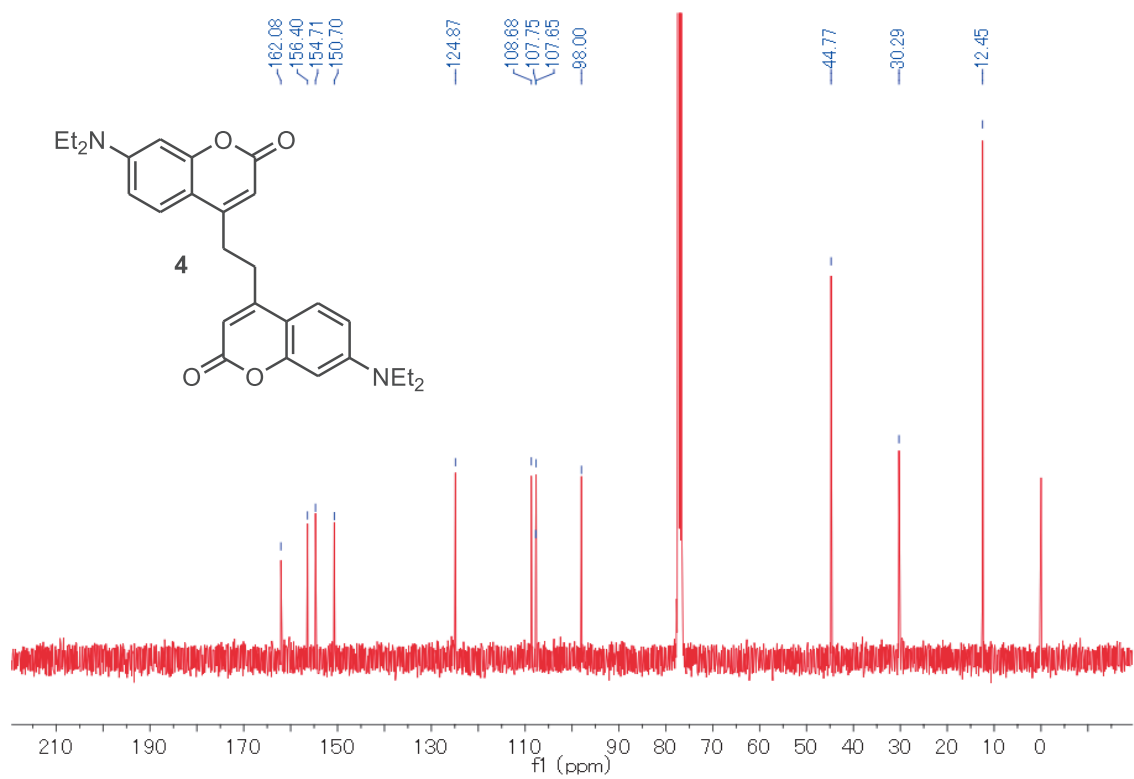
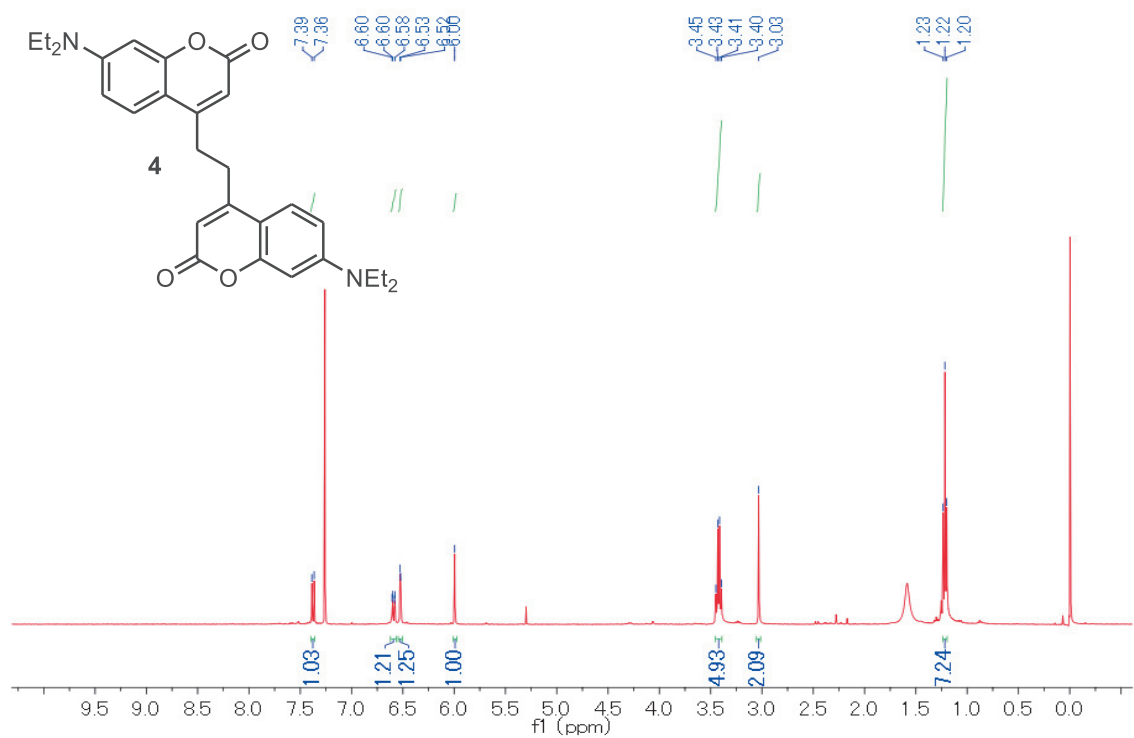


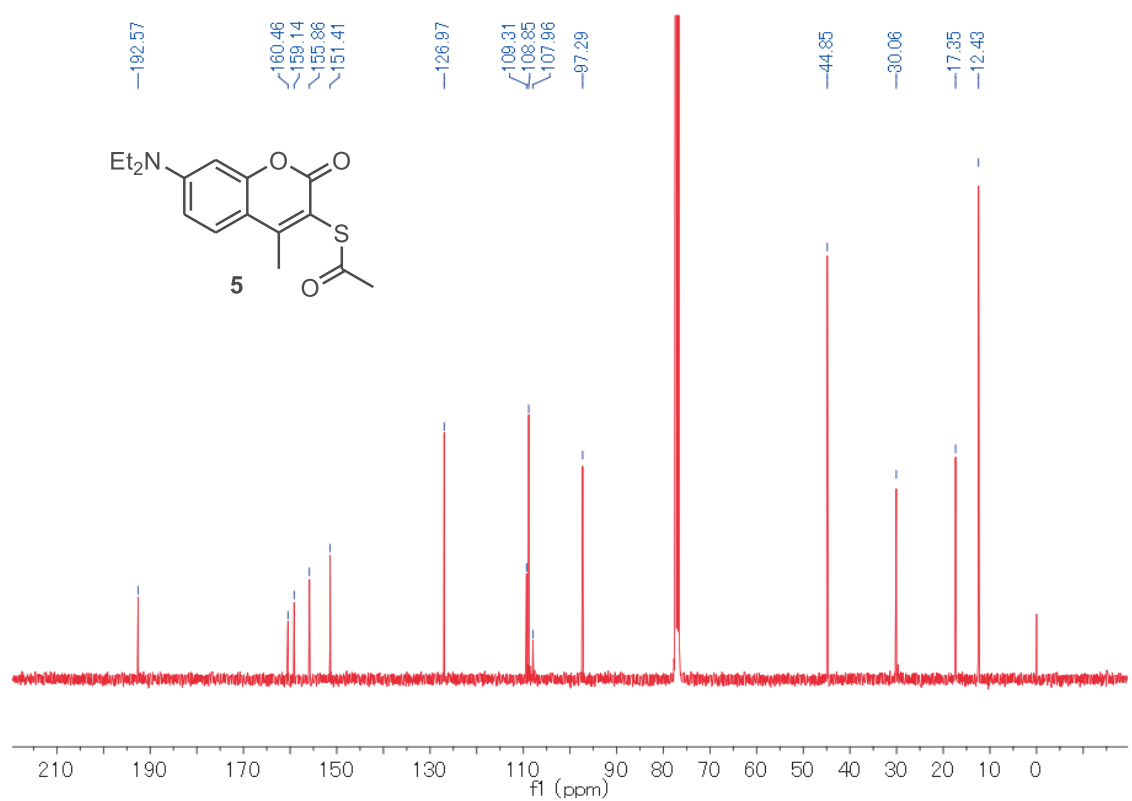
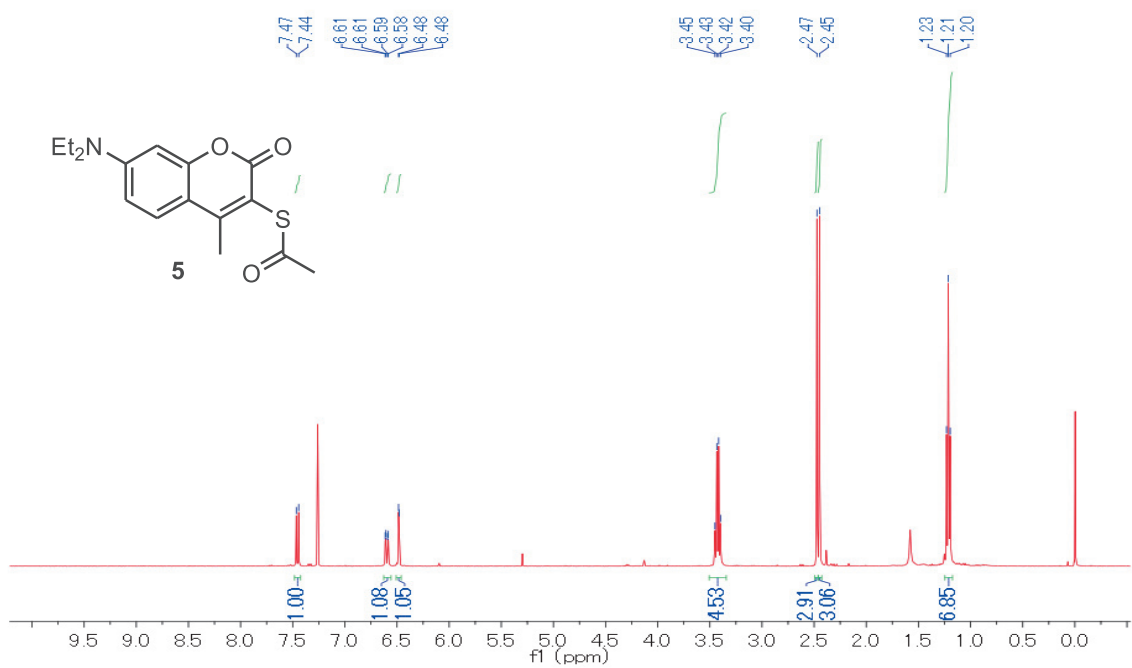


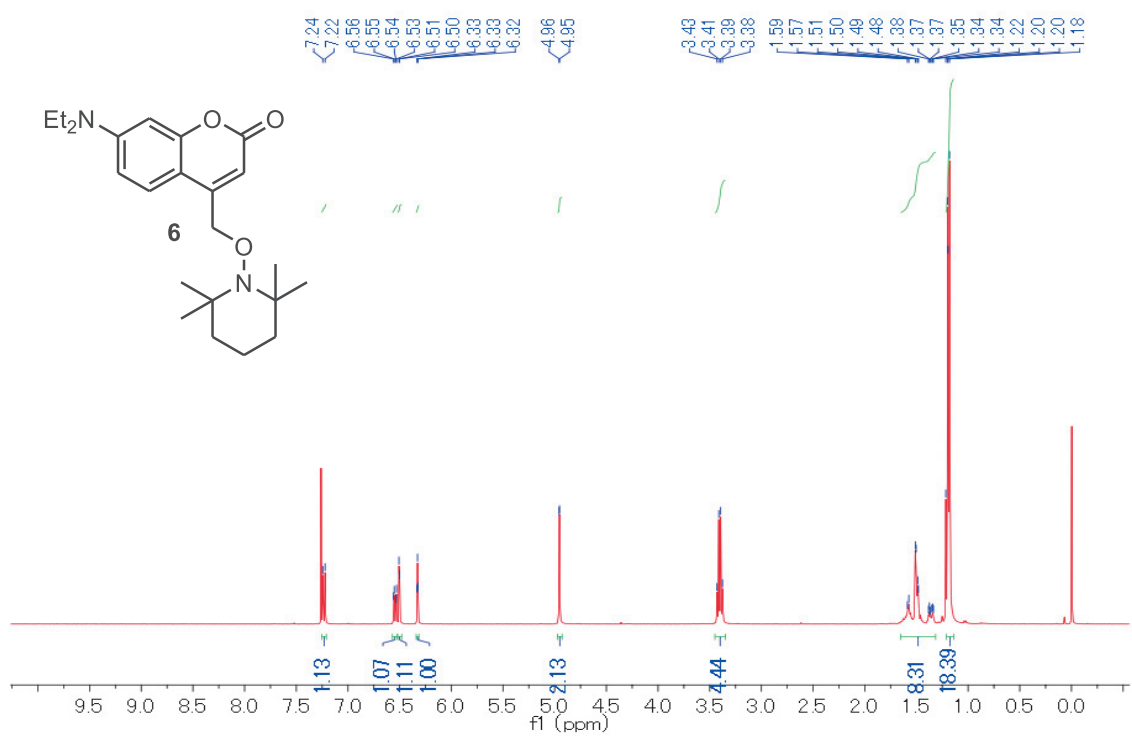


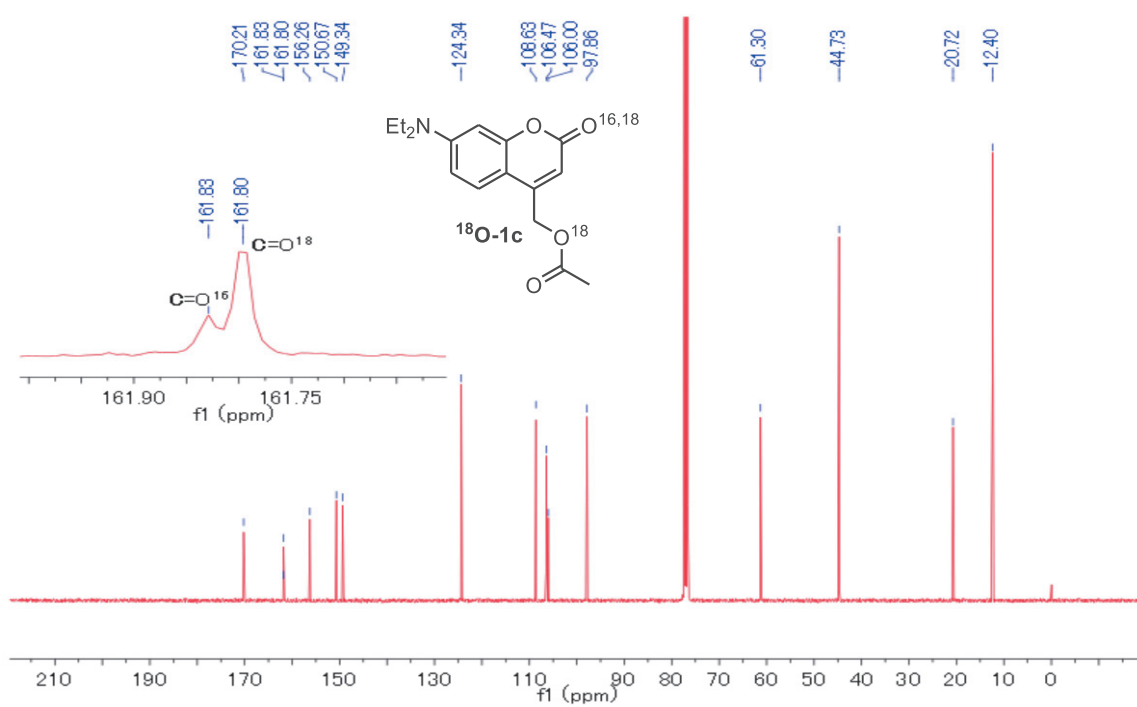
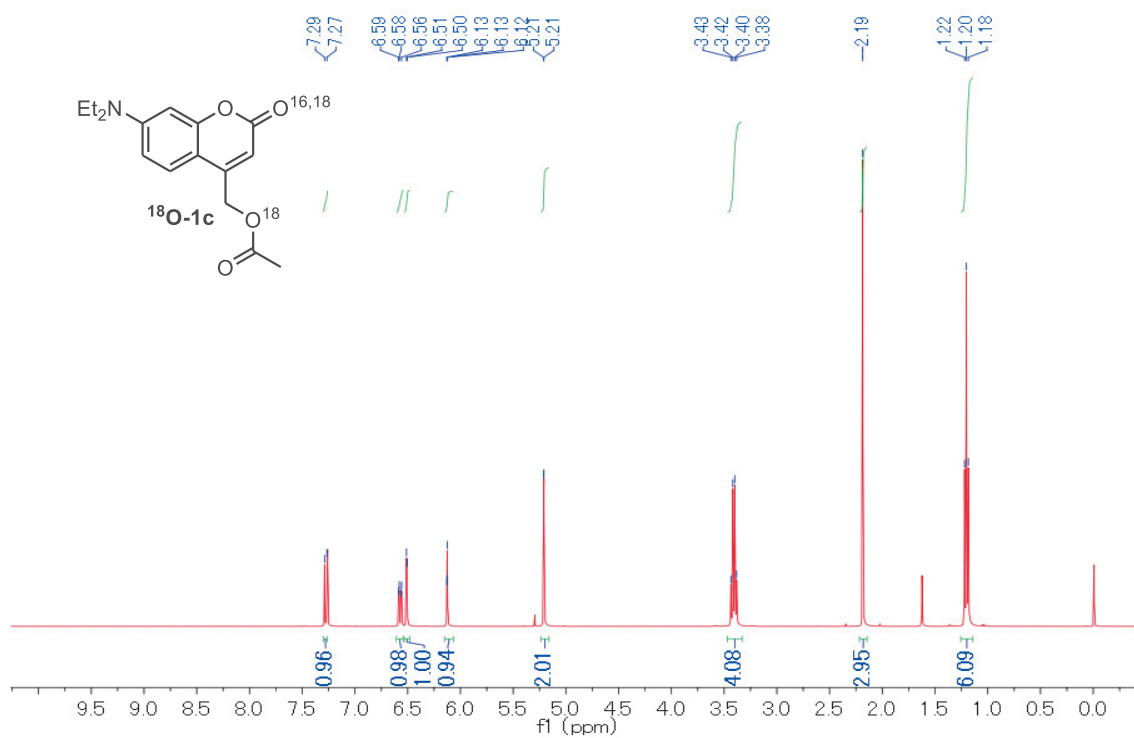












2-13. References

- (68) Li, Z.; Su, K.; Jiang, Z.; Yu, Y.; You, Q.; Zhang, X. Photoactivatable Prolyl Hydroxylase 2 Inhibitors for Stabilizing the Hypoxia-Inducible Factor with Light. *J Med Chem* **2019**, 62 (16), 7583–7588. <https://doi.org/10.1021/acs.jmedchem.9b00688>.
- (69) Katritzky, A. R.; Witek, R. M.; Rodriguez-Garcia, V.; Mohapatra, P. P.; Rogers, J. W.; Cusido, J.; Abdel-Fattah, A. A. A.; Steel, P. J. Benzotriazole-Assisted Thioacylation. *Journal of Organic Chemistry* **2005**, 70 (20), 7866–7881. <https://doi.org/10.1021/jo050670t>.
- (70) Shalaby, M. A.; Rapoport, H. A General and Efficient Route to Thionoesters via Thionoacyl Nitrobenzotriazoles. *Journal of Organic Chemistry* **1999**, 64 (3), 1065–1070. <https://doi.org/10.1021/jo981985u>.
- (71) Weinrich, T.; Gränz, M.; Grünewald, C.; Prisner, T. F.; Göbel, M. W. Synthesis of a Cytidine Phosphoramidite with Protected Nitroxide Spin Label for EPR Experiments with RNA. *European J Org Chem* **2017**, 2017 (3), 491–496. <https://doi.org/10.1002/ejoc.201601174>.
- (72) Takano, M. A.; Abe, M. Photoreaction of 4-(Bromomethyl)-7-(Diethylamino)Coumarin: Generation of a Radical and Cation Triplet Diradical during the C-Br Bond Cleavage. *Org Lett* **2022**, 24 (15), 2804–2808. <https://doi.org/10.1021/acs.orglett.2c00694>.
- (73) Roth, H. G.; Romero, N. A.; Nicewicz, D. A. Experimental and Calculated Electrochemical Potentials of Common Organic Molecules for Applications to Single-Electron Redox Chemistry. *Synlett* **2016**, 27 (5), 714–723. <https://doi.org/10.1055/s-0035-1561297>.
- (74) Isse, A. A.; Gennaro, A. Absolute Potential of the Standard Hydrogen Electrode and the Problem of Interconversion of Potentials in Different Solvents. *Journal of Physical Chemistry B* **2010**, 114 (23), 7894–7899. <https://doi.org/10.1021/jp100402x>.

- (75) Nicovich, J. M.; Kreutter, K. D.; Van Dijk, C. A.; Wine, P. H. Temperature-Dependent Kinetics Studies of the Reactions Bromine Atom($2P_{3/2}$) + Hydrogen Sulfide .Tautm. Mercapto + Hydrogen Bromide and Bromine Atom($2P_{3/2}$) + Methanethiol .Tautm. Methylthiol + Hydrogen Bromide. Heats of Formation of Mercapto and Methylthio Radicals. *J Phys Chem* **1992**, *96* (6), 2518–2528. <https://doi.org/10.1021/j100185a025>.

Chapter 3

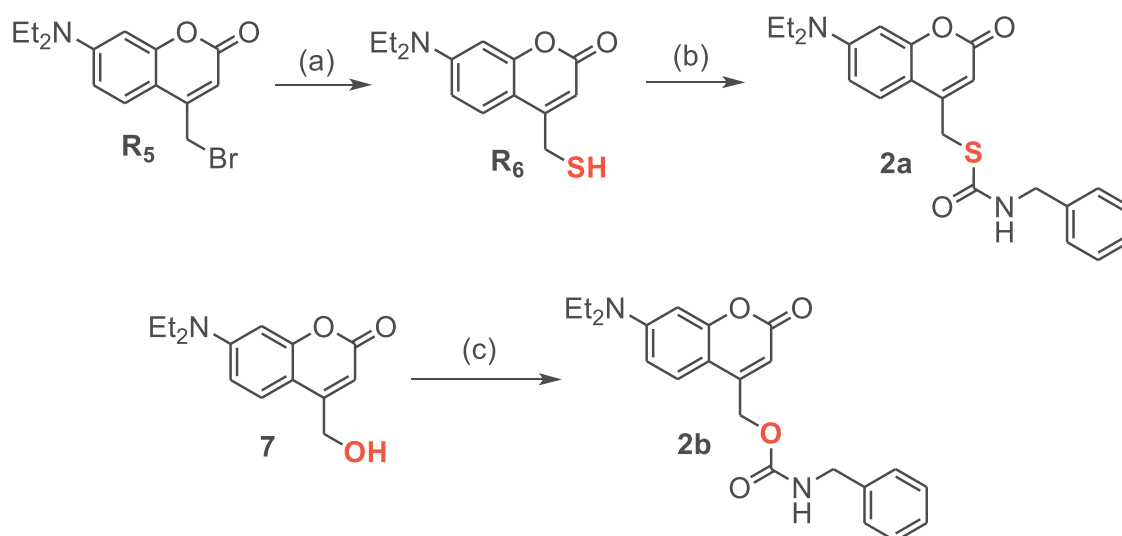
Sulfur Atom Effect on the Uncaging Reaction of DEACM-based Caged Amines

3-1. Introduction

In chapter 2, it was shown that the photochemical quantum yield of thioester **1a** (Φ^{air}) is 0.026, which is much higher than that of ester **1c** (Φ^{air}), indicating a positive effect of sulfur atom on the photorelease of carboxylic acid. Getting motivated by this result, we predicted that the sulfur atom also has a large influence on the release of amines from the carbamate linker. To this end, in this chapter, we synthesized DEACM-based thiocarbamate-containing caged benzyl amine **2a** and DEACM-based carbamate-containing caged benzyl amine **2b** and examined the photochemical properties of these two compounds to clarify the sulfur atom effect on photochemistry of caged amine.

3-2. Synthesis of **2a** and **2b**

Compound **2a** and **2b** were synthesized by the following synthetic routes.



Scheme 4. Synthetic routes for **2a** and **2b**. (a) AcSK, K_2CO_3 , 0 °C to RT, 49% yield. (b) 4-nitrophenylchloroformate, benzylamine, DMAP, 0 °C, 34% yield. (c) 4-nitrophenylchloroformate, benzylamine, DIPEA, 0 °C, 53% yield.

3-3. Photophysical properties of **2a** and **2b** in DMSO

Table 4. Photophysical properties of **2a** and **2b** in DMSO

	Absorption			Emission	
	λ_{max} (nm)	ϵ_{max} (M ⁻¹ cm ⁻¹)	λ_{emi} (nm)	Φ_{f}	τ (ns)
2a	385	22,014 \pm 391	445	0.14	1.7
2b	380	24,472 \pm 454	466	0.56	2.6

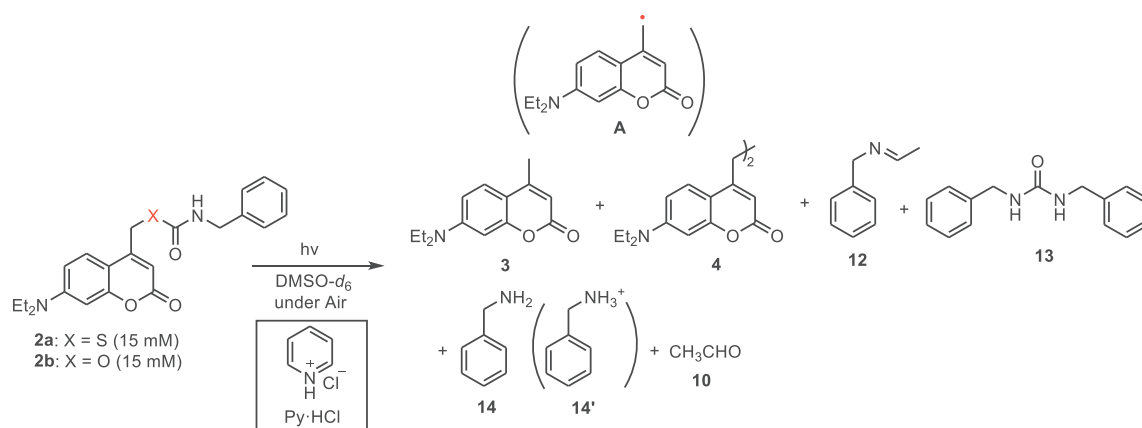
The photophysical properties of **2a** and **2b** were observed in DMSO, summarized in Table 4. It can be seen that **2a** and **2b** have the absorption maxima (λ_{max}) around 385 nm and 380 nm, respectively, with relatively high extinction coefficients ($\epsilon_{\text{max}} > 22000 \text{ M}^{-1}\text{cm}^{-1}$). On the other hand, **2a** shows the emission maxima (λ_{emi}) around 445 nm, while **2b** possess an emission maxima around 466 nm, which reveals a larger Stokes shift as compared to **2a**. Notably, the fluorescence quantum yields (Φ_{f}) of **2a** are significantly lower than that value of **2b**, which could derive from the lower photochemical quantum yield of **2b** in comparison with **2a**.

3-4. Photochemical properties of **2a** and **2b**

The photoreactions of compounds **2a** and **2b** were carried out in air-saturated DMSO-*d*₆, utilizing a 405 nm (± 20 nm) LED lamp as the light source, followed by ¹H NMR spectroscopy. The chemical yields of the photoproducts were quantified by incorporating triphenylmethane as an internal standard, with results compiled in Table 5. In entry 1, irradiation of a 15 mM solution of **2a** led to the formation of compound **3** (18%) and compound **4** (11%), which are possibly derived from DEACM radical **A**. Additionally, benzylamine **14** was released in a relatively low yield of 36%, likely due to subsequent reactions between compound **14** and other species within the reaction mixture. It should be noted that urea **13** (6%) would originate from the reaction between **14** and **2a** (Figure 7). To mitigate these side reactions, the photoreaction was conducted with the addition of pyridinium hydrochloride (Py·HCl, 150 mM) to protonate the liberated benzylamine **14** (Entry 2, Table 5). Consequently, the yield of the protonated

form of compound **14** (**14'**) significantly increased to 70%, while the formation of compound **13** was entirely suppressed.

Table 5. Summary of photochemistry of **2a** and **2b**



			Products and Yields (%) ^a					
Entry	2	Conditions	3	4	10	12	13	14 (14')
1	2a	without Py.HCl	18	11	n.d ^b	n.d ^b	9	36
2	X = S	150 mM Py.HCl	11	12	3	n.d ^b	n.d ^b	70
3	2b	without Py.HCl	17	2	n.d ^b	9	n.d ^b	29
4	X = O	150 mM Py.HCl	6	n.d ^b	24	n.d ^b	n.d ^b	89

^aDetermined by ¹H NMR (400 MHz) using triphenylmethane as the internal standard. ^bNot determined.

The photoreaction of compound **2b** in air-saturated DMSO-*d*₆ (entry 3, Table 2) primarily produced compound **3** (17%), a coumarin-based product. Compound **14** was obtained with a yield of 29%. This relatively low yield is likely due to the side reactions involving **14**, a primary amine, as observed in entry 1. It is noteworthy that urea **13** was absent from the reaction mixture in entry 3, suggesting that the nucleophilic addition of benzylamine **14** to the

carbamate moiety of **2b** did not occur. This can be attributed to the lower leaving ability of DEACM-O⁻ compared to DEACM-S⁻. Instead of compound **13**, compound **12** (9%) was produced upon irradiation of **2b**, resulting from the reaction between **14** and acetaldehyde **10** (Figure 7). This side reaction was confirmed by the absence of compound **12** and the presence of compound **10** (24%) when the photoreaction of **2b** was conducted with Py·HCl (150 mM) (entry 4, Table 2). Additionally, the yield of the protonated form of **14** (**14'**) was approximately three times higher than that of **14** in entry 3, further indicating that the low yield of **14** in entry 3 was due to its side reactions. The formation of compound **10** could be explained by the reaction of singlet oxygen with the diethylamine moiety (Figure 7).^{63,64}

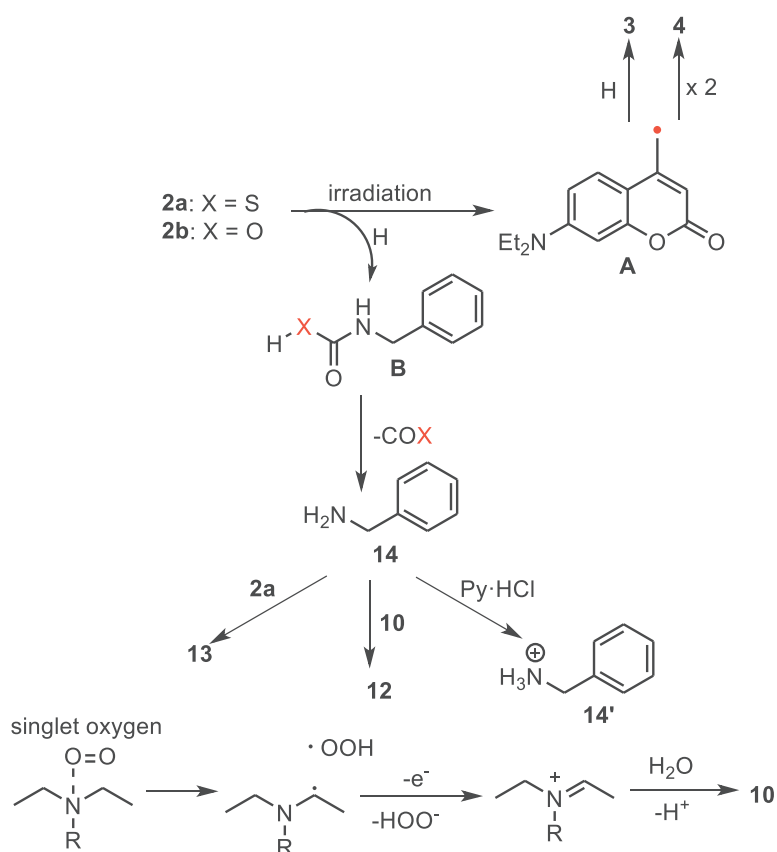


Figure 8. Proposed mechanism for photochemistry of **2a** and **2b**.

To elucidate the effect of the sulfur atom on the release rate of compound **14**, the photochemical quantum yields of **2a** and **2b** (0.49 mM) were determined in air-saturated DMSO utilizing a 405 nm (\pm 20 nm) LED lamp and a ferrioxalate complex as a chemical actinometer. The photoreactions were performed in the presence of Py·HCl (4.9 mM) to prevent side reactions between compound **7** and the starting materials **2**. The conversion of the starting materials during irradiation was monitored using HPLC analysis.

It was observed that the photodecomposition rate of compound **2a** was approximately 27 times faster than that of compound **2b** (Figure 8). The photochemical quantum yield of **2a** (Φ_{2a}) was determined to be 0.024, which is 20 times greater than that of **2b** (Φ_{2b} = 0.0012). This finding is consistent with our previous study, where the photochemical quantum yield of thioester **1a** was also 20 times higher than that of **1c**. The higher photochemical quantum yield of **2a** can be attributed to the lower bond dissociation energy (BDE) of the C–S bond (BDE = 73.6 kcal/mol, CH₃S–CH₃) compared to the C–O bond (BDE = 83.2 kcal/mol, CH₃O–CH₃).⁷⁵ These observations suggest that the presence of a sulfur atom significantly enhances the photochemical yield of the caged amine.

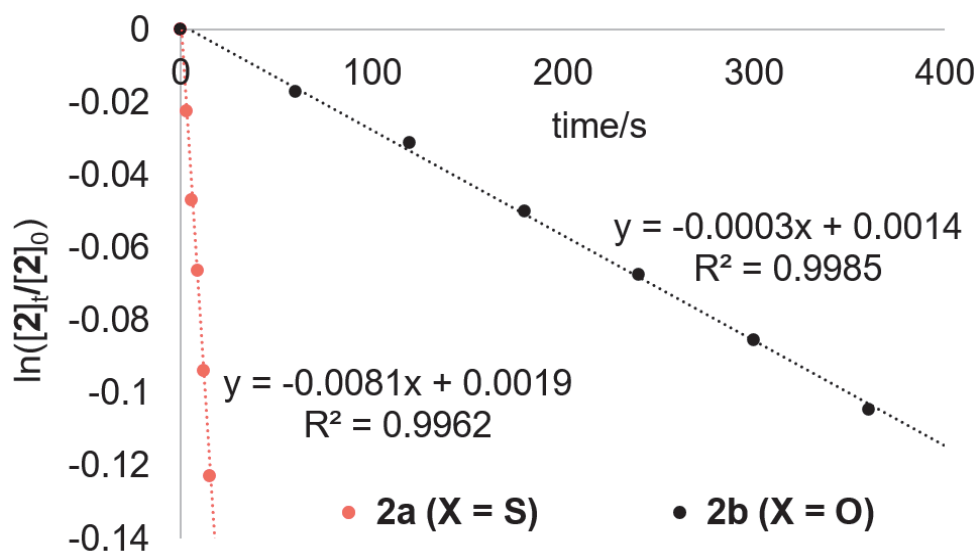


Figure 9. Time profile of the photoreactions of **2a** (0.35 mM) and **2b** (0.49 mM) in air-saturated DMSO at 22 °C. The ratios $[2]_t/[2]_0$ were determined by HPLC analysis.

3-5. DFT calculations

To rationalize the photodecomposition rates of compounds **2a** and **2b**, the activation energies for the C–S bond dissociation in the triplet state (**³2a**) and the C–O bond dissociation in the triplet state (**³2b**) were computed using the UB3LYP/6-31G+(d) (SMD = DMSO) level of theory for quantum mechanical calculations. The energy barrier for the C–S bond cleavage was found to be approximately half that of the C–O bond cleavage, indicating a faster decomposition of **2a** compared to **2b**. Based on these findings, the more rapid photodecomposition of **2a** can be rationalized by the lower activation energy required for the homolytic dissociation of the C–S bond compared to the C–O bond in **2b**. According to the Arrhenius equation ($k = Ae^{-E_a/RT}$), the photodecomposition of **2a** is about 26 times faster than that of **2b** (Figure 9). This theoretical result aligns with experimental observations, where the photochemical quantum yield of **2a** is approximately 20 times higher than that of **2b**. These findings suggest that the faster photodecomposition of **2a** compared to **2b** can be attributed to the higher activation energy required for

the homolytic dissociation of the C–O bond in **2b**, compared to the C–S bond in **2a**.

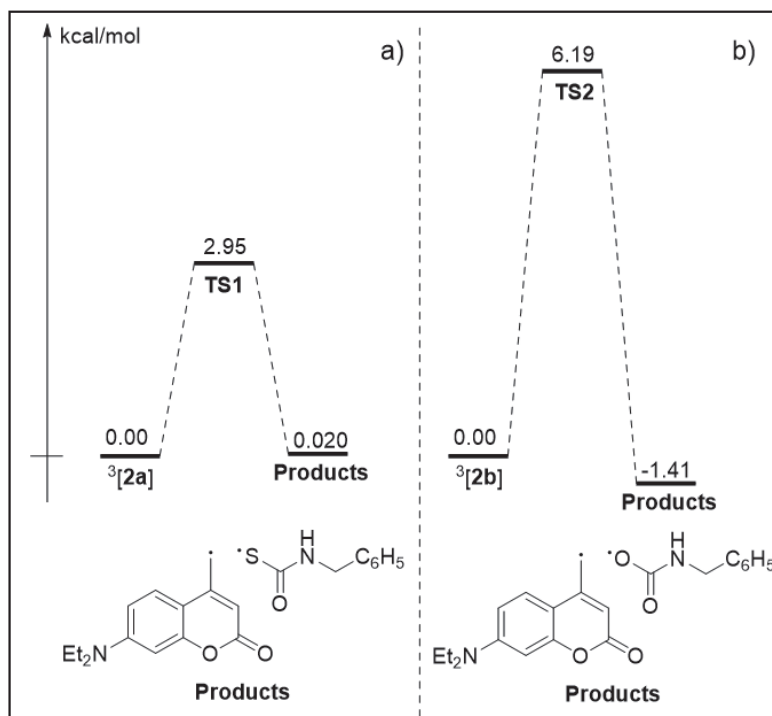


Figure 10. Computed relative energies of a) $^3[2a]$, **TS1**, products and b) $^3[2b]$, **TS2**. Products at UB3LYP/6-31G+(d) (SMD = DMSO) level of theory.

3-6. References

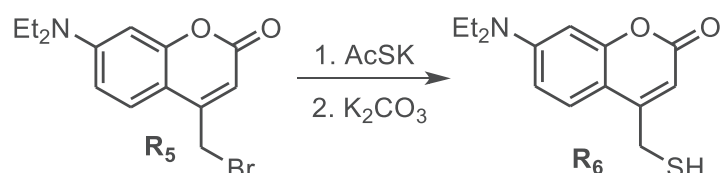
- (74) Isse, A. A.; Gennaro, A. Absolute Potential of the Standard Hydrogen Electrode and the Problem of Interconversion of Potentials in Different Solvents. *Journal of Physical Chemistry B* **2010**, *114* (23), 7894–7899. <https://doi.org/10.1021/jp100402x>.
- (75) Nicovich, J. M.; Kreutter, K. D.; Van Dijk, C. A.; Wine, P. H. Temperature-Dependent Kinetics Studies of the Reactions Bromine Atom($2P_{3/2}$) + Hydrogen Sulfide .Tautm. Mercapto + Hydrogen Bromide and Bromine Atom($2P_{3/2}$) + Methanethiol .Tautm. Methylthiol + Hydrogen Bromide. Heats of Formation of Mercapto and Methylthio

Radicals. *J Phys Chem* **1992**, 96 (6), 2518–2528.
<https://doi.org/10.1021/j100185a025>.

3-7. Experimental section

All commercially available chemical reagents were purchased from TCI, Wako, or Sigma-Aldrich and directly used without any further purification. NMR spectra were recorded on Bruker Ascend 400 (^1H NMR: 400 MHz, ^{13}C NMR: 100 Hz) spectrometer at 298 K. Coupling constants (J) are denoted in Hz and chemical shift (δ) in ppm. The abbreviations s, d, t, q and dd denote the resonance multiplicities singlet, doublet, triplet, quartet, and double of doublets, respectively. IR spectrum was recorded on a JASCO MCT-6000M. Mass spectrometric data were observed with Thermo Fisher Scientific LTQ Orbitrap XL. UV-Vis spectra were recorded on a SHIMADZU UV-3600 Plus spectrometer. The spectra were observed at room temperature using a slit width of 1 nm with middle scan rate.

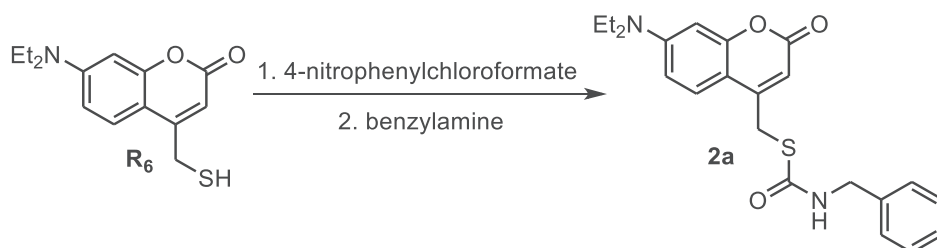
Synthesis of 7-(diethylamino)-4-(mercaptomethyl)-2H-chromen-2-one (**R**₆)



R₅ (55.6 mg, 0.18 mmol, 1.0 equiv.) and potassium thioacetate (24.3 mg, 0.21 mmol, 1.2 equiv.) were dissolved in 0.6 mL MeOH. The solution was stirred under N₂ atmosphere at room temperature. After 30 minutes, the solvent was removed under reduced pressure to observe the residue, which was then dissolved in CHCl₃ and washed with H₂O. The organic layer was dried with Na₂SO₄, then concentrated to obtain the residue. The residue was then dissolved in deoxygenated MeOH, followed by the addition of potassium carbonate (29.2 mg, 0.21 mmol, 1.2 equiv.) at 0 °C. The mixture was stirred under N₂ atmosphere while the temperature was increased gradually to room

temperature for 30 minutes before quenched with 1M HCl. The solution was then concentrated under reduced pressure before dissolved again in CHCl₃ and washed with water. The organic layer was dried over Na₂SO₄, concentrated under reduced pressure to obtain the crude product, which was then purified by gel permeation chromatography to afforded compound **R₆** as a yellow solid (23.2 mg, 49%). Mp: 67 °C. ¹H NMR (400 MHz, CDCl₃) δ 7.42 (d, *J* = 9.0 Hz, 1H), 6.60 (dd, *J* = 9.0, 2.3 Hz, 1H), 6.51 (d, *J* = 2.3, 1H), 6.08 (s, 1H), 3.72 (d, *J* = 7.9 Hz, 2H), 3.41 (q, *J* = 7.1 Hz, 4H), 1.87 (t, *J* = 7.9 Hz, 1H), 1.21 (t, *J* = 7.1 Hz, 6H). ¹³C NMR (101 MHz, CDCl₃) δ 161.6 (s), 156.1 (s), 154.1 (s), 150.2 (s), 124.8 (s), 108.2 (s), 107.1 (s), 106.1 (s), 97.2 (s), 44.3 (s), 24.4 (s), 12.1 (s). HRMS (ESI⁺) *m/z*: [M + H]⁺ calcd for C₁₄H₁₈NO₂S⁺ 264.10528, found 264.10519. IR (film, cm⁻¹): 3072, 2971, 2930, 1715, 1608, 1527, 1416, 1357, 1270, 1232, 1199, 1138, 1074, 825.

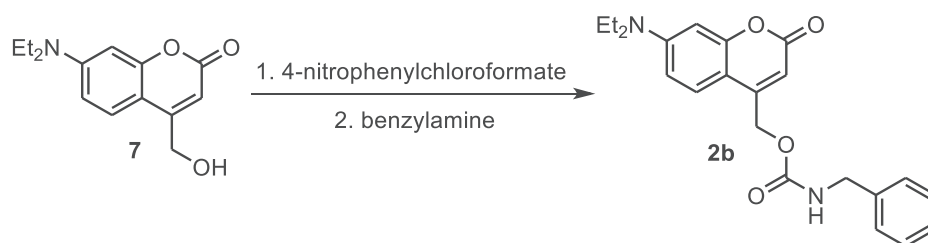
Synthesis of 2a



Compound **R₆** (122.4 mg, 0.46 mmol, 1.0 equiv.) and 4-nitrophenylchloroformate (112.6 mg, 0.55 mmol, 1.2 equiv.) were dissolved in deoxygenated THF. DIPEA (0.1 mL, 0.55 mmol, 1.2 equiv.) was added at 0 °C. The reaction mixture was then stirred at room temperature under N₂ atmosphere for 1 hour before concentrated to obtain the residue. The residue and DMAP (69.1 mg, 0.55 mmol, 1.2 equiv.) were dissolved in dry DMF. Benzylamine (0.06 mL, 0.55 mmol, 1.2 equiv.) was injected into the solution at 0 °C. The reaction mixture was stirred under N₂ atmosphere at 0 °C for 1.5 hours before extracted with CHCl₃. The organic layer was dried over Na₂SO₄ and concentrated to afforded the crude product, which was then purified by silica-gel column chromatography to observe compound **2a** as a yellow solid (61.3 mg, 34%). Mp: 110 °C. ¹H NMR (400 MHz, CDCl₃) δ 7.46 (d, *J* = 9.0

Hz, 1H), 7.41 – 7.25 (m, 5H), 6.60 (dd, $J = 9.0, 2.6$ Hz, 1H), 6.50 (d, $J = 2.6$ Hz, 1H), 6.16 (s, 1H), 5.95 (t, $J = 5.4$ Hz, 1H), 4.52 (d, $J = 5.4$ Hz, 2H), 4.22 (s, 2H), 3.42 (q, $J = 7.1$ Hz, 4H), 1.22 (t, $J = 7.1$ Hz, 6H). ^{13}C NMR (101 MHz, CDCl_3) δ 165.5 (s), 162.0 (s), 156.5 (s), 151.9 (s), 150.7 (s), 137.4 (s), 128.8 (s), 127.80 (s), 127.75 (s), 125.4 (s), 109.0 (s), 108.7 (s), 107.2 (s), 97.8 (s), 45.7 (s), 44.8 (s), 30.0 (s), 12.5 (s). HRMS (ESI $^+$) m/z : $[\text{M} + \text{H}]^+$ calcd for $\text{C}_{22}\text{H}_{24}\text{N}_2\text{O}_3\text{SNa}^+$ 419.13998, found 419.13971. IR (film, cm^{-1}): 2971, 2925, 1702, 1680, 1616, 1598, 1525, 1416, 1354, 1273, 1271, 1138.

Synthesis of 2b



Compound **7** (173.5 mg, 0.70 mmol, 1.0 equiv.) and 4-nitrophenylchloroformate (284.7 mg, 1.40 mmol, 2.0 equiv.) were dissolved in dry THF (2.3 mL). DIPEA (0.24 mL, 1.40 mmol, 2.0 equiv.) was added at 0 °C. The reaction mixture was then stirred at room temperature under N_2 atmosphere for 8 hours before concentrated to obtain the residue. The residue and DMAP (102.2 mg, 0.84 mmol, 1.2 equiv.) were dissolved in dry DMF (4.5 mL). Benzylamine (0.1 mL, 0.92 mmol, 1.3 equiv.) was injected into the solution at 0 °C. The reaction mixture was stirred under N_2 atmosphere at 0 °C for 3 hours before extracted with CHCl_3 . The organic layer was dried over Na_2SO_4 and concentrated to afford the crude product, which was then purified by silica-gel column chromatography to observe compound **2b** as a yellow solid (142.0 mg, 53%). ^1H NMR (400 MHz, CDCl_3) δ 7.41 – 7.23 (m, 1H), 6.57 (dd, $J = 9.0, 2.2$ Hz, 1H), 6.50 (d, $J = 2.2$ Hz, 1H), 6.14 (s, 1H), 5.54 (s, 1H), 5.25 (s, 2H), 4.43 (d, $J = 6.0$ Hz, 2H), 3.41 (q, $J = 7.1$ Hz, 4H), 1.21 (t, $J = 7.1$ Hz, 6H). ^{13}C NMR (101 MHz, CDCl_3) δ 161.9 (s), 156.2 (s), 155.6 (s), 150.6 (s), 150.2 (s), 138.0 (s), 128.7 (s), 127.6 (s), 127.5 (s), 124.3 (s), 108.6 (s), 106.1 (s), 106.0 (s), 97.7 (s), 61.8 (s), 45.2 (s), 44.7 (s), 12.4 (s). HRMS

(ESI⁺) *m/z*: [M + H]⁺ calcd for C₂₂H₂₄N₂O₄Na⁺403.16283, found 403.16296.
IR (film, cm⁻¹): 2971, 2925, 1700, 1604, 1525, 1420, 1354, 1234, 1133, 1077, 1062.

Photophysical properties of 2a and 2b

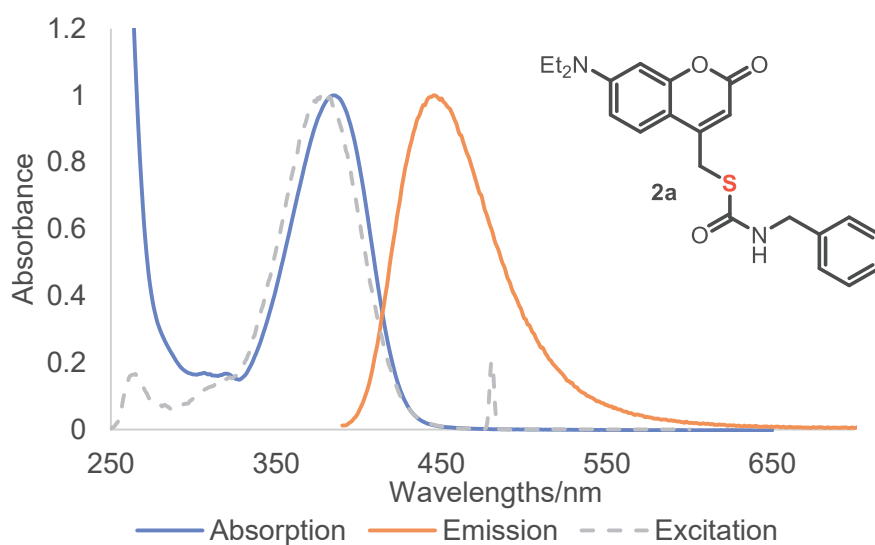


Figure S32. Absorption, emission and excitation spectra of **2a** in DMSO

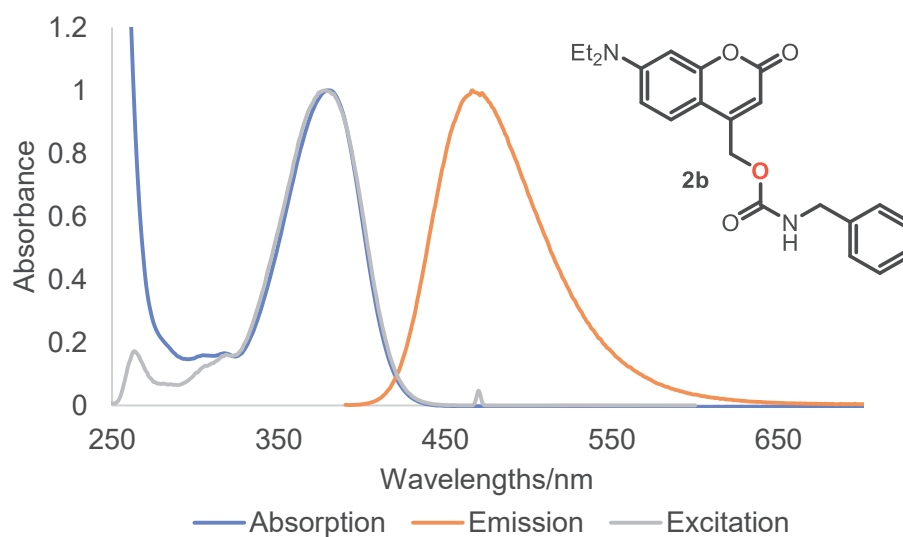


Figure S33. Absorption, emission and excitation spectra of **2b** in DMSO

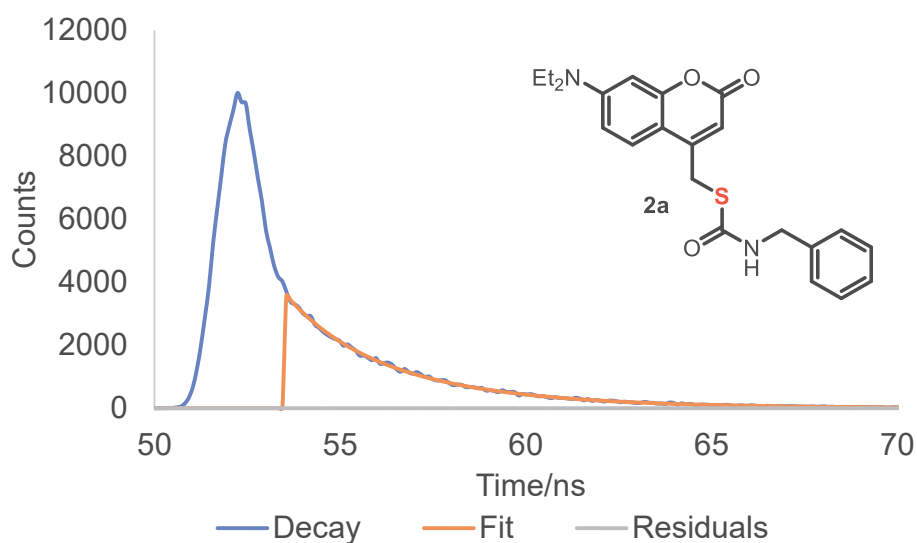


Figure S34. Time profile of the excited state **2a** in air-saturated DMSO monitored at 440 nm (excited at 390 nm).

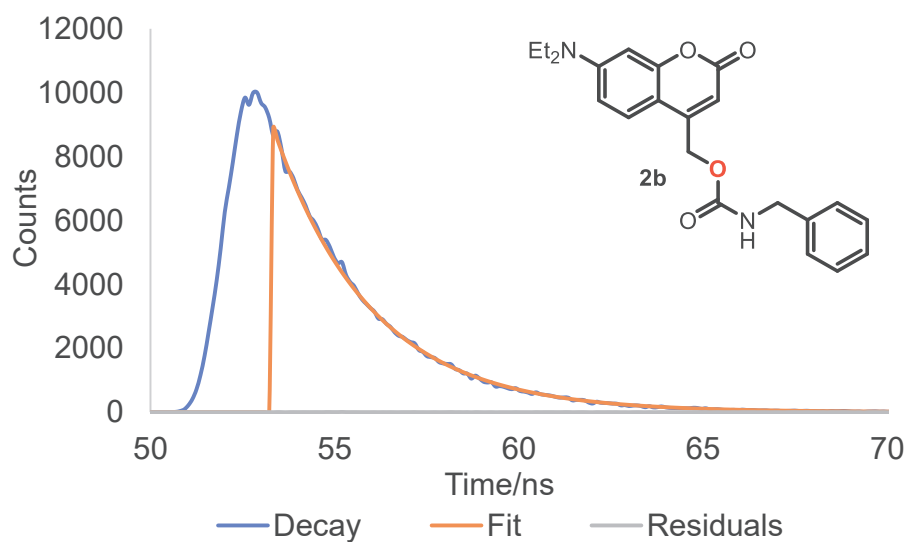


Figure S35. Time profile of the excited state **2b** in air-saturated DMSO monitored at 440 nm (excited at 390 nm).

Photoreactions of **2a** and **2b** in DMSO-*d*₆

General procedure for experiments in the absence of pyridinium hydrochloride: A solution of compound **2a** or **2b** ($C_M = 15$ mM) in DMSO-*d*₆ was irradiated at $\lambda = 405$ nm (LED lamp). The chemical yields of photoproducts were determined by ¹H NMR spectroscopy using triphenylmethane (TPM) as an internal standard.

General procedure for experiments in the presence of pyridinium hydrochloride: A solution of compound **2a** or **2b** ($C_M = 15$ mM) and pyridinium hydrochloride ($C_M = 150$ mM) in DMSO-*d*₆ was irradiated at $\lambda = 405$ nm (LED lamp). After irradiation, DMSO-*d*₆ was removed under reduce pressure to observe the residue. The residue and triphenylmethane (TPM) were dissolved in CD₃OD. The chemical yields were determined by ¹H NMR spectroscopy.

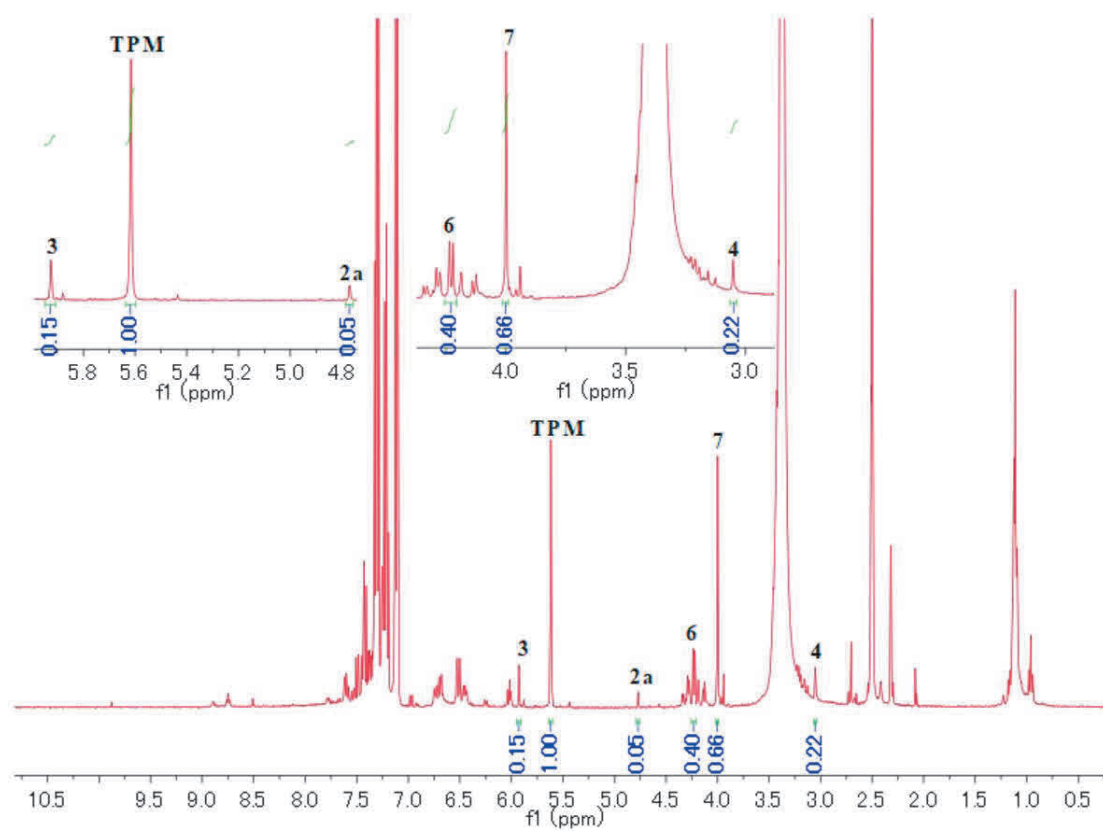


Figure S36. ^1H NMR analysis of the photoreaction of **2a** (400 MHz, $\text{DMSO-}d_6$) (entry 1)

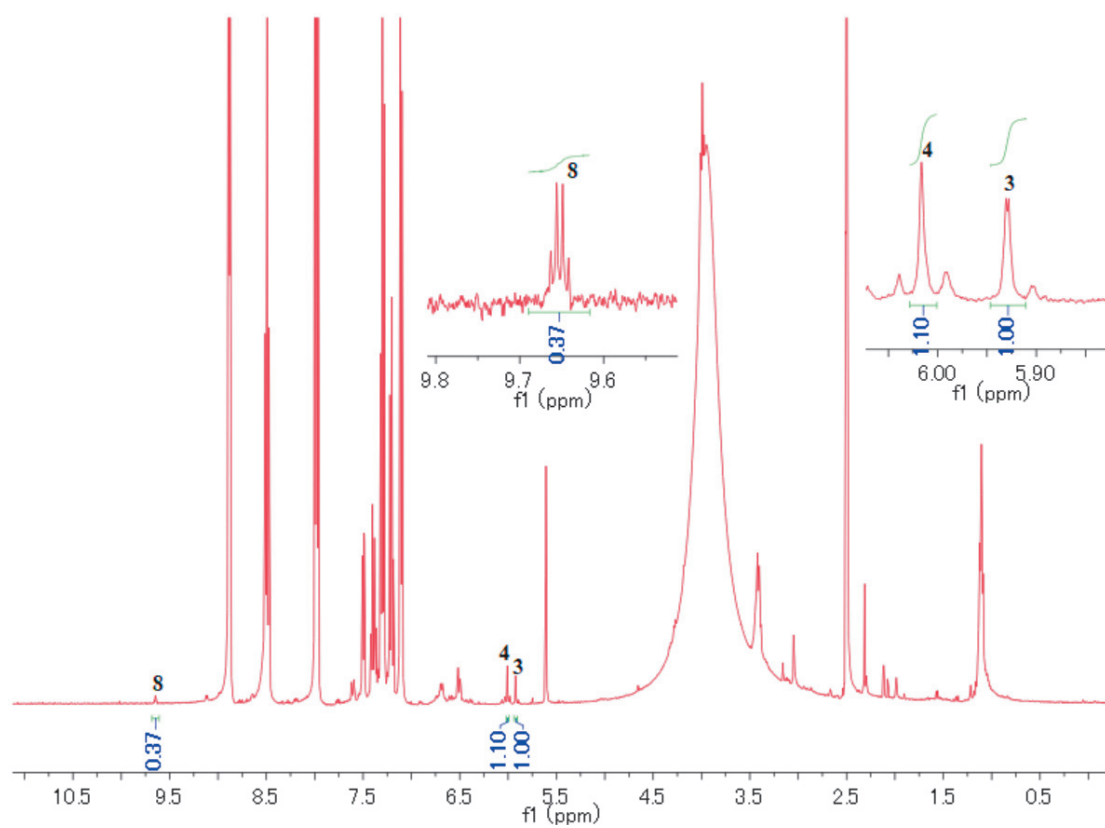


Figure S37. ^1H NMR analysis of the photoreaction of **2a** (400 MHz, $\text{DMSO-}d_6$) (entry 2)

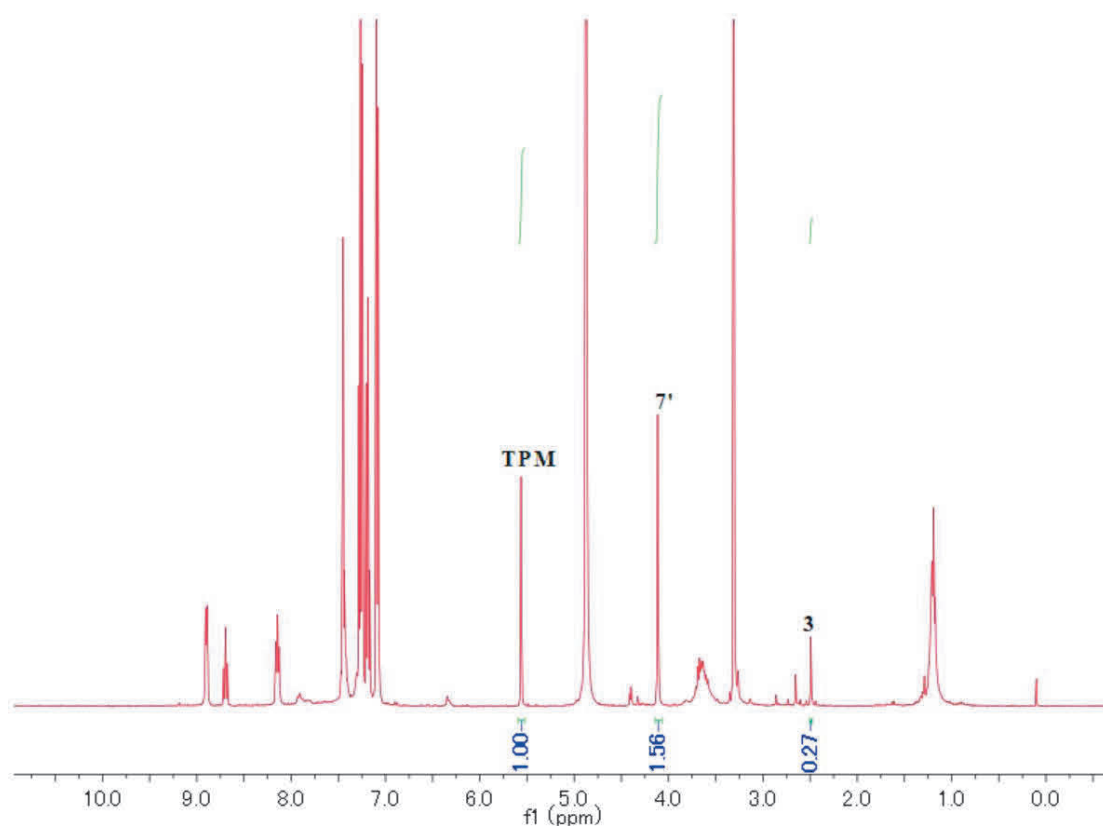


Figure S38. ^1H NMR analysis of the photoreaction of **2a** (400 MHz, CD_3OD) (entry 3)

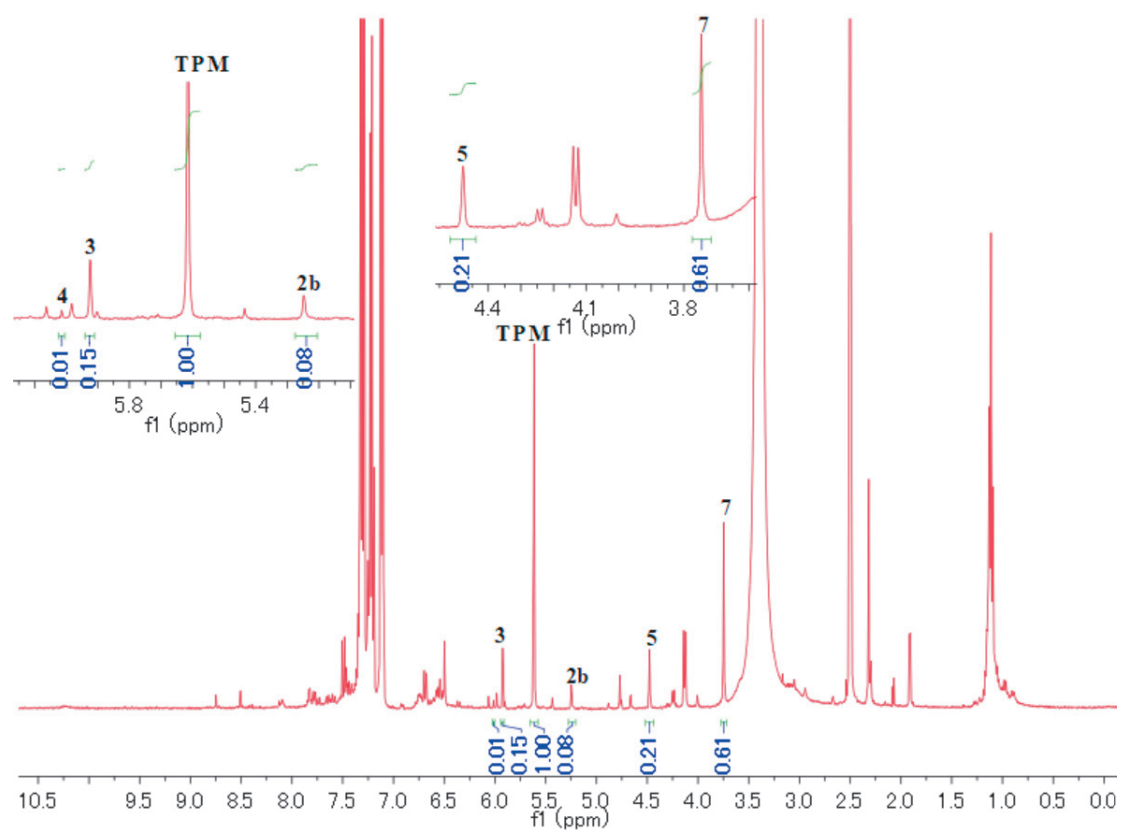


Figure S39. ^1H NMR analysis of the photoreaction of **2b** (400 MHz, $\text{DMSO-}d_6$) (entry 3)

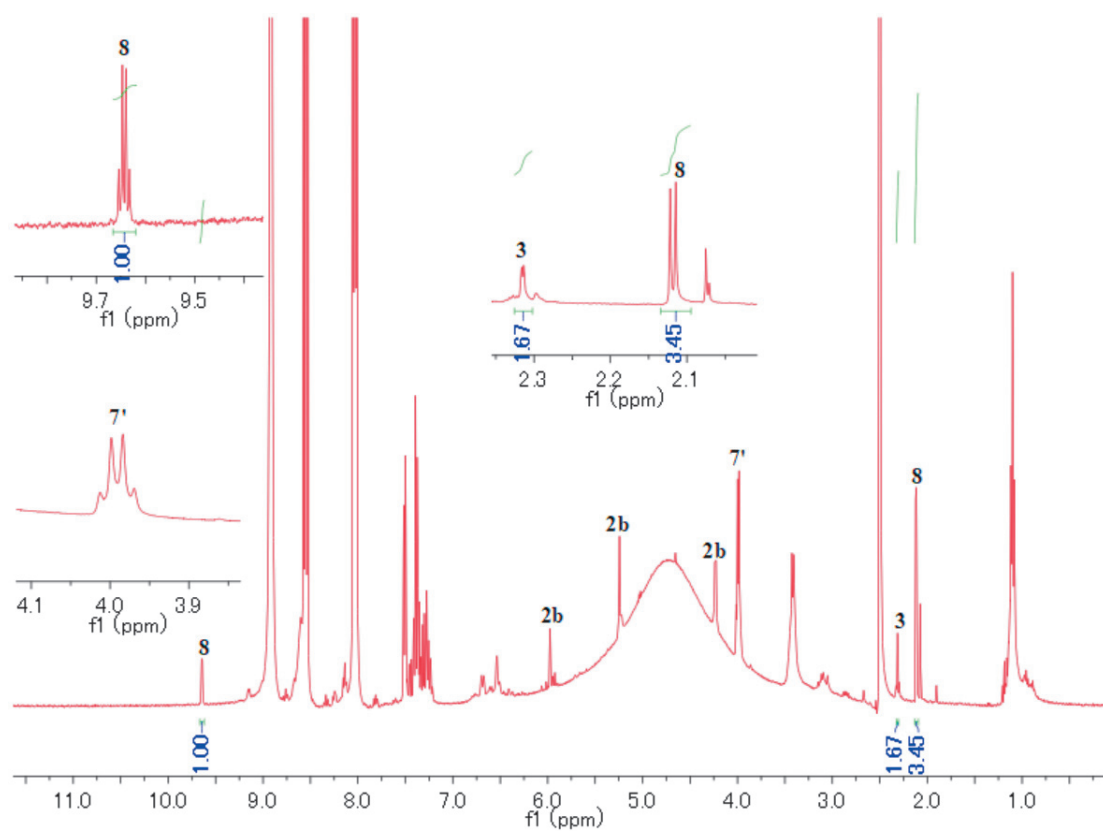


Figure S40. ^1H NMR analysis of the photoreaction of **2b** (400 MHz, $\text{DMSO-}d_6$) (entry 4)

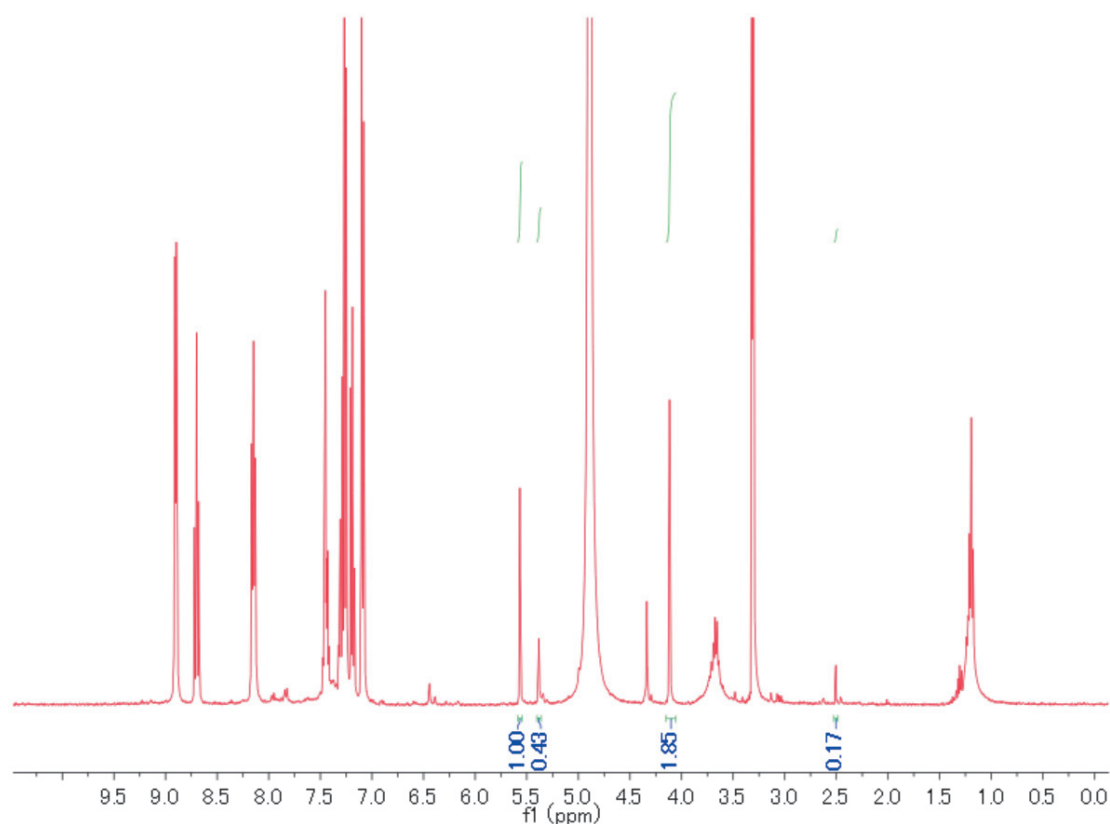


Figure S41. ^1H NMR analysis of the photoreaction of **2b** (400 MHz, CD_3OD) (entry 4).

Photochemical quantum yield measurements of photoreactions of **2a** and **2b**

General procedure: 3.0 mL of solution of **2a** ($C_M = 0.35$ mM, $\text{Abs}_{405} = 5$) or **2b** ($C_M = 0.49$ mM, $\text{Abs}_{405} = 5$) and pyridinium hydrochloride ($C_M = 3.5$ or 4.9 mM) in DMSO were irradiated by using 405 nm LED lamp. The number of photons of LED lamp was determined by using Ferrioxalate complex as the actinometer. The conversion of the starting material at a certain time was calculated by HPLC analysis. A conversion vs time graph was sketched, and the slope of the linear line was observed as the conversion rate. The photochemical quantum yield values were calculated by using the following equation:

$$\Phi = \frac{\text{conversion rate (s}^{-1}\text{)} \times C_{\text{starting material (mM)}} \times V \text{ (L)}}{\text{moles of photons (mmol} \times \text{s}^{-1}\text{)}}$$

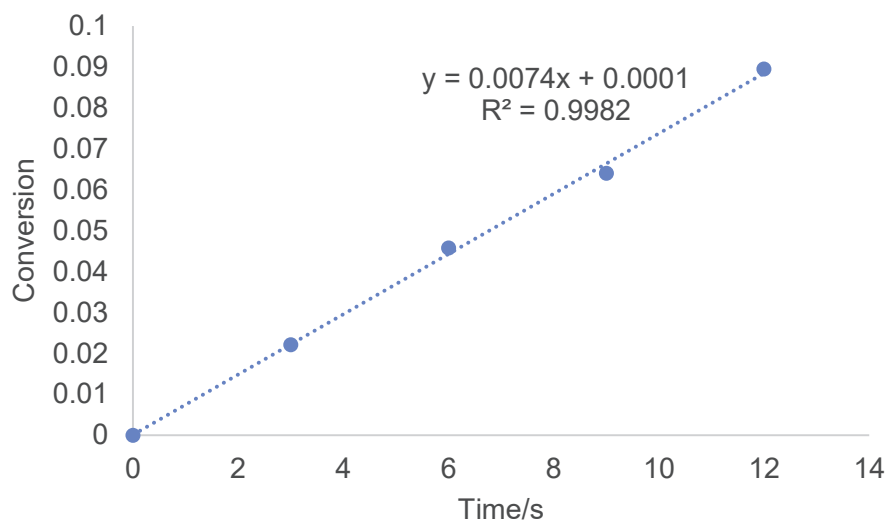


Figure S42. Time profile of the photoreaction of **2a** in DMSO

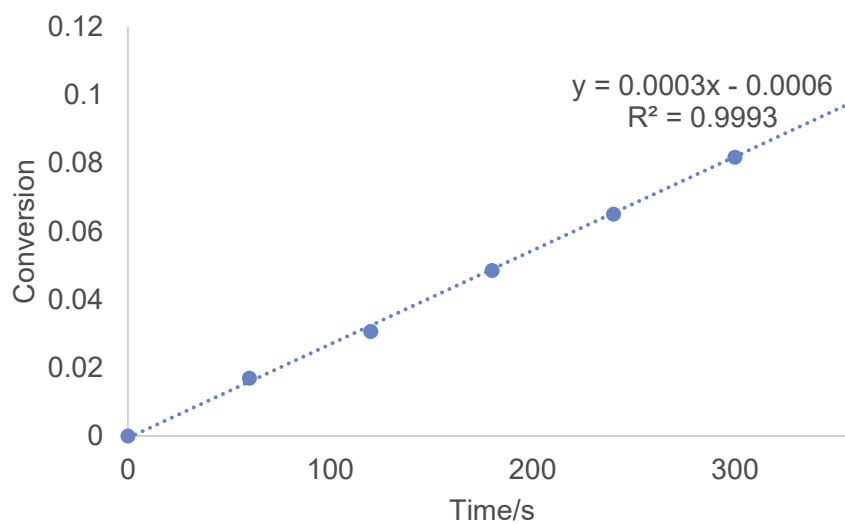


Figure S43. Time profile of the photoreaction of **2b** in DMSO

3-8. Calculation details

All calculations were performed by using the Gaussian 16 programming package. Charge, spin multiplicity, number of imaginary frequencies, energies (in Hartree) and Cartesian coordinates (in Å) of computed geometries were simulated by each calculation. The energy minimum structures and the energy maxima (TS) structures were confirmed by vibrational frequency analysis.

Calculation of energy barriers of C–S and C–O bond dissociations

The energy profile of the C–S and C–O bond dissociations of **2a** and **2b** were computed at the UB3LYP/6-31+(d) (SMD = DMSO) level of theory to estimate the energy barriers.

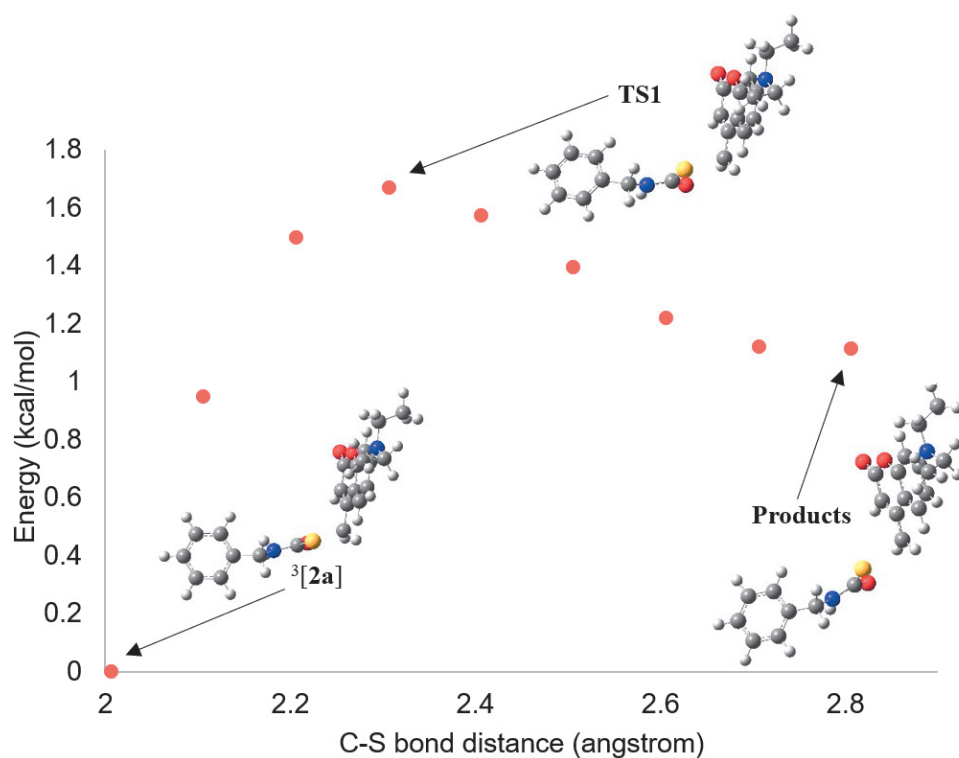


Figure S44. Energy profile of the C–S bond dissociation at UB3LYP/6-31+(d)

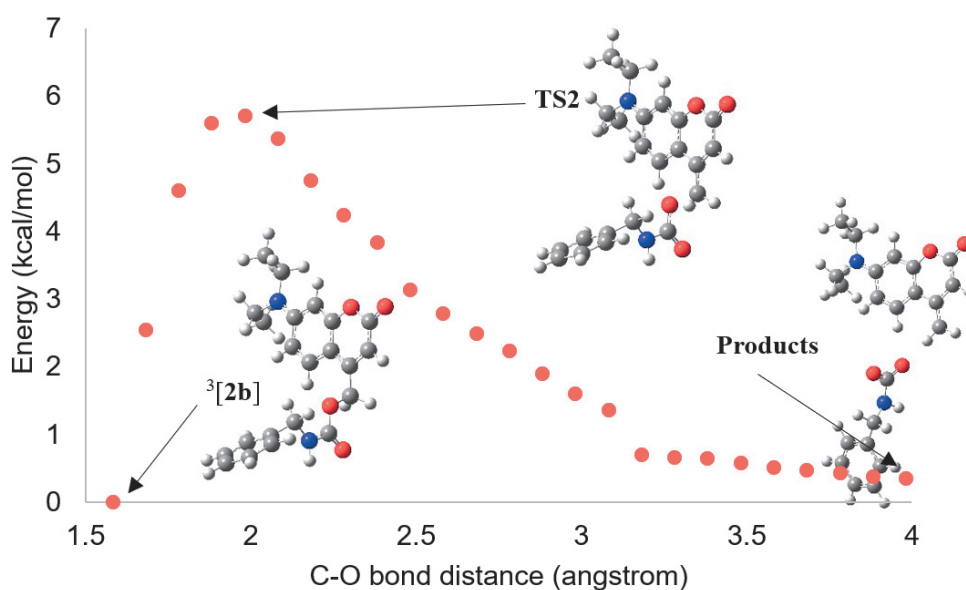


Figure S45. Energy profile of the C–O bond dissociation at UB3LYP/6-31+(d)

Triplet state of 2a

opt freq ub3lyp/6-31+g(d) scrf=(smd,solvent=dmsol); 0, 3

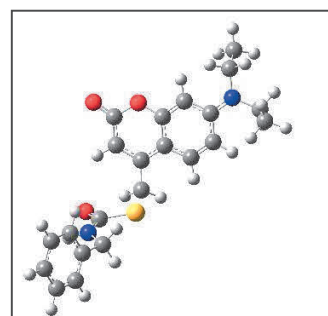
Number of Imaginary Frequencies = 0

Sum of electronic and zero-point Energies = -1585.768095

Sum of electronic and thermal Energies = -1585.740675

Sum of electronic and thermal Enthalpy = -1585.739730

Sum of electronic and thermal Free Energy = -1585.832560



Atom	Cartesian coordinate		
	X	Y	Z
H	-4.39768	-0.7182	1.63007
C	-3.81491	0.40759	-0.77229
C	-2.25682	-0.2937	1.44124
C	-2.68587	1.12966	-0.47398
C	-4.21803	-0.70077	0.04156
C	-3.39225	-1.02534	1.15908

C	-1.84719	0.83101	0.65638
H	-3.63121	-1.86866	1.79477
H	-1.65742	-0.58866	2.29605
O	-2.4081	-2.18124	1.32007
C	-1.23719	2.95396	-1.16308
O	-1.06665	3.82808	-2.02154
C	-0.7075	1.63845	0.90835
C	-0.41174	2.65997	-0.05593
H	0.47933	3.26927	0.05258
C	0.22213	1.39717	2.03496
H	0.77682	2.29861	2.30353
H	-0.27054	1.00935	2.92901
S	1.59096	0.11303	1.69921
C	2.96449	1.22258	1.26923
O	2.89385	2.44618	1.38866
N	-5.34633	-1.41737	-0.25274
C	-5.83709	-2.50069	0.61422
H	-5.64099	-2.24626	1.65752
H	-6.92327	-2.52997	0.49074
C	-5.23436	-3.863	0.25549
H	-4.14853	-3.86924	0.39886
H	-5.45033	-4.12638	-0.78616
H	-5.67351	-4.63217	0.90184
C	-6.1551	-1.16149	-1.45548
H	-6.61718	-2.11438	-1.72832
H	-5.49847	-0.87728	-2.27999
C	-7.2394	-0.10366	-1.22352
H	-7.91113	-0.40094	-0.41028
H	-7.83516	0.00707	-2.13731
H	-6.80162	0.86939	-0.97611
N	4.07705	0.59459	0.81328
H	4.8793	1.20584	0.6855
C	4.32183	-0.85092	0.72195
H	3.41899	-1.32983	0.329
H	4.51936	-1.26977	1.71658
C	5.49143	-1.13291	-0.19816
C	6.80065	-0.83234	0.20001
C	5.27903	-1.70053	-1.46485

C	7.882	-1.0949	-0.64961
H	-6.9755	0.3933	1.18005
C	6.35567	-1.96054	-2.31601
H	4.26641	-1.94121	-1.78209
C	7.66156	-1.65841	-1.90955
H	8.89274	-0.85816	-0.32603
H	6.17751	-2.40289	-3.29329
H	8.49997	-1.8636	-2.57078

Triplet state of 2b

opt freq ub3lyp/6-31+g(d) scrf=(smd,solvent=dmsol); 0, 3

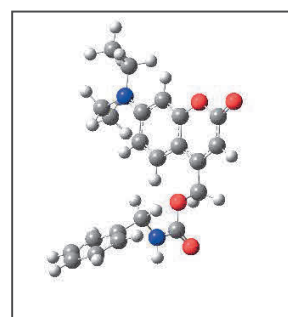
Number of Imaginary Frequencies = 0

Sum of electronic and zero-point Energies = -1262.802764

Sum of electronic and thermal Energies = -1262.776008

Sum of electronic and thermal Enthalpy = -1262.775064

Sum of electronic and thermal Free Energy = -1262.866582



Cartesian coordinate			
Atom	X	Y	Z
H	4.47954	1.96484	0.15383
C	3.95209	1.02204	0.087
C	2.45522	-1.32746	-0.12817
C	2.56723	1.04918	0.16212
C	4.63607	-0.20634	-0.09683
C	3.83237	-1.38652	-0.20247
C	1.76421	-0.1068	0.05801
H	4.29843	-2.35617	-0.32435
H	1.89693	-2.25556	-0.20843
O	6.00206	-0.26238	-0.16714
C	6.83997	0.9225	0.05418
O	6.38819	1.54685	0.83123
C	7.79279	0.56829	0.46042

C	6.7209	-1.5078	-0.46513
H	7.65049	-1.22591	-0.97022
C	6.14811	-2.09671	-1.18744
H	7.04385	-2.34264	0.77791
H	7.60783	-3.23896	0.48983
O	6.13206	-2.66398	1.29426
C	7.65499	-1.76991	1.48601
O	7.09429	1.74047	-1.21598
N	6.16086	2.12929	-1.63856
C	7.5892	1.13022	-1.98117
H	7.74646	2.59278	-0.98659
H	1.99699	2.28703	0.33801
C	0.62573	2.46832	0.42636
H	0.23302	3.61808	0.58247
H	-0.20001	1.29136	0.3264
H	-1.26799	1.4502	0.39929
C	0.33528	0.04571	0.14871
H	-0.52187	-1.18787	0.04216
H	-0.35993	-1.67986	-0.92341
C	-0.25665	-1.90269	0.82835
H	-1.9054	-0.82724	0.16971
H	-2.79298	-1.85738	0.12594
H	-2.46075	-3.03564	0.016
N	-4.07437	-1.42165	0.19667
H	-4.76408	-2.15842	0.29425
C	-4.50862	-0.04654	0.48092
H	-4.37495	0.18423	1.54532
H	-3.87319	0.63421	-0.09136
C	-5.95965	0.14166	0.09
C	-6.95123	0.28097	1.07015
C	-6.33319	0.17595	-1.2633
C	-8.2928	0.45338	0.70844
H	-6.67247	0.25736	2.12161
C	-7.67106	0.34521	-1.62764
H	-5.57057	0.0724	-2.03267
C	-8.65547	0.48471	-0.64101
H	-9.05061	0.56246	1.48065
H	-7.94568	0.37358	-2.67944

H	-9.6966	0.61932	-0.92429
---	---------	---------	----------

TS1

opt = (calcfc,ts,noeigentest) freq ub3lyp/6-31+g(d)

scrf=(smd,solvent=dms0); 0, 3

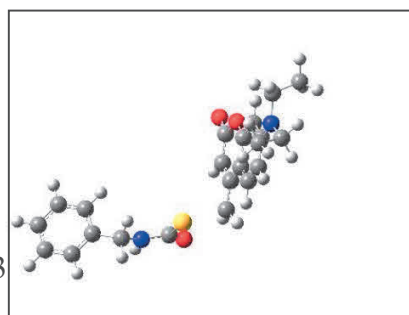
Number of Imaginary Frequencies = 1

Sum of electronic and zero-point Energies = -1585.764633

Sum of electronic and thermal Energies = -1585.737781

Sum of electronic and thermal Enthalpy = -1585.736837

Sum of electronic and thermal Free Energy = -1585.827864



Cartesian coordinate			
Atom	X	Y	Z
H	4.49141	1.01496	1.56531
C	3.94476	0.57179	0.74338
C	2.47485	-0.4676	-1.39565
C	2.78417	1.19119	0.33435
C	4.41523	-0.59998	0.07912
C	3.63158	-1.1038	-1.01157
C	1.99996	0.7109	-0.75698
H	3.92621	-2.00534	-1.53238
H	1.9051	-0.88933	-2.21653
O	2.43381	2.31327	1.04293
C	1.24778	3.00722	0.76066
O	1.01429	3.97655	1.48402
C	0.80291	1.42188	-1.14121
C	0.45547	2.53751	-0.31829
H	-0.45263	3.0969	-0.51812

C	-0.05548	1.00153	-2.18748
H	-0.7952	1.71328	-2.54149
H	0.34004	0.34931	-2.95819
S	-1.66504	-0.47695	-1.45115
C	-3.11218	0.54491	-1.73461
O	-3.08701	1.58971	-2.40091
N	5.5598	-1.2191	0.4702
C	6.1318	-2.36333	-0.26512
H	5.93806	-2.23828	-1.33132
H	7.21457	-2.3078	-0.12549
C	5.60472	-3.70834	0.24279
H	4.52454	-3.7983	0.08628
H	5.81593	-3.83731	1.31015
H	6.10347	-4.5159	-0.30561
C	6.32743	-0.79335	1.65553
H	6.81614	-1.69057	2.04437
H	5.63773	-0.44475	2.42572
C	7.3749	0.27337	1.32196
H	8.07984	-0.09046	0.56617
H	7.93922	0.51378	2.23043
H	6.90671	1.19141	0.95153
N	-4.28055	0.12203	-1.16285
H	-5.09559	0.6539	-1.45678
C	-4.54015	-1.14391	-0.47489
H	-3.64919	-1.39949	0.10673
H	-4.70462	-1.95382	-1.19812
C	-5.74179	-1.02487	0.44085
C	-6.90522	-1.76496	0.19192
C	-5.70487	-0.17699	1.56022
C	-8.0119	-1.66537	1.04428
H	-6.94535	-2.42434	-0.67275
C	-6.80765	-0.07326	2.4111
H	-4.80602	0.40097	1.76544
C	-7.96606	-0.81841	2.155
H	-8.90715	-2.24691	0.837
H	-6.76345	0.58486	3.27577
H	-8.82398	-0.73907	2.81838

TS2

opt = (calcfc,ts,noeigentest) freq ub3lyp/6-31+g(d)

scrf=(smd,solvent=dmsd); 0, 3

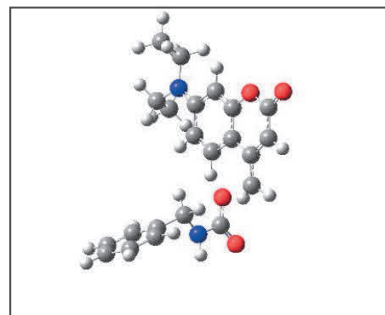
Number of Imaginary Frequencies = 1

Sum of electronic and zero-point Energies = -1262.792957

Sum of electronic and thermal Energies = -1262.766489

Sum of electronic and thermal Enthalpy = -1262.765545

Sum of electronic and thermal Free Energy = -1262.856712



Cartesian coordinate			
Atom	X	Y	Z
H	4.36606	0.38717	-1.48308
C	3.65234	0.2633	-0.67943
C	1.72304	0.01165	1.33051
C	2.71445	1.25447	-0.49065
C	3.65217	-0.89992	0.14606
C	2.64316	-0.99515	1.16273
C	1.71618	1.18185	0.52493
H	2.60241	-1.85136	1.82295
H	0.97907	-0.09731	2.11185
N	4.57425	-1.88061	-0.02645
C	5.67794	-1.76762	-0.99951
H	6.00831	-0.72941	-1.05204
H	6.5078	-2.35005	-0.59154
C	4.55049	-3.14024	0.74318
H	4.99333	-3.90145	0.09599
H	3.51582	-3.43312	0.92534
C	5.34009	-3.03688	2.05135
H	5.32888	-4.01303	2.54971
H	4.89746	-2.29699	2.7265
H	6.38295	-2.75985	1.86167
C	5.28881	-2.30075	-2.3817
H	4.47384	-1.71585	-2.82084

H	4.9774	-3.3496	-2.32552
H	6.15943	-2.2358	-3.04432
O	2.80109	2.31993	-1.35021
C	1.88775	3.38232	-1.28899
O	2.04621	4.27001	-2.12602
C	0.89168	3.33021	-0.278
H	0.20079	4.16643	-0.24645
C	0.7783	2.27593	0.67551
C	-0.24765	2.29014	1.63793
H	-0.21079	1.63228	2.49553
H	-0.78106	3.21937	1.79594
O	-1.80795	1.37601	0.82571
C	-2.84641	1.30928	1.60292
O	-2.94613	1.7939	2.75112
N	-3.92515	0.58358	1.08547
H	-4.7924	0.77149	1.57851
C	-4.07071	0.29703	-0.34358
H	-4.31217	1.20613	-0.91475
H	-3.10409	-0.06514	-0.70421
C	-5.14373	-0.74642	-0.58338
C	-6.33583	-0.41174	-1.24006
C	-4.96246	-2.07115	-0.15145
C	-7.32697	-1.37575	-1.4644
H	-6.4896	0.61044	-1.58055
C	-5.94858	-3.03569	-0.37142
H	-4.04124	-2.34574	0.3586
C	-7.13612	-2.6902	-1.02987
H	-8.24506	-1.09757	-1.97685
H	-5.79075	-4.05756	-0.034
H	-7.90356	-3.44102	-1.20244

Products from the C–S bond dissociation (2a)

opt freq ub3lyp/6-31+g(d) scrf=(smd,solvent=dmsd); 0, 3

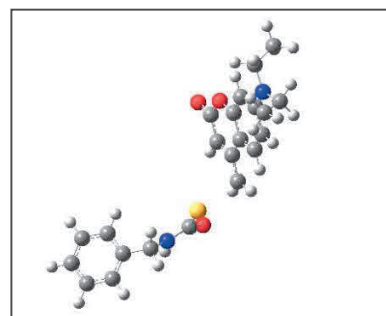
Number of Imaginary Frequencies = 0

Sum of electronic and zero-point Energies = -1585.765968

Sum of electronic and thermal Energies = -1585.738073

Sum of electronic and thermal Enthalpy = -1585.737129

Sum of electronic and thermal Free Energy = -1585.832528



Cartesian coordinate			
Atom	X	Y	Z
H	4.72232	1.20981	1.40297
C	4.16707	0.66338	0.65223
C	2.67104	-0.64258	-1.32038
C	2.99256	1.21542	0.18803
C	4.6359	-0.57621	0.12618
C	3.83869	-1.2176	-0.88333
C	2.19832	0.5969	-0.81555
H	4.13499	-2.17321	-1.29501
H	2.09047	-1.16309	-2.07403
O	2.64152	2.41361	0.7578
C	1.4676	3.0692	0.4002
O	1.23531	4.12426	0.98019
C	0.97443	1.24452	-1.2597
C	0.65081	2.46263	-0.60458
H	-0.25584	2.9974	-0.86682
C	0.13192	0.72601	-2.2421
H	-0.72805	1.29467	-2.57514
H	0.40578	-0.13941	-2.83095
S	-1.88225	-0.82561	-1.05439
C	-3.24842	0.14365	-1.6572
O	-3.12254	1.05631	-2.49355
N	5.79116	-1.13173	0.56609
C	6.36047	-2.35811	-0.02713
H	6.13801	-2.37825	-1.09437

H	7.44523	-2.27163	0.07582
C	5.86406	-3.62776	0.67105
H	4.78209	-3.74954	0.55331
H	6.10149	-3.60869	1.74043
H	6.36238	-4.49544	0.22366
C	6.57959	-0.55374	1.67195
H	7.08834	-1.39166	2.15484
H	5.90203	-0.11953	2.40837
C	7.60539	0.47321	1.1822
H	8.29655	0.02472	0.46015
H	8.18737	0.82831	2.04037
H	7.11764	1.3343	0.71336
N	-4.4982	-0.12381	-1.15038
H	-5.24389	0.37324	-1.63028
C	-4.90649	-1.25405	-0.31863
H	-4.06698	-1.501	0.33775
H	-5.11185	-2.14083	-0.9348
C	-6.13365	-0.91192	0.50316
C	-7.34665	-1.58034	0.29031
C	-6.07348	0.0784	1.49792
C	-8.479	-1.27007	1.05397
H	-7.40644	-2.34894	-0.47779
C	-7.20073	0.39166	2.26079
H	-5.13724	0.60421	1.67419
C	-8.40892	-0.28281	2.0406
H	-9.41262	-1.79826	0.87471
H	-7.13727	1.15847	3.02949
H	-9.28654	-0.03932	2.6347

Products from the C–O bond dissociation (2b)

opt freq ub3lyp/6-31+g(d) scrf=(smd,solvent=dmsd); 0, 3

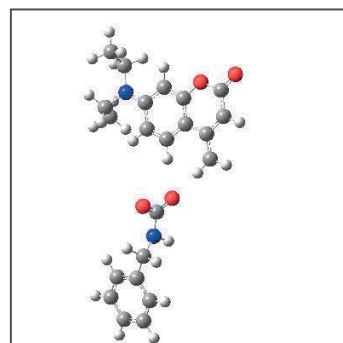
Number of Imaginary Frequencies = 0

Sum of electronic and zero-point Energies = -1262.802480

Sum of electronic and thermal Energies = -1262.774969

Sum of electronic and thermal Enthalpy = -1262.774024

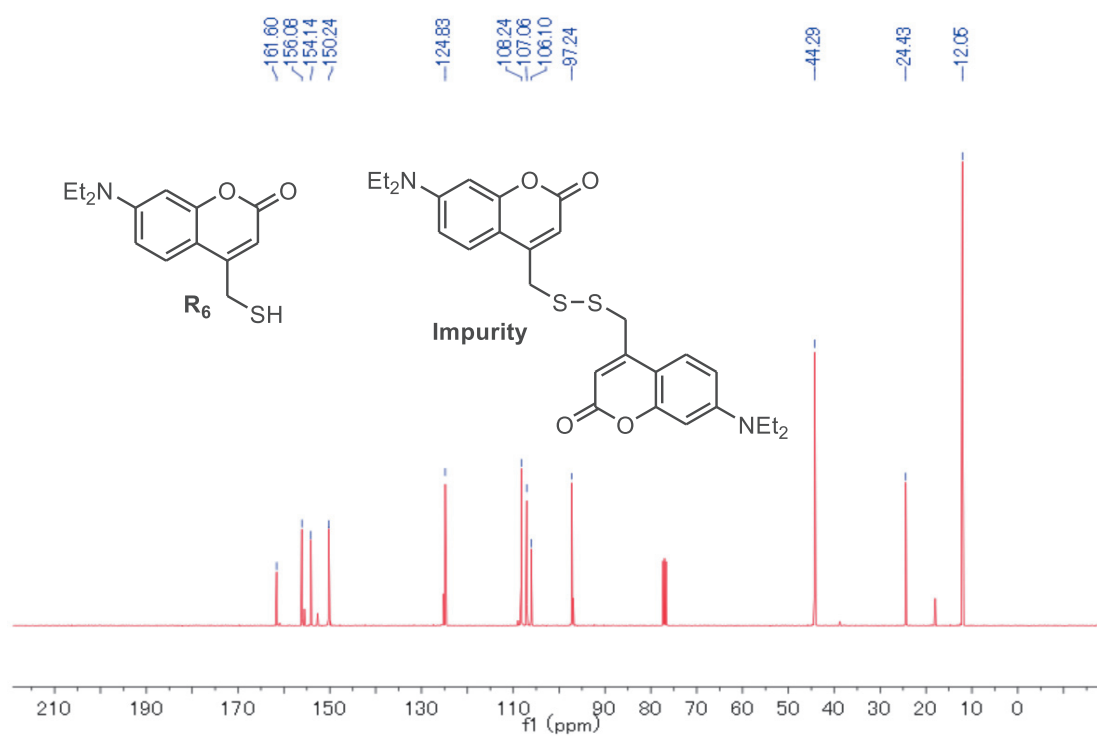
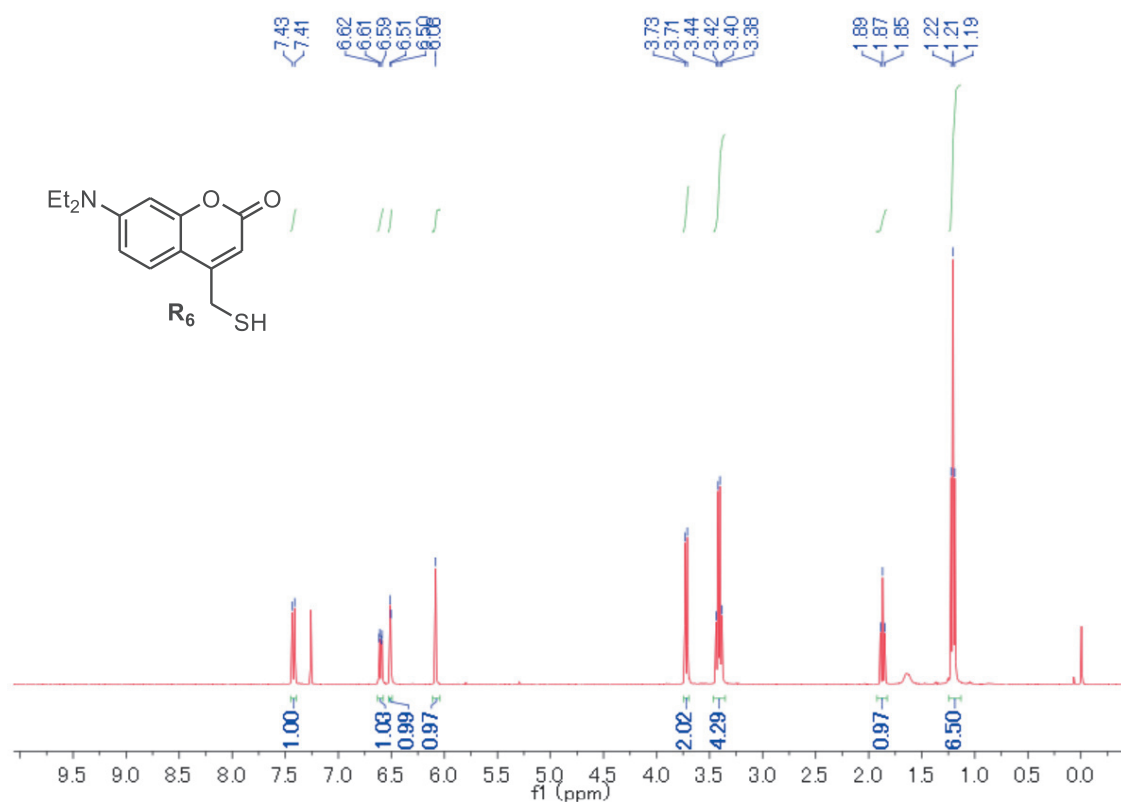
Sum of electronic and thermal Free Energy = -1262.868824

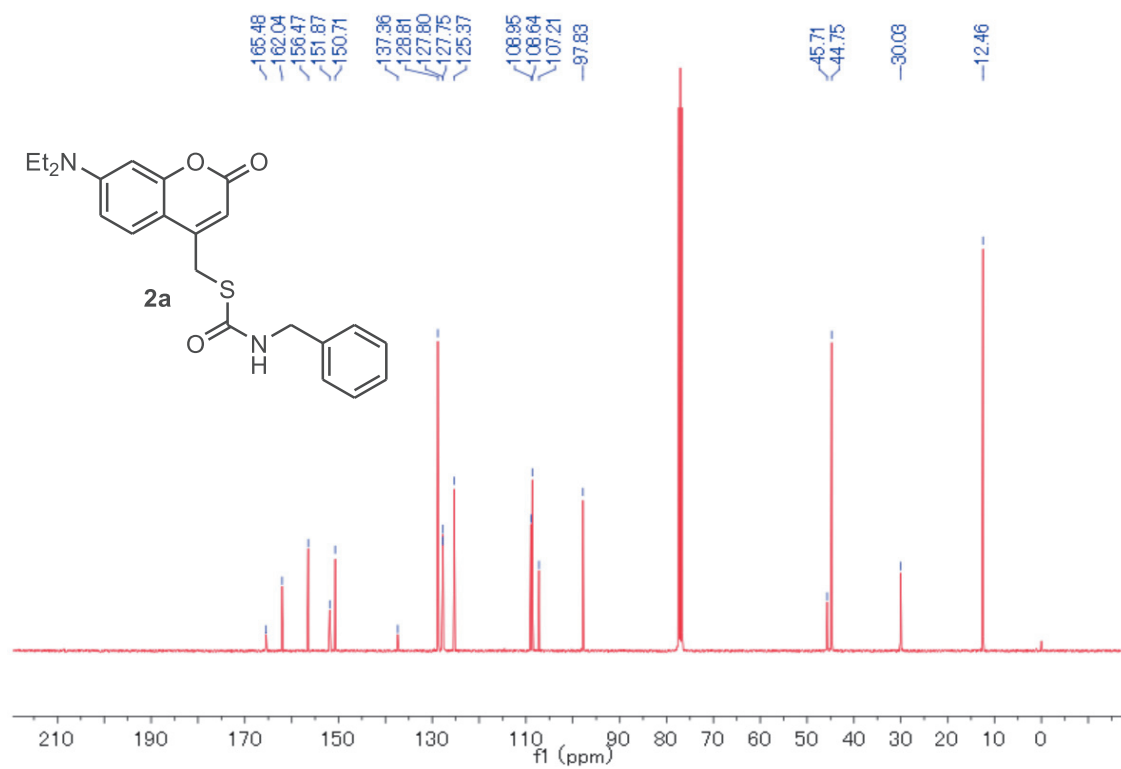
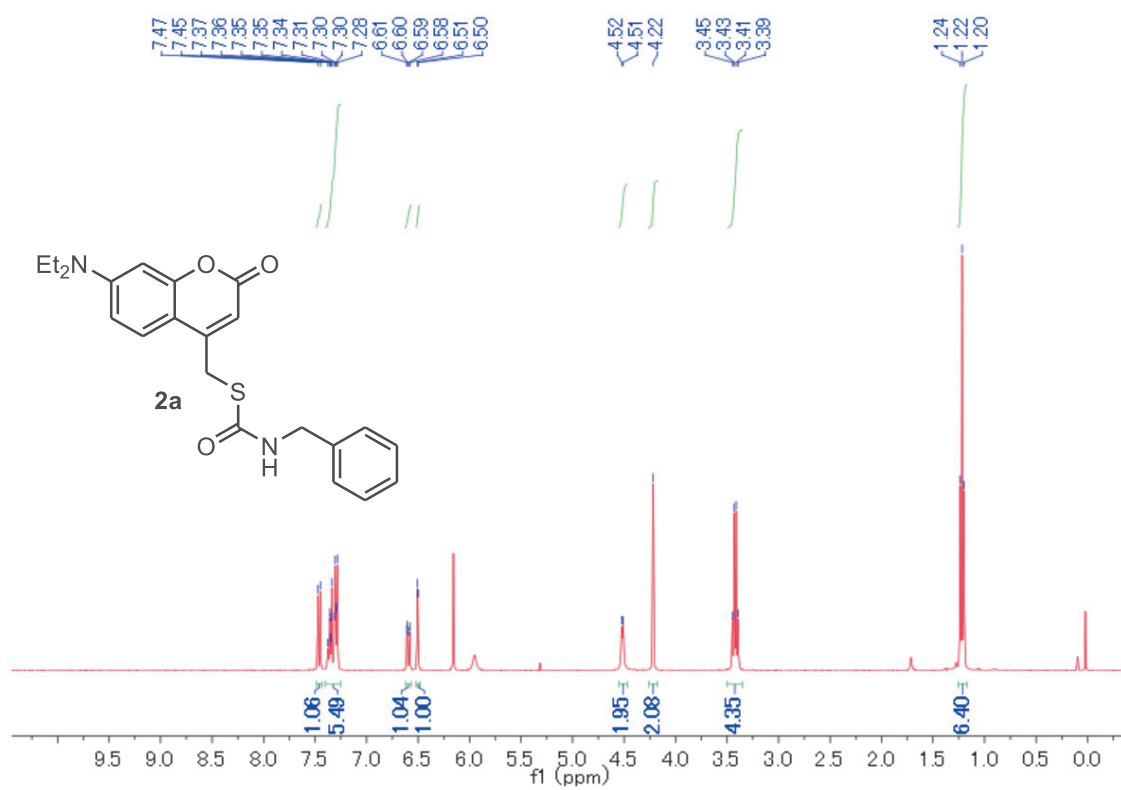


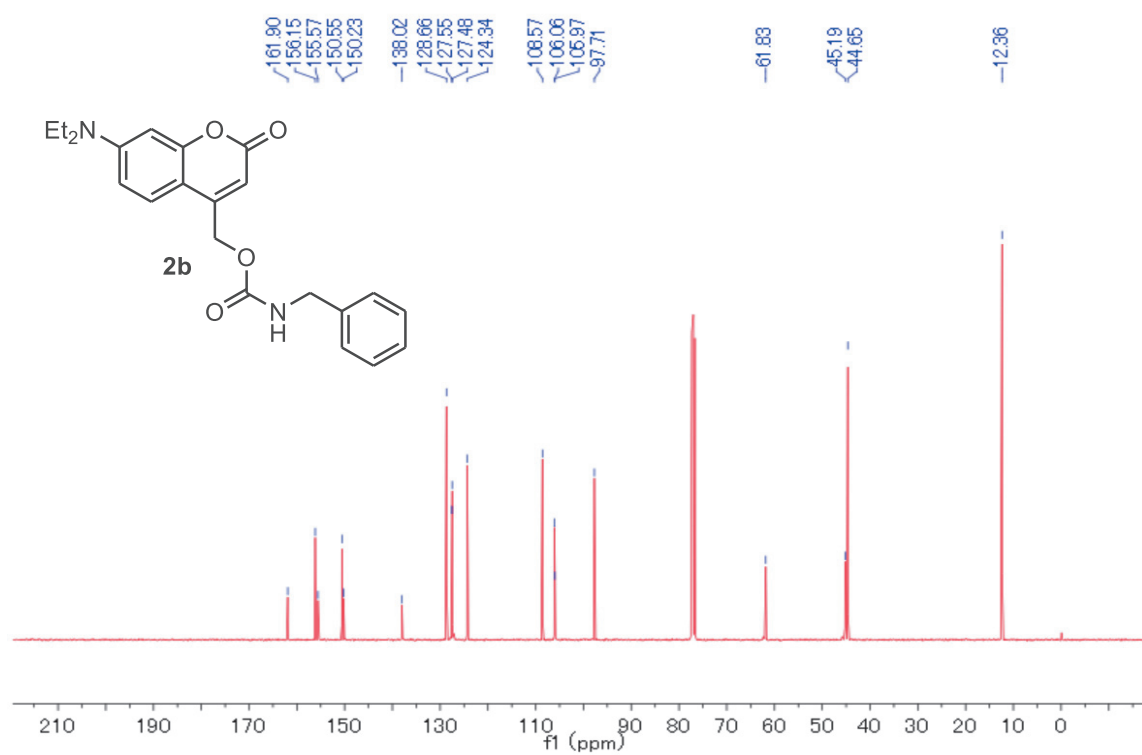
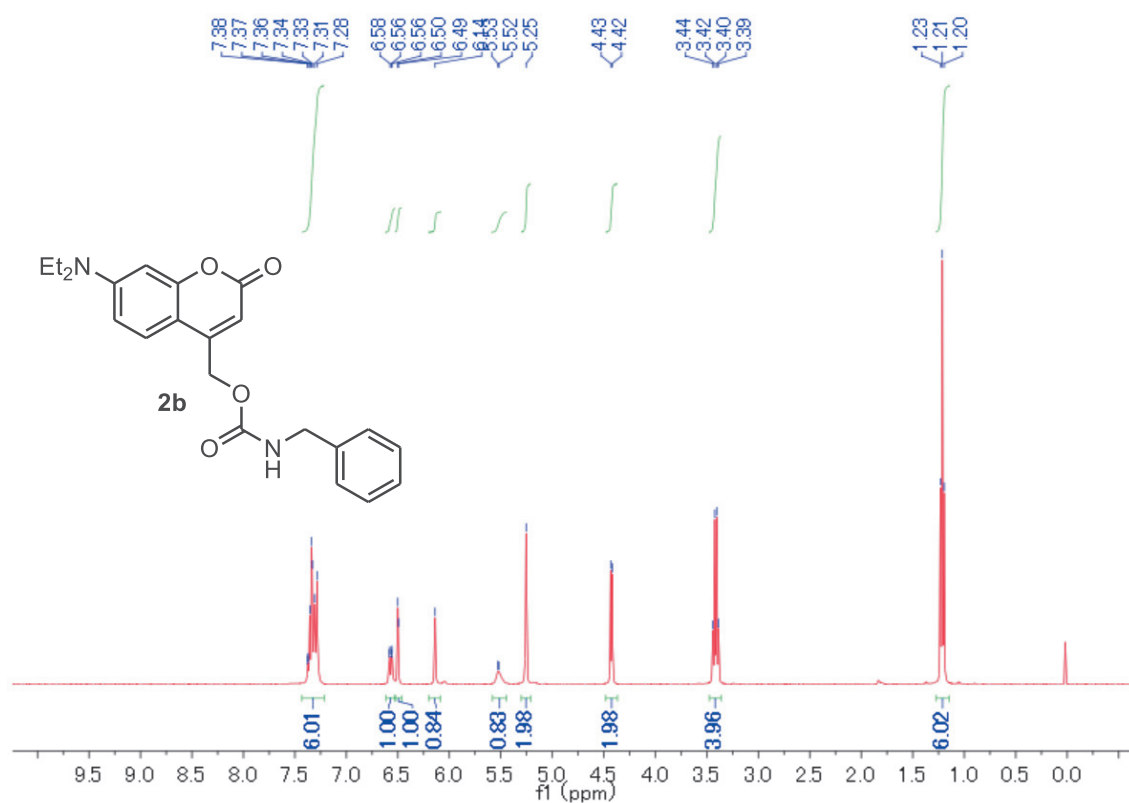
Cartesian coordinate			
Atom	X	Y	Z
H	5.33146	-0.52884	0.04006
C	4.26586	-0.3465	0.08021
C	1.51116	0.2313	0.13988
C	3.82722	0.95803	0.11594
C	3.31801	-1.41376	0.06322
C	1.91951	-1.07867	0.09341
C	2.44765	1.29816	0.14884
H	1.16946	-1.85825	0.10303
H	0.44285	0.44757	0.17648
N	3.72389	-2.70354	0.02339
C	5.14622	-3.09608	0.09687
H	5.67655	-2.40307	0.75012
H	5.1644	-4.07805	0.57548
C	2.77695	-3.8322	-0.09072
H	3.30794	-4.61992	-0.63028
H	1.929	-3.52932	-0.70454
C	2.32533	-4.34006	1.28188
H	1.67224	-5.20769	1.13597
H	1.76781	-3.57106	1.82641
H	3.18222	-4.6515	1.88889
C	5.79459	-3.17202	-1.2888
H	5.80212	-2.19359	-1.78015
H	5.26989	-3.88644	-1.93203
H	6.82989	-3.51098	-1.17058

O	4.80999	1.91612	0.11338
C	4.51406	3.26962	0.14395
O	5.45916	4.04311	0.13679
C	3.12361	3.64289	0.18248
H	2.91328	4.70671	0.20801
C	2.07091	2.70584	0.18917
C	0.74152	3.13384	0.23117
H	-0.10138	2.44376	0.24321
H	0.53498	4.20055	0.2562
O	-2.42233	1.48559	-1.53879
C	-2.53535	1.01372	-0.37478
O	-1.61337	0.87217	0.4919
N	-3.81614	0.54045	0.02755
H	-3.8953	0.46543	1.037
C	-5.02913	1.02405	-0.6313
H	-5.23969	2.07694	-0.38163
H	-4.84695	0.98058	-1.70865
C	-6.23279	0.17783	-0.26567
C	-7.24934	0.68864	0.55356
C	-6.35178	-1.1407	-0.73737
C	-8.35954	-0.09405	0.89601
H	-7.17294	1.70874	0.92555
C	-7.45675	-1.9257	-0.39938
H	-5.5723	-1.55126	-1.37637
C	-8.46596	-1.40407	0.4209
H	-9.13766	0.32097	1.53269
H	-7.53436	-2.94247	-0.77798
H	-9.32717	-2.01398	0.68346

3-9. Spectra







Chapter 4

Conclusions

4-1. Conclusions

In this study, a series of DEACM-based caged carboxylic acid and caged amines were synthesized. The photochemical properties of these compounds were examined by product analysis, ^{18}O -labeling method and laser flash photolysis. In the case of caged carboxylic acid, sulfur atom has a profound influence on the uncaging mechanism of the caged compounds. The distribution of intermediates (radical pairs, ion pairs) was controlled by the type of bond which is broken under light irradiation (C–O or C–S). Furthermore, sulfur atom improved the photochemical quantum yield as this value of thioester **1a** was much higher than that of **1c**. In the case of caged amines, the photochemical quantum yield was significantly improved (from 0.0012 to 0.024) when the carbamate linker was substituted by the thiocarbamate linker. This observation suggests that thiocarbamate linker is a promising substitution for the conventional carbamate linker to enhance the photochemical quantum yield of caged amines.

List of Publications

Articles

(1) "Crucial Roles of Leaving Group and Open-Shell Cation in Photoreaction of (Coumarin-4-yl)methyl Derivatives"

Hai Dang Nguyen and Manabu Abe*

J. Am. Chem. Soc. **2024**, 146, 10993-11001.

(2) "Sulfur Atom Effect on the Photochemical Release of Benzylamine from Caged Amines"

Hai Dang Nguyen and Manabu Abe*

Chem. Lett. **2024**, 53, 1-4.

Thesis Supplements

(1) "Crucial Roles of Leaving Group and Open-Shell Cation in Photoreaction of (Coumarin-4-yl)methyl Derivatives"

Hai Dang Nguyen and Manabu Abe*

J. Am. Chem. Soc. **2024**, 146, 10993-11001.

(2) "Sulfur Atom Effect on the Photochemical Release of Benzylamine from Caged Amines"

Hai Dang Nguyen and Manabu Abe*

Chem. Lett. **2024**, 53, 1-4.

(3) "Development of a Two-Photon-Responsive Chromophore, 2-(*p*-Aminophenyl)-5,6-dimethoxy-1-(hydroxyinden-3-yl)methyl Derivatives, as a Photoremovable Protecting Group"

Tuan Phong Nguyen, Hai Dang Nguyen and Manabu Abe*

J. Org. Chem. **2024**, 89, 4691-4701.

Acknowledgement

All the research studies included in this dissertation have been conducted under the supervision of Professor Manabu Abe at the Department of Chemistry, Graduate School of Science, Hiroshima University. My research was supported by JST CREST (JPMJCR18R4).

At first, I would like to express my deepest appreciation to Professor Manabu Abe for his profound support, advice and encouragement thought out my research in Hiroshima University.

I would like to extend my sincere thanks to Dr. Ryukichi Takagi for his kind support and valuable discussions during my research works. I am also grateful to Dr. Sayaka Hatano for her great helps during my time in the lab.

I would like to express my special thanks to all lab members for their helps and creating a friendly environment in the lab.

Finally, I could not have undertaken this journey without my family, who always stand by my side in hardest times. Additionally, words cannot express my gratitude to my wife, who always give me great motivations in my career.